

**INVESTIGATING THE ROLE OF LIPOCALIN-2 AS A DIAGNOSTIC INDICATOR FOR
NONALCOHOLIC STEATOHEPATITIS IN A FRUCTOSE-INDUCED RAT FATTY LIVER MODEL:
FIRST EXPERIMENTAL STUDIES**



Dissertation

for the award of the degree
"Doctor rerum naturalium" (Dr. rer. nat.)
of the Georg-August-University Goettingen

within

the Georg-August University School of Science (GAUSS) doctoral program

Submitted by

Salamah Mohammad ALWAHSH

from Bethlehem, PALESTINE

2013

Goettingen, GERMANY

Thesis Committee

Reviewer: Prof. Dr. Uwe Groß

(Institute for Medical Microbiology, Faculty of Medicine, Georg-August-University, Goettingen, Germany)

Second reviewer: Prof. Dr. Michael Hoppert

(Department General Microbiology, Institute of Microbiology and Genetics, Georg-August-University Goettingen, Goettingen, Germany)

Members of the Examination Board

Prof. Dr. J. Wilting

(Anatomy & Cell Biology Institute, University Medical Center, Goettingen)

Prof. Dr. A. Mansouri

(Biophysics Chemistry, Max-Planck-Institute, Goettingen)

Prof. Dr. W. Kramer

(Institut für Microbiology and Genetic, Department of Molecular Genetic)

Prof. Dr. S. Rizzoli

(STED Microscopy of Synaptic Function, European Neuroscience Institute (ENI))

Date of the oral examination: December 12th, 2013

Declaration

I hereby declare that this doctoral thesis entitled **”Investigating the role of lipocalin-2 as a diagnostic indicator for nonalcoholic steatohepatitis in a fructose-induced rat fatty liver model: First experimental studies“** is my own work and effort and that it has not been submitted anywhere for any award. I have accomplished this work independently without any informal aids than quoted.

Salamah M. Alwahsh

Contents

Declaration	3
Contents	4
List of figures	8
List of tables	9
Summary	11
Abbreviations.....	14
1. INTRODUCTION	17
1.1. <i>Liver anatomy</i>	17
1.1.1. Liver macroscopy	17
1.1.2. Liver microscopy.....	18
1.2. <i>Liver physiology</i>	19
1.3. <i>Liver pathophysiology</i>	20
1.3.1. Nonalcoholic fatty liver disease (NAFLD)	20
1.3.1.1.1. Fat metabolism in the liver	21
1.3.1.1.2. Accumulation of fat in the liver	22
1.3.1.1.3. Transition from fat accumulation into inflammation and fibrosis.....	22
1.4. <i>Fructose</i>	27
1.4.1. Definition	27
1.4.2. Fructose metabolism	28
1.4.3. Fructose and liver diseases.....	29
1.4.4. Fructose and oxidative stress and lipid peroxidation	30
1.5. <i>Lipocalin-2</i>	31
1.5.1. Definition	31
1.5.2. LCN2, oxidative stress and lipid peroxidation	33
1.5.3. LCN2 receptor	33
1.6. <i>Study Motivations</i>	34
1.7. <i>Research Hypotheses and Aims</i>	35
2. MATERIALS AND METHODS	36
2.1. <i>Materials</i>	36
2.1.1. Chemicals.....	36
2.1.2. Equipment	37
2.1.3. Antibodies.....	38
2.1.4. Oligonucleotides	38
2.1.5. Software	39
2.2. <i>Methods</i>	40
2.2.1. Experimental animals and diets.....	40
2.2.2. Fructose-containing Lieber-DeCarli diet	40
2.2.3. Induction of nonalcoholic fatty liver in rats.....	40
2.2.4. Collection of blood and liver samples	41
2.2.5. Histological (morphological) staining	42

2.2.5.1.1. Principle	42
2.2.5.1.2. Solutions' preparation	42
2.2.5.1.3. Oil Red O staining procedure.....	42
2.2.5.2.1. Nile red staining protocol.....	44
2.2.6. Biochemical studies	45
2.2.7. qRT-PCR analysis	46
2.2.8. Western immunoblots.....	49
2.2.9. Double immunofluorescent analysis for LCN2 and MPO or ED1.....	51
2.2.10. Enzyme-linked immunoadsorbent assay (ELISA) for serum LCN2	51
2.2.11. Two-dimensional gel electrophoresis (2-DE).....	53
2.2.12. <i>In vitro</i> studies	55
2.2.12.1.1. Animal preparation.....	55
2.2.12.1.2. Liver perfusion	56
2.2.12.1.3. HCs treatment.....	57
2.3. <i>Statistical analysis</i>	58
3. RESULTS	59
3.1. <i>Animal phenotypes and biophysical parameters</i>	59
3.1.1. L-HFr fed rats exhibited increases of food intake	59
3.1.2. Variations in the body and liver weights	59
3.2. <i>Fatty liver developed in the LDC and the L-HFr group</i>	61
3.2.1. Hepatic lipid partitioning in the animal groups	62
3.1.2. HE staining manifested macrosteatosis, HCs ballooning, and moderate inflammation in the L-HFr group	63
3.2.3. Stages of liver fibrosis in the experimental groups	66
3.3. <i>Biochemical Studies</i>	67
3.3.1. Hepatic TG content.....	67
3.3.2. Plasma biochemical profiles differed markedly in the L-HFr model	68
3.3.3. Changes in serum leptin levels.....	69
3.4. <i>Changes of hepatic inflammation- and metabolism-related genes</i>	70
3.4.1. mRNA transcript of <i>Lcn2</i> increased significantly in the L-HFr group.....	70
3.4.2. Expression of inflammation-related genes in the liver samples	71
3.4.3. Hepatic <i>Glut5</i> and <i>Lep-r</i> transcripts were elevated in the L-HFr regimen	72
3.5. <i>Changes of the hepatic LCN2 expression at protein levels</i>	73
3.6. <i>Immunohistochemical detection of LCN2, MPO and ED1 in rat liver</i>	74
3.7. <i>Serum levels of LCN2</i>	76
3.8. <i>Modulations of hepatic expression of inflammation-related proteins</i>	77
3.9. <i>Metabolism and oxidative stress related indicators</i>	77
3.10. <i>2-DE data analysis</i>	79
3.10.1. Proteins with significantly altered amount.....	79
3.11. <i>Expression of LCN2 in vitro</i>	81

4. DISCUSSION	83
4.1. <i>Animal phenotypes and NAFLD.....</i>	83
4.2. <i>The effect of the diets on the histopathological manifestations of NAFLD</i>	85
4.3. <i>Metabolic syndrome and serum transaminase.....</i>	86
4.4. <i>LCN2 expression in the liver and serum of L-HFr fed rats</i>	87
4.5. <i>Localization and possible role of LCN2 in the liver.....</i>	88
4.6. <i>Conclusion</i>	92
5. Outlook	94
6. References	95
Appendix.....	104
Acknowledgments	107
Publications and Conferences	108
Resume	109

List of figures

Figure 1.1 Diagram of liver architecture.....	17
Figure 1.2 Spectrum of NAFLD	22
Figure 1.3 The cyclic (5-ring) structure of D-fructose according to IUPAC	28
Figure 1.4 Utilization of fructose and glucose in the liver.....	29
Figure 1.5 Lipocalin/ cytosolic fatty-acid binding protein family	32
Figure 2.1 Diet categories and feeding periods	41
Figure 2.2 Simplified Jablonski diagram	44
Figure 2.3 qRT-PCR phases	48
Figure 2.4 The status of rat liver during HC isolation.....	57
Figure 3.1 Phenotypes of the animals	60
Figure 3.2 An overview of the rat liver and visceral adipose tissue after laparotomy.....	61
Figure 3.3 Representative micrographs illustrate lipid deposition.....	62
Figure 3.4 Photomicrographs of Nile red stained liver sections	63
Figure 3.5A HE-stained livers at wk 4.....	64
Figure 3.5B Photomicrographs of HE staining of wk 8 hepatic tissue.....	65
Figure 3.5C Percentage of fat-laden HCs.....	66
Figure 3.6 Masson's Trichrome stained liver slices	67
Figure 3.7 Triglyceride content in the rat liver.....	68
Figure 3.8 Fasting serum leptin levels	70
Figure 3.9 Bar plot shows relative expression of <i>Lcn2</i> in the liver	71
Figure 3.10 Changes of specific mRNA transcription in the liver	72
Figure 3.11 Modulations of <i>Glut5</i> and <i>Lep-r</i> mRNA in the liver.....	73
Figure 3.12 Changes in LCN2 protein expression in the rat liver.....	73
Figure 3.13 Immunolocalization of hepatic LCN2	75
Figure 3.14 Upregulation of systemic LCN2 levels was seen in the L-HFr group	76
Figure 3.15 Changes in the expression of liver inflammation-related proteins.....	77
Figure 3.16 Changes in oxidative stress related proteins in the liver.....	78
Figure 3.17 Representation of two gel images warped by the software Delta2D.....	79
Figure 3.18 Representative protein spots of phospho and silver stained 2-DE gels.....	80
Figure 3.19 Changes of <i>Lcn2</i> expression in the isolated primary HCs	81
Figure 3.20A Changes of LCN2 protein expression in cultured HCs	82
Figure 3.20B Densitometric analysis (I) and fold change (II) LCN2 expression.....	82
Figure 4.1 Hypothetical model of the mechanism of hepatic LCN2 production in L-HFr 91	
Appendix Figure 1 Kinetic HE staining for rat liver sections on 1, 2, 4, 8 wks.....	104
Appendix Figure 2 Illustration of rat fatty liver models induced by various diets	105

List of tables:

Table 1.1 Noninvasive predictors of NASH in human beings	24
Table 1.2 NAFLD, histological classification/changes.	26
Table 2.1 List of the chemicals and materials that were used in this study.	36
Table 2.2 The technical equipment that were utilized in this study.	37
Table 2.3 List of the antibodies that were used in this study.....	38
Table 2.4 List of gene-specific primers used for qRT-PCR analysis.....	39
Table 2.5 List of the scientific software that were applied in this study.	39
Table 2.6 Lysis buffer used for protein extraction in Western blots.	50
Table 2.12 The composition of the phase 1 and 2 gels.	54
Table 2.14 Buffer I: Pre-perfusion, Ca-free KRB + EGTA pH (7.4) KRB.	57
Table 3.1 Data of plasma biochemistry of the rats during 8 wks of feeding.	69
Appendix Table 1 Summary of LCN2 studies in recent literature	106

Summary

The liver is the vital organ for fat and carbohydrate metabolism as well as detoxification and excretion of metabolites. Any functional impairment will thus affect the whole organism and is absolutely undesirable. Nonalcoholic fatty liver disease (NAFLD) is a multifactorial worldwide disease which coincides with metabolic syndrome. The spectrum of NAFLD ranges from simple steatosis to nonalcoholic steatohepatitis (NASH), with consecutive fibrosis, cirrhosis, and might ultimately lead to hepatocellular carcinoma. The prevalence of NAFLD is estimated to be 20-30% of the general population in Europe, and it is paralleling with the increase in fructose consumption. Fructose, a monosaccharide, is naturally present in fruit, and it can be metabolized into glucose and lipid within the liver. Industrially, fructose is used in soft drinks as a sweetener, and it is integrated in pre-packed food as an additive. Fructose is considered a risk factor for NAFLD. Previous reports found an upregulation of liver lipocalin-2 (LCN2) expression in inflammation and metabolic syndrome. LCN2 is a 25-kDa secretory glycoprotein, found abundantly in tissues that are exposed to microorganisms. It can bind a variety of lipophilic substances.

Study motivations. Although ultrasonography, CT scan, and MRI are reliable tools for detecting a fatty liver, they are inadequate to classify the disease. Instead, a liver biopsy is needed to distinguish between simple steatosis and NASH. However, this is an invasive procedure which carries the risk of bleeding and injury to gallbladder, lungs and kidney. Thus, serum biomarkers would be most welcome. In addition, the pathogenesis of NAFLD is still poorly defined. The available animal models, such as *Lcn2^{-/-}*, *db/db*, *ob/ob*, and ZF *fa/fa* do not mimic the physiological and/or histological features of NAFLD seen in humans. Since fructose is included in commercial/fast food as well as juice beverages and as it has been proposed to induce the most NAFLD manifestations noticed in humans; this study selected fructose as an inducer for metabolic syndrome and NAFLD.

This study aimed to establish diet-induced fatty liver models in non-genetically-modified rats, to compare the expressional changes of inflammatory and metabolic parameters and LCN2 in these models, to explore whether serum LCN2 is a diagnostic indicator for NASH, and to investigate the potential mechanism(s) that induce(s) hepatic LCN2 expression.

Male Sprague-Dawley rats were randomly assigned (n= 4 per group/ time point) as follows: chow pellets (control (Co)), liquid Lieber-DeCarli (LDC, high fat), and LDC + high (70% of the total calorie) fructose (L-HFr) diet. After feeding for 4 or 8 wks; the animals were deprived of any food 10 h before sacrifice.

Blood from the *vena cava* and liver samples were harvested. Blood samples were examined for fasting glucose, lipid profile, serum transaminases activities, and leptin concentration. Histochemical studies for lipid deposition, inflammation, and fibrosis were performed on the liver sections. In addition, the hepatic transcript of *Lcn2*, the inflammatory mediators *Il-8*, *Mcp-1 (Ccl2)*, alpha-2 macroglobulin ($\alpha 2m$), *Tnf- α* , *Inos*, *Tlr4*, and fructose transporter (*Glut5*) and leptin receptor (*Lep-r*) were evaluated by qRT-PCR. Furthermore, ELISA and Western blots were performed to assess LCN2 levels in serum, while the localization of LCN2 in liver tissue was detected by double-immunofluorescence staining. Western immunoblots for hepatic LCN2, CD14, I κ B1 α , pMAPK, casp 9, Cyt c, 4-hydroxynonenal (4-HNE adducts): by-products of lipid peroxidation, GRP78: an ER chaperone, and PGC-1 α : a mitochondrial-biogenic protein, were carried out. *In vitro* experiments were done as well to study *Lcn2* transcription. Primary hepatocytes (HCs) were isolated from control rats and cultured in M199 media supplemented with either 20 mM glucose or fructose for 0, 3, 6, 12, and 24 h.

Hallmarks of the metabolic syndrome, including a significant elevation of fasting blood glucose and triglycerides as well as a decrease in HDL-cholesterol levels, were observed in the LHF_r group. The activities of AST and ALT were augmented in L-HFr fed rats. Concurrently, feeding with L-HFr augmented fasting leptin levels by about 3-fold vs. Co ($P < 0.001$). Histologically, hepatic simple steatosis was featured in the LDC group. Parallel to the metabolic syndrome, the L-HFr group evidenced NASH criteria, such as inflammation (grade 2) and mild fibrosis (stage 2) in the portal triads, and hepatocellular ballooning in the centrilobular areas. Hepatic *Glut5* and *Lep-r* expressions were substantially upregulated in the L-HFr group. While most tested biochemical parameters under the LDC regimen were slightly higher than in control rats, a significant increase in the plasma triglyceride level was seen in this group at wk 4.

In the liver, specific transcripts of *Mcp-1*, $\alpha 2-m$, and *Il-8* were increased in the L-HFr group at both time points ($P < 0.001$), whereas the transcription of *Tlr4*, *Inos*, and *Tnf- α* was significantly enhanced at wk 4 and then dropped to the control level at wk 8. In

contrast, no significant change was observed in the LDC group. Interestingly, of the studied parameters, hepatic transcription of *Lcn2* mRNA was the most pronounced (90- and 507-fold higher in the L-HFr rats vs. control at wk 4 and 8, respectively ($P < 0.001$)). These data were further validated by Western blots. Of note, while hepatic LCN2 expression reached its maximum at wk 8, the expression of inflammatory mediators in the liver decreased to control levels pointing to a possible hepatoprotective effect of LCN2. Likewise, a significant elevation of systemic LCN2 levels was observed in the L-HFr regimen. In contrast to the mild changes seen in the LDC group, the hepatic expression of CD14, pMAPK, casp 9, Cyt c and 4-HNE proteins was increased in the L-HFr group. Conversely, the expression of PGC-1 α in the liver was reduced in the L-HFr group at wk 8. In the liver, the localization of LCN2 was restricted to MPO⁺ recruited granulocytes. LCN2 showed a high consecutive expression in fructose-treated primary HCs compared to glucose treatment.

Conclusion

Both LDC and L-HFr diets led NAFLD. While the LDC diet resulted in a simple steatosis, the L-HFr diet led to NASH. Fructose supplementation appears to worsen liver pathology. The features of the metabolic syndrome and NASH with progressive fibrosis obtained with fructose-enriched diet represent an animal model broadly similar to the conditions in human liver disease. These findings highlight the impact of dietary composition in the development of NAFLD. The fructose diet upregulates hepatic *Lcn2* gene expression in fructose-induced NASH. This correlates with the increased indicators of inflammation, oxidative stress and mitochondrial dysfunction. This novel study could introduce serum LCN2 as a useful new diagnostic to discriminate between simple steatosis and NASH. Evidently, an interaction exists between the metabolic impetus and inflammatory processes in the animals. The current model is valuable for investigation of the role(s) of LCN2 and other markers for inflammation and metabolism in greater depth and the development of new insights for preventing NASH.

Abbreviations

ATP	Adenosine triphosphate
α 2-m	Alpha 2 macroglobin
BSA	Bovine serum albumin
°C	Degrees Celsius
cDNA	Complementary DNA
cAMP	Cyclic adenosine monophosphate
Ct	Threshold cycle
CO ₂	Carbon dioxide
ddH ₂ O	Double distilled water
DMEM	Dulbecco's Modified Eagle Medium
DNA	Deoxyribonucleic acid
dNTP	Deoxynucleotide phosphate
DTT	Dithiothreitol
EDTA	Ethylendiamintetra acidic acid
ED1	Ectodysplasin-1
EGTA	Ethylene glycol tetraacetic acid
ELISA	Enzyme-linked immunosorbent assay
ER	Endoplasmatic reticulum
FCS	Fetal calf serum
FFA	Free fatty acid
Glut5	Glucose transporter 5 (fructose transporter)
HCS	Hepatocytes
HEPES	4-(2-hydroxyethyl)-1-piperazineethanesulfonic acid
HDL-C	High-density lipoprotein containing cholesterol
HSCs	Hepatic stellate cells
4-HNE	Hydroxynonenal adducts
h	Hour
IF	Immunofluorescent
IPG	Immobilized pH gradient
IEF	Isoelectric focusing
Il-8	Interleukin 8
iNOS	Inducible nitric oxide synthase

IR	Insulin resistance
KCs	Kupffer cells
kDa	Kilodalton
KRB	Krebs-Ringer Buffer
LDL-C	Low-density lipoprotein containing cholesterol
Lep-r	Leptin receptor
LCN2	Lipocalin-2
LPS	Lipopolysaccharides
MAPK	Mitogen-associated protein kinase
MCP-1	Monocyte chemotactic protein-1
min	Minute
μL	Microliter
mL	Milliliter
NF-κB	Nuclear factor kappa-light-chain-enhancer of activated B-cells
NAFLD	Nonalcoholic fatty liver disease
NASH	Nonalcoholic steatohepatitis
OD	Optical density
P	p-value
PBS	phosphate-buffered saline
PMN	Polymorphonuclear neutrophils
PMSF	Phenylmethyl sulfonylfluoride
phospho	Phosphorylated
qRT-PCR	Quantitative reverse transcriptase-polymerase chain reaction
RNA	ribonucleic acid
RNase	RNA ribonuclease
ROS	Reaction oxygen species
RT	Room temperature
rpm	Round per minute
SDS	Sodium dodecyl sulphate
SDS-PAGE	SDS-polyacrylamide gel electrophoresis
sec	Second
2-DE	Two-dimensional gel electrophoresis
TEMED	Tetramethyl ethylene diamine
TG	Triglyceride

TLR4	Toll-like receptor 4
TNF- α	Tumor necrosis factor alpha
Tris	Tris-(hydroxymethyl)-aminomethane

1. INTRODUCTION

1.1. Liver anatomy

The human liver is located in the upper right quadrant of the abdomen, just under the diaphragm. It is the largest (1.5 - 1.8 kg in adult) organ of the body, accounting for approximately 2 - 3% of the average body weight.

1.1.1. Liver macroscopy

In humans, the liver consists of unequal right and left lobes divided by the falciform ligament, both of which are made up of thousands of lobules (Gregory and Wing 2002). These are the functional units of the liver. Each lobule is about 1 mm in diameter. Liver lobules are hexagonal structures consisting of cords of hepatocytes that are separated by sinusoids. At each of the six corners of a lobule is a portal triad (branch of portal vein, branch of hepatic artery, and bile duct). The portal triad components with hepatic nerves plexus enter the liver via the so-called porta hepatis (a deep, transverse fissure on the right lobe). There are two distinct sources that supply blood to the liver (Figure 1.1), oxygenated blood flows through the hepatic artery (20%) and nutrient-rich blood flows from the hepatic portal vein (80%) (Tygstrup *et al.* 1962). There is also superficial and deep lymph drainage.

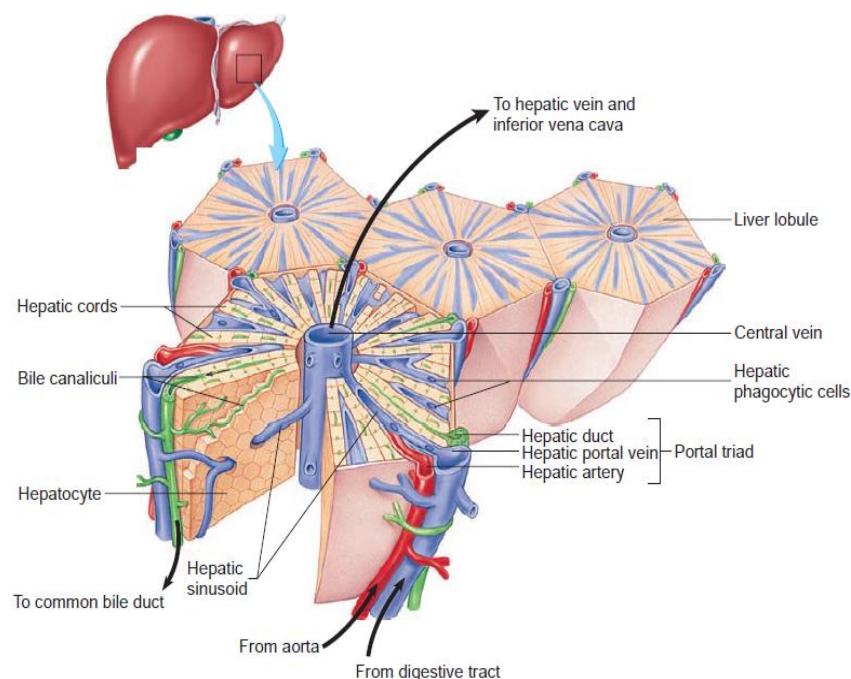


Figure 1.1 Diagram of liver architecture (Seeley *et al.* 2008).

1.1.2. Liver microscopy

The liver lobule is formed by parenchymal and nonparenchymal cells. Hepatocytes and cholangiocytes are two major components of liver epithelia (Lee 2008). Hepatocytes (HCs), parenchymal cells, form almost 80% of the total liver volume and 60% of the total number of liver cells. The typical hepatocyte forms a cubical cell of 15 µm sides. Mammalian HCs are normally characterized by a polyploidy, and 30-40% of HCs in human adults are polyploidy (tetrapolyploid and other degrees) with dispersed chromatin and prominent nucleoli (Celton-Morizur *et al.* 2010). Hepatocyte turnover in the normal adult liver is slow — the life span of a HC ranges from 200 to 400 days in mice and rats (Malato *et al.* 2011). The HCs are separated from the sinusoids by the space of Disse. In addition, the HCs contain thousands of enzymes essential to perform vital metabolic functions, e.g. maintenance of glucose, amino acid, ammonia and bicarbonate homeostasis in the body, the synthesis of most plasma proteins, the storage and processing of signal molecules, bile salt excretion and, last but not least, they participate in the acute phase reaction (Dufour and Clavien 2005).

Nonparenchymal liver cells, which contribute to only 6.5% to the liver volume but 40% of total liver cells, are localized in the sinusoidal compartment of the tissue. Of these cells, cholangiocytes, sinusoidal endothelial cells (SECs), Kupffer cells (KCs), hepatic stellate cells (HSCs, formerly called Ito cells), and natural killer lymphocytes (Kmiec 2001). Endothelial cells, fat-storing cells, and parenchymal cells are sessile cells. In contrast, KCs and pit cells seem to be mobile cells and adhere to the endothelial lining.

Cholangiocytes (biliary epithelial cells) are epithelial cells that line the intra- and extrahepatic ducts of the biliary tree (Tabibian *et al.* 2013). Three percent of the total liver mass is composed of cholangiocytes (Alpini *et al.* 2002). The primary physiological function of cholangiocytes is the modification of bile of canalicular origin and drainage of bile from the liver. They participate also in the detoxification of xenobiotics (Wise *et al.* 2008). Cholangiocytes are also targets in several human diseases including primary sclerosing cholangitis, primary biliary cirrhosis (PBC), IgG4 autoimmune cholangitis, and may lead to cholangiocarcinoma (Lee 2008). SECs constitute the sinusoidal wall of the hepatic sinusoid. They perform an important

filtration function due to the presence of small fenestrations that allow free diffusion of many substances that are smaller than chylomicrons between the blood and the hepatocyte surface. Hepatic sinusoidal lining cells have a huge endocytic capacity for many ligands including glycoproteins, components of the extracellular matrix (such as hyaluronate and proteoglycan), immune complexes and others (Saile *et al.* 1999). They are also active in the secretion of cytokines, endothelin-1 and nitric oxide (Kmiec 2001). SECs are vital in the development of fibrosis in chronic liver disease (Saile *et al.* 1999).

KCs are resident macrophages, which adhere to the endothelial lining, and are preferentially located in the periportal sinusoids. Structurally, KCs mostly show an abundant clear cytoplasm which often contains lysosomes. They present as irregular cell coat, wormlike structures, and fuzzy-coated vacuoles (Wisse 1974). The intrasinusoidal localization is compatible with the pronounced endocytic and phagocytic capacity of tissue macrophages which are in constant contact with gut-derived particulate materials and soluble bacterial products. Hepatic macrophages secrete potent mediators of the inflammatory response (reactive oxygen species (ROS), eicosanoids, nitric oxide, carbon monoxide, tumor necrosis factor alpha (TNF- α), and other cytokines) and thus control the early phase of liver inflammation, playing an important role in the innate immune defense. Apart from typical macrophage activities, KCs also play an important role in the clearance of senescent and damaged erythrocytes (Kmiec 2001).

1.2. Liver physiology

The liver is considered as the largest exocrine gland, i.e. liver cells produce the bile which is transported via hepatic bile duct to the gallbladder and via the ductus choledochus to the duodenum. Liver functions arise from a collective physiology of its cells. The liver is central to a multitude of physiologic functions, including (Seeley *et al.* 2008):

- Clearance of damaged red blood cells and bacteria by phagocytosis
- Synthesis of its own proteins and secreted plasma proteins such as albumin, globulin, protein C, insulin-like growth factor, clotting factors etc.
- Biotransformation of toxins, hormones and drugs
- Detoxification of ammonia by converting it into urea

- Vitamin and mineral storage
- Nutrient management involving the carbohydrate, fat and protein metabolism

1.3. Liver pathophysiology

There are many types of liver disease, the most common of which are viral hepatitis, alcoholic liver disease, nonalcoholic fatty liver disease (NAFLD), autoimmune hepatitis and others which may progress to cirrhosis and ultimately primary liver cancer. The field of interest in this study is the NAFLD.

1.3.1. Nonalcoholic fatty liver disease (NAFLD)

The NAFLD is a disease of globally increasing prevalence. It is defined as hepatic fat content exceeding 5% of liver weight (Garg and Misra 2002). NAFLD is closely associated with the metabolic syndrome, which consists of a constellation of insulin resistance (IR), central obesity (excessive fat around the abdomen), hypertension and dyslipidemia (Marchesini *et al.* 2003). For this reason, NAFLD and its progressive disease subtype nonalcoholic steatohepatitis (NASH) have been regarded as hepatic manifestation of the metabolic syndrome (Marchesini *et al.* 2001; Ong and Younossi 2007). It is characterized by hepatic steatosis in the absence of a history of significant alcohol use or other known liver disease (Kleiner *et al.* 2005). Physiologically, IR is a condition where higher (than normal) insulin concentrations are needed to achieve normal metabolic responses or when normal insulin concentrations fail to achieve a normal metabolic response (Kahn 1978).

To date, in the majority of patients, fatty liver is attributed either to "excessive" alcohol consumption, i.e. alcoholic fatty liver disease (AFLD), or to overweight/obesity (in most cases), i.e. NAFLD (Ekstedt *et al.* 2009). When other known causes of steatosis, such as certain drugs and toxins, have been excluded, the cut-off level for what is considered to be tolerable alcohol consumption ranging from abstinence (Diehl *et al.* 1988) to, most commonly, 20 g/day, is used to differentiate between AFLD and NAFLD (McCullough 2004).

The spectrum of NAFLD ranges from simple steatosis, whereby fat is abnormally accumulated in hepatocytes, to NASH, fibrosis, cirrhosis, which ultimately may lead to hepatocellular carcinoma (Sanyal 2011). Several studies suggest that the

accumulation of fat in the liver is benign. However, recently it has been shown that fatty livers are more vulnerable to progress to the later stages of the disease (e.g. NASH, fibrosis) (Figure 1.2) (Adams *et al.* 2005). The prevalence of NAFLD rises from 10 - 30%, while in the obese population; it is increased to 75–92% (Angulo 2002). Clinical relevance of NAFLD indicates that 20-30% of patients of NAFLD will develop NASH. Importantly, up to 20% of patients have long-standing NASH and may develop fibrosis, cirrhosis, or even hepatocellular carcinoma over their lifetime (Figure 1.2) (Adams *et al.* 2005; Edmison and Mccullough 2007; Ekstedt *et al.* 2006). Hence, on the basis of the U.S. population in the year 2000, an estimated 30.1 million obese adults in this country may have steatosis, and about 8.6 million may have steatohepatitis (Angulo 2002).

1.3.1.1. Pathogenesis of NAFLD

The nonalcohol related causes of NAFLD can be nutritional, due to drugs (medications), inborn metabolic disorders and others. During the 20th century, an extraordinary change in the pattern of caloric availability occurred in Western societies, which together with a more sedentary lifestyle has led to a state of chronic overnutrition (Neel 1999).

1.3.1.1.1. Fat metabolism in the liver

Dietary fats (macronutrient) are digested in the intestine and lipolytic products cross into the enterocyte. In the enterocytes, triglyceride (TG), cholesterol, phospholipids, and apolipoproteins are packaged into chylomicrons which enter the lymph system and then the venous circulation. The free fatty acids (FFAs) pool in the liver arises from hepatic *de novo* synthesis or from the released FFAs as a result of lipolysis in adipose tissue (the blood delivers these FFAs to the liver).

Depending on the energy state, fatty acids are either stored as TG or they undergo β -oxidation in the mitochondria or peroxisomes of the HCs. The excess fatty acids are converted to TG for storage or are transported into the circulation by very low density lipoprotein (VLDL). *De novo* liver lipogenesis only contributes to 8% in the feeding state (4% in the fasting state) of the fatty acids incorporated into the VLDL particle, whereas adipose tissue contributes to 44%, chylomicrons to 15%, and dietary acids to 10% (Barrows and Parks 2006).

1.3.1.1.2. Accumulation of fat in the liver

The primary metabolic abnormalities leading to TG retention in the HCs are not well understood, but they possibly include alterations in the uptake pathways, synthesis (*de novo* lipogenesis), degradation (β -oxidation), and/or secretion and exportation of the hepatic lipid resulting from IR (Charlton *et al.* 2002; Donnelly *et al.* 2005).

1.3.1.1.3. Transition from fat accumulation into inflammation and fibrosis

Fat accumulation in HCs has been regarded to be benign. The reason why a fatty liver progresses to develop inflammation and/or fibrosis, i.e. NASH, which is considered as the most violent form of NAFLD, is not fully understood. The development and progression of NAFLD to NASH occurs via a “two-hit” process involving the interaction of genetic and environment factors (Carniel-Haggai *et al.* 2005; Day 2002; Day and James 1998), which implicate steatosis as the first hit, increasing the sensitivity of the liver to secondary triggers, such as cytokines, mitochondrial dysfunction, lipotoxicity, oxidative stress and lipid peroxidation. IR, which is the main driving cause of liver steatosis, is also proposed as a transition factor from liver steatosis to steatohepatitis (Bugianesi *et al.* 2005). It induces higher hepatic glucose output and lipolysis, whereas steatosis is exacerbated to NASH by higher amounts of circulating FFAs released from white adipose tissue (Tordjman *et al.* 2008). IR and increased FFAs may both affect mitochondrial oxidation of the fatty acids causing free radical generation in HCs (Grattagliano *et al.* 2000).

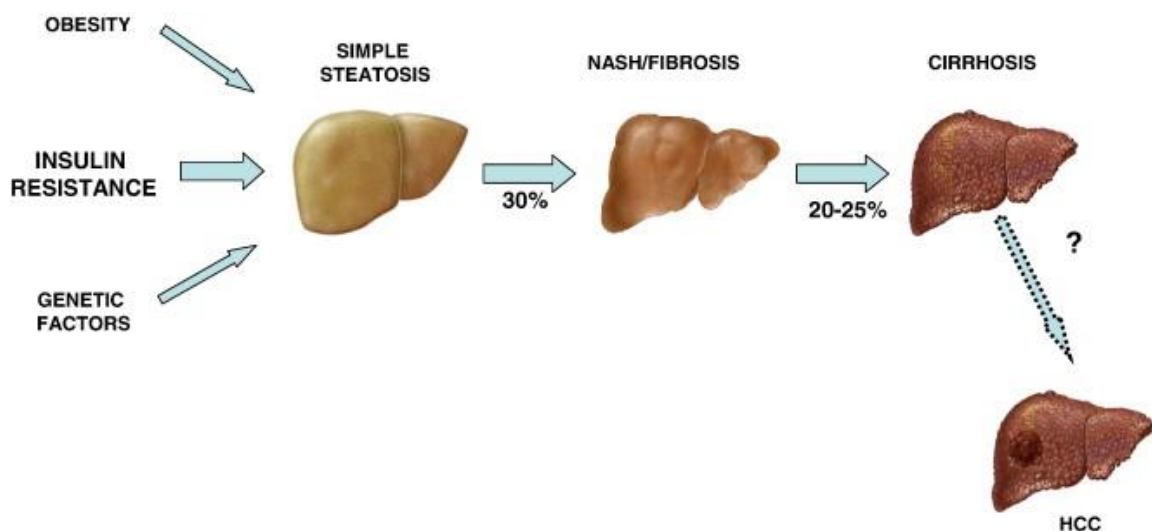


Figure 1.2 Spectrum of NAFLD. Schematic of progression of the disease. Obesity, genetic factors and IR contribute to fat deposition in the liver. Around 30% of the patients with NAFLD have NASH

which involves the presence of various degrees of inflammation and fibrosis and may progress to cirrhosis in 20–25% within 20 years. An unknown percentage of patients will develop hepatocellular carcinoma (HCC) (Trauner *et al.* 2010).

Conceptually, overnutrition in rodent models should lead to metabolic syndrome and liver steatosis and/or steatohepatitis, as in patients. However, in overfeeding conditions, rodents can adapt by modulating their intake and use of food (Baumgardner *et al.* 2008). Results from human studies indicate that patients with NAFLD are frequently overweight and suffer from IR. Both conditions have been identified to as risk factors in the development of NAFLD (Bedogni *et al.* 2005; Marchesini and Babini 2006). Furthermore, it has been suggested that the occurrence of NAFLD in humans is frequently associated with alteration of the intestinal barrier function (Miele *et al.* 2009). In line with these findings, results from animal models suggest that an increased translocation of bacterial endotoxin may induce lipid peroxidation in the liver, subsequently leading to an induction of TNF α (Bergheim *et al.* 2008). Furthermore, the role of the gut microbiota and other new mechanisms in the development of NAFLD have recently been discovered (Podrini *et al.* 2013).

1.3.1.2. Assessment of NAFLD

Most patients with nonalcoholic fatty liver disease have no symptoms or signs of liver disease at the time of diagnosis, although many patients report fatigue or malaise and a sensation of fullness or discomfort on the right side of the upper abdomen (Angulo 2002). Up to 56% of NALFD patients present obesity and hepatomegaly in the physical examination (De Lusong *et al.* 2008; Paschos and Paletas 2009). Other reports suggest that hepatomegaly is the only physical finding in 75% of the cases, but it is not easy to detect it owing to the high prevalence of obesity in NAFLD patients (Angulo 2002).

In general, NAFLD is linked with metabolic syndrome including visceral obesity, IR, type II diabetes, dyslipidemia, and hypertension (Vanni *et al.* 2010). Circulating alanine aminotransferase (ALT) and aspartate transaminase (AST) are indicative of hepatocyte injury and present in very low concentrations in the circulation of healthy individuals (Yuzer *et al.* 2009). On contrast, most of patients with NAFLD are usually

clinically asymptomatic, while their serum transaminases activities are elevated, most frequently serum ALT (Table 1.1) ([Ekstedt et al. 2006](#); [Yu and Keeffe 2003](#)).

Table 1.1 Noninvasive predictors of NASH in human beings ([Mauss et al. 2012a](#))

HAIR index (hypertension; ALT >40 U/L; insulin resistance)

≥2 are 80% sensitive, 89% specific for NASH

BAAT index (BMI >28; Age >50 years; ALT >2x UNL; increased TGs)

≤1 has 100% negative predictive value for NASH

BMI: body mass index, TG: triglycerides, UNL: upper normal limit

While ultrasound, computerized tomography (CT) and magnetic resonance imaging (MRI) can detect liver steatosis, these methods cannot differentiate simple steatosis from NASH ([Tarasow et al. 2002](#)) and none of them has a capacity to detect fibrosis. For this reason, (percutaneous) liver biopsy remains the "gold standard" in the diagnosis of the pathology with two main limitations: technical issues (due to the invasive procedure) and the very limited size of the biopsy specimen with respect to histological heterogeneity ([Bravo et al. 2001](#)). In addition, an ethical perspective exists as human liver biopsy is not performed casually owing to its invasiveness. This has contributed to the delay in clarification of the pathological details of NASH ([Semba et al. 2013](#)).

There are currently several methods available for obtaining liver tissue: percutaneous biopsy, laparoscopic biopsy and fine-needle aspiration. As a result of its invasive nature, liver biopsy can cause serious complications. In a French prospective study, severe complications were observed in about 0.6% of the patients ([Cadranel et al. 2000](#)). Complications include intraperitoneal hemorrhage, mild to severe biliary ascites, transient bacteremia and injury of gallbladder, kidney and lungs ([Bravo et al. 2001](#)). In addition, hospitalization due to complications resulting from a liver biopsy occurs in 1 - 3 % of patients. Whether the use of ultrasonography to guide the biopsy can lower the complication rates or may provide a higher diagnostic yield, is still debated ([Bravo et al. 2001](#)).

Ultrasonography of the liver is safe and relatively inexpensive ([Torres and Harrison 2008](#)). Fatty infiltration of the liver produces an increased echogenicity when

compared to the echogenicity of the kidneys. The increased echogenicity is due to the fact that fat attenuates ultrasound more than normal liver parenchyma (Quinn and Gosink 1985). Therefore, when used in prevalence studies, ultrasonography underestimates the prevalence of fatty liver (Saadeh *et al.* 2002). Interestingly, there is a noninvasive marker to assess the fibrosis: fibroscan and (transient) elastography. It works like ultrasound and gives a number for determining a fibrotic score (Sandrin *et al.* 2003).

1.3.1.3. Histopathology of NAFLD

Histologically, steatosis is defined as an increase of fat content in hepatocytes (Attar and Van Thiel 2013). There are different scores or grades of steatosis assessed in liver biopsies via a morphological semiquantitative approach. For example, the degree of fatty infiltration in NAFLD is graded according to the percentage of HCs with fat deposits: mild steatosis involves less than 30% HCs, moderate NAFLD up to 60%, and severe NAFLD above 60% (Ploeg *et al.* 1993). It has been suggested that < 5% of HCs involved should be considered normal (Adams and Angulo 2005).

In the case of NASH, the first histological criterion is liver steatosis (usually macrovesicular and centrilobular). The second is hepatocellular ballooning, characterized by enlarged swollen HCs, with reticulated cytoplasm, denoting cellular injury with cytoskeleton alterations (Lackner *et al.* 2008). Ballooned cells are the most characteristic feature of necroinflammation and hepatocellular injury in NAFLD, and they are often associated with steatotic perivenular HCs. Importantly, hepatocellular ballooning is considered a key feature of the evolution from simple steatosis to NASH and cirrhosis (Brunt *et al.* 2004). The third feature involves lobular inflammation which is usually mild and composed of mononuclear or polymorphonuclear neutrophil (PMN) cells (or both). As the disease progresses, liver fibrosis may develop (Kleiner *et al.* 2005) (Table 1.2). Mallory bodies are occasionally seen but are not necessary for the diagnosis. The presence of these features, alone or in combination, accounts for the wide spectrum of NAFLD (Angulo 2002). A finding of fibrosis in NAFLD suggests more advanced and severe liver injury (Angulo 2002), while steatosis and hepatocellular ballooning regress as the fibrosis stage progresses. In some patients with cirrhosis, the features of steatosis and necroinflammatory activity may no longer be present (Bacon *et al.* 1994).

Table 1.2 NAFLD, histological classification/changes (Tilg 2004).**1. NAFL (nonalcoholic fatty liver)**

Simple steatosis	Type 1; simple fatty liver
NASH	Type 2; predominantly macrovesicular steatosis, lobular inflammation
	Type 3; additional ballooning degeneration (dying enlarged hepatocytes)
	Type 4; in addition Mallory bodies (rather periportal) fibrosis

2. AFL (alcoholic fatty liver)

Ballooning degeneration (enlarged dying hepatocytes)
Prominent infiltrate with neutrophils (rather located at Mallory bodies)
Necrotic hepatocytes, focal
Mallory bodies (rather perivenular)

1.3.1.4. Treatment

Moderate weight loss as a result of dietary and life-style modifications is the only therapy proven to be effective in NAFLD. Complete alcohol abstinence and good control of diabetes mellitus are probably also important to reduce the risk of severe liver disease in NASH (Mauss *et al.* 2012). Vitamin E, metformin, rosiglitazone and lipid-lowering agents (e.g. statin (Merat *et al.* 2003)) have yielded promising results, such as improvement in values of the liver-tests as well as histological findings in the patients. However, these medications require further evaluation in carefully controlled clinical trials (Angulo 2002). Avoiding the extensive consumption of fast food and fructose-enriched foods and more physical exercises are some recommendations given to lessen the disease occurrence.

1.3.1.5. Animal models for NAFLD

Various animal models have been established to investigate the disease. Existing models of NAFLD/NASH have several disadvantages in the reproduction of complete features of NAFLD when compared to humans. For example, a possible model of steatohepatitis induction (with or without fibrosis) failed to provide features of the metabolic syndrome. In contrast, reproduction of the metabolic syndrome was successful, yet with incomplete histological features of NASH (Charlton *et al.* 2011). Although there are small animal platforms that summarize some of the histological features of simple steatosis, only some of them are NASH models with consistent hepatocellular ballooning and progressive fibrosis, physiologically reproducing a

metabolic profile of the human condition ([Charlton et al. 2011](#)). Thus, a representative model is required to study the pathogenesis of NAFLD, specifically the progression from simple steatosis to NASH.

Of the genetically engineered models, the obese Zucker fatty rat (ZF *fa/fa*), whose defective leptin receptor leads to a poor binding affinity for its ligand, develops obesity, hyperphagia, IR and hypertriglyceridemia ([Gary-Bobo et al. 2007](#)). A more recent overnutrition-based model like the fast food diet mouse model has demonstrated substantial metabolic similarity to humans with NAFLD type I and NASH, but it incompletely reproduces the histological features of NASH ([Shiri-Sverdlov et al. 2006](#)). For instance, no macrosteatosis, HCs ballooning, or fibrosis were not found, instead only CD68⁺ cells were present in the liver tissues. The *ob/ob* mouse develops obesity but it is leptin-deficient and lacks the inflammatory and fibrosis components of NASH ([Leclercq et al. 2002](#)). Furthermore, a model of a high-fat diet in male C57BL/6J mice led to the development of features of the metabolic syndrome and steatohepatitis but only mild fibrosis after 50 wks ([Ito et al. 2007](#)). The methionine and choline deficient diet was also used to induce NASH in C57BL/6 mice. This model, however, does not mimic human physiological condition, and the metabolic profile is opposite to the typical features of human NASH, as well ([Takahashi et al. 2012](#)).

The addition of fructose to a diet high in saturated fat and cholesterol has been proposed to reproduce all of the features of NASH, including ballooning in large animals, which is also a typical feature of the diet of humans with NASH ([Charlton et al. 2011](#)). However, LCN2 was not investigated in that study. Since fructose is included in commercial/fast food as well as juice beverages and as it has been suggested to induce the most NAFLD manifestations noticed in humans, this study selected fructose as an inducer for metabolic syndrome and NAFLD.

1.4. Fructose

1.4.1. Definition

D-fructose is a simple sugar (monosaccharide) found naturally in fruit, honey, sucrose, and vegetables. Normally, it is metabolized in HCs into glucose, glycogen, and lipid. Industrially, fructose is frequently found in soft drinks, juice beverages, and it

is integrated into convenient pre-packaged foods (Akar *et al.* 2012). The five-ring structure (Figure 1.3) has more sweetness than the six-ring structure which results after heating.

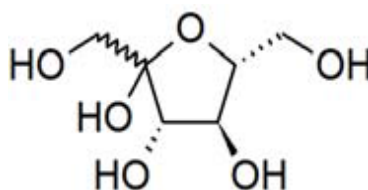


Figure 1.3 The cyclic (5-ring) structure of D-fructose according to IUPAC.

1.4.2. Fructose metabolism

Fructose is transported from the small intestine (enterocytes) via a specific glucose transporter, GLUT5 and exits actively or facilitated (or both) via GLUT2 and GLUT5 transporters (Wiernsperger *et al.* 2010). Upon intestinal absorption, both fructose and glucose are delivered via the portal vein to the liver. It is believed that the ability of the liver to metabolize high doses of fructose is responsible for the disruption in energy stores and fuel metabolism (Commerford *et al.* 2002; Daly *et al.* 1997). There are marked variations in estimates of blood fructose concentrations arising from differences in methods of collection and analysis (Douard and Ferraris 2008). Serum fructose concentration was estimated to be 0.008 mM in normal humans, while plasma fructose was 0.030 mM. These variations can also arise from differences in fructose consumption, which is a potent regulator of intestinal fructose transport (Douard and Ferraris 2008).

In contrast to glucose, the phosphorylated product, fructose 1-P, is directly metabolized into glyceraldehyde and dihydroxyacetone phosphate by aldolase B (EC 4.1.2.13) independent of insulin. Thus, fructose can then readily converge with the glycolytic/gluconeogenic pathways at the level of triose phosphate (Van Den Berghe 1986) (Figure 1.4). Fructose catabolism is able to by-pass the main regulatory step of glycolysis: the conversion of glucose 6-P to fructose 1,6P₂, controlled by phosphofructokinase (EC 2.7.1.11). Hence, while the glucose metabolism is negatively regulated by phosphofructokinase, which, in turn, is allosterically inhibited

associated diseases such as type 2 diabetes and fatty liver (Bantle 2009). The exposure of the liver to large quantities of fructose (to date 85–100 grams per day) leads to rapid stimulation of lipogenesis and TG accumulation. The latter may contribute in reduced insulin sensitivity and hepatic IR. Increased fructose consumption is associated with fibrosis severity in patients with NAFLD (Abdelmalek *et al.* 2010).

Moreover, previous studies stated that a chronic fructose intake may, at least partly, contribute to the development of the early phase of NAFLD (Cummings 1988) through mechanisms involving intestinal bacterial overgrowth and/or an increased intestinal permeability and translocation of bacterial endotoxin, and subsequent activation of KCs through a TLR-4-dependent mechanism mediated through MyD88-dependent signaling pathways (Brun *et al.* 2007; Cani *et al.* 2008). Specifically, it has been shown that MyD88 (an adapter protein involved in the Toll-like receptor signaling pathway in the innate immune response) is involved in the rapid activation of nuclear factor B (NFB) and the consequent increase of TNF- α (Velayudham *et al.* 2009). This leads to an increased formation of ROS (Zimmet *et al.* 2001) through its entering the cellular metabolism independent of insulin and results in increased *de novo* lipogenesis (Spruss *et al.* 2009). Protection of the intestinal epithelial cells against the loss of tight junction proteins (e.g. occludin), resulting either from direct or indirect effects of the chronic intake of fructose on the intestinal mucosa, seems to be a key factor (Volynets *et al.* 2010). It has been shown that bile acids may protect the liver from the onset of NAFLD.

A typical feature of fructose is the induction of hypertriglyceridemia. This is remarkably because of reduced clearance (Wiernsperger *et al.* 2010) accompanied with IR. In addition to its effects on TGs, fructose also decreases high density lipoprotein-bound cholesterol (HDL-C) levels (Wiernsperger *et al.* 2010). Furthermore, diets specifically high in fructose have been shown to contribute to a metabolic disturbance in animal models resulting in weight gain and hyperlipidemia (Kasim-Karakas *et al.* 1996).

1.4.4. Fructose and oxidative stress and lipid peroxidation

Unlike glucose, which is widely used by tissues throughout the body, fructose is primarily metabolized in the liver and it facilitates oxidative damage and lipid peroxidation (Anurag and Anuradha 2002), a process in which unsaturated lipids

become oxidatively degraded to a variety of products at sites of inflammation. The degradation of lipids occurs, whereby free ROS capture electrons from lipids in cell membranes. One of the end products of lipid peroxidation is 4-hydroxynonenal (4-HNE), a specific, stable, and highly reactive product, which exhibits a chemotactic activity toward neutrophils *in vitro* and *in vivo* (Quinn *et al.* 1995). Apoptosis is also induced by the products of lipid peroxidation (Ribeiro *et al.* 2004). In mice, a chronic moderate fructose intake (e.g. 30% fructose solution as only fluid source) was shown to be associated with an increased translocation of lipopolysaccharide (LPS, endotoxin) from the intestine into the portal vein as a result of bacterial overgrowth and increased intestinal permeability. This may cause a further activation of hepatic Kupffer cells and formation of ROS in the liver and an NF- κ B-dependent induction of hepatic TNF- α expression (Spruss *et al.* 2009).

The metabolic process produces acetaldehyde, a toxic and reactive compound that impairs mitochondrial function leading to increases in ROS production (Dey and Cederbaum 2006). ROS is important for certain cellular functions, e.g. it can be cytotoxic to foreign bacteria (Arteel 2003). In addition, ROS production is detrimental when excessive amounts are produced leading to tissue damage. ROS can act as a second messenger and induce apoptosis, in part, by signaling through the mitogen-activated protein kinase (MAPK) pathway (Lu *et al.* 2007). Increases in ROS production also cause necrotic cell death by depleting endogenous antioxidants (Wu and Cederbaum 2001). Oxidative stress and 4-HNE induce apoptosis in HSCs by increasing the expression of apoptotic regulatory proteins and adaptors, such as Fas ligand and FasL receptor, caspase-2 (casp 2), casp 3 and Bax (De Villiers *et al.* 2007). Apoptosis, also known as programmed cell death, is a cascade of reactions culminating in a non-inflammatory elimination of a cell without disrupting the surrounding tissue and maintaining homeostasis (Henson and Hume 2006).

1.5. Lipocalin-2

1.5.1. Definition

Previous reports studied the role of lipocalin-2 (LCN2) in inflammation and in metabolic syndrome. LCN2, a neutrophil gelatinase-associated lipocalin (NGAL), is a member of the lipocalin subfamily (25-kDa) known as secretory glycoprotein initially

identified from human neutrophils (Chen *et al.* 2005) and cells and tissues that are exposed to microorganisms e.g. the gastrointestinal tract (Cowland and Borregaard 1997). The lipocalin family in general plays the role of transporters with various functions, e.g. regulation of immune responses (Yang *et al.* 2002). By forming a cup-shaped hydrophobic cavity; lipocalins bind and transport a wide variety of small lipophilic substances, such as retinoids, arachidonic acid, iron, lipids and various steroids (Flower 1996).

In addition, LCN2 (Figure 1.5) is a pleiotropic protein which presents abundantly in the circulation, and it has also been detected in adipocytes and macrophages (Zhang *et al.* 2008). Immunologically, LCN2 plays a key role in implementing the acute-phase response (Liu and Nilsen-Hamilton 1995), and it also has a role in the regulation of apoptosis (Devireddy *et al.* 2001). It was demonstrated that the liver is the main source of serum LCN2, which is highly expressed in the turpentine-oil model (Borkham-Kamphorst *et al.* 2011; Sultan *et al.* 2013; Sultan *et al.* 2012). It preferably binds to lipophilic substances and plays a role in iron metabolism, regulates hematopoiesis, modulates inflammatory processes and restoration of tissue homeostasis following LPS-induced injury (Borkham-Kamphorst *et al.* 2011).

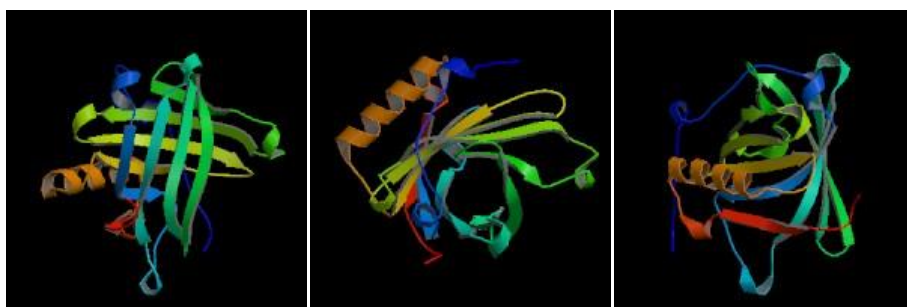


Figure 1.5 Lipocalin/ cytosolic fatty-acid binding protein family (www.ncRNA.org (rat gene *Lcn2* (X13295) description and page index)).

Interestingly, LCN2 has been characterized as a critical regulator of energy metabolism, glucose and lipid homeostasis, and IR in *Lcn2*-deficient mice (Guo *et al.* 2010). It has also been reported that LCN2 suppression attenuates obesity-induced IR by modulating 12-lipoxygenase and TNF- α levels in adipose tissue (Law *et al.* 2010). In humans, elevated serum LCN2 concentration was also observed among

diabetic patients and this increase could be reversed by the insulin-sensitizing drug rosiglitazone (Wang *et al.* 2007). Recent research showed that LCN2 was provoked in a rat model after *in vivo* liver γ -irradiation in response to the development of ROS (Sultan *et al.* 2013).

LCN2 has also been shown to be a bacteriostatic agent capable of binding iron in the form of siderophores by a non-heme compound which consequently sequesters it from inflammation and infection sites (Berger *et al.* 2006; Flo *et al.* 2004). Promoter regions of *Lcn2* and its murine homolog 24p3 have been found to contain consensus sequences for several different transcription factors, including NF- κ B, C/EBP and cAMP response element-binding protein (CREB) (Cowland *et al.* 2006).

1.5.2. LCN2, oxidative stress and lipid peroxidation

Increased *Lcn2* gene expression has been found in oxidative stress induced by chemicals such as diethylnitrosamine, which is a major producer of ROS (Lechner *et al.* 2001). Several studies have reported an LCN2 expression under stress conditions to be caused by free radicals, such as inflammation, toxicity, chronic kidney disease, myocardial infarction and burn injury, infections and several types of cancers (Mishra *et al.* 2006). In the absence of cellular stress, LCN2 maintains a low steady-state level and exerts very little if any effect on the fate of tissue (Sultan *et al.* 2012). *Lcn2* gene expression has been studied both in *Lcn2*^{-/-} models and in several NAFLD models, such as *ob/ob* and *db/db* (Jin *et al.* 2011; Jun *et al.* 2011; Law *et al.* 2010; Wang *et al.* 2007). While an important role for *Lcn2* gene expression in inflammatory and glucose metabolism processes could be identified, LCN2 was not previously evaluated in (high)fructose induced NASH. In addition, LCN2 protein localization in the cell population of the liver is controversially discussed, and the LCN2-expressing cell type in the liver is still being debated.

1.5.3. LCN2 receptor

The LCN2/NGAL/24p3 receptor (24p3-R) is poorly understood and incompletely identified in the liver to date. In rodent distal nephron, the 24p3-R is expressed where it mediates protein endocytosis (Langelueddecke *et al.* 2013). Therefore, state-of-the-art methods are urgently required to pursue and understand the function and localization of LCN2 in the liver.

1.6. Study Motivations

While ultrasonography, CT scan and MRI are reliable and sensitive methods for detecting steatosis, but the grade and stage of the disease can be determined only with a liver biopsy (Angulo 2007). Instead, liver biopsy is needed to detect the switch from simple steatosis to NASH. However, this is an invasive (puncture) procedure with a risk of bleeding and injury to gallbladder, lungs and kidney. Thus, research for noninvasive (serological) diagnostic markers is required. The pathogenesis of NAFLD remains unknown. *Lcn2* gene expression has been studied in *Lcn2*^{-/-} models and in several NAFLD models, such as *db/db*, *ob/ob*, ZF *fa/fa*, etc. which do not greatly mimic the physiological and/or histological features of NAFLD seen in humans. In addition, the following technical aspects have to be taken into account prior to establishing a suitable animal model:

- Reproducibility.
- Commercial availability.
- Time schedule and feeding in accordance with animal welfare.
- Costs.
- The food composition.

Some of the available animal models showed the feature of NAFLD after 50 wks. Hence, there is a need for an animal model that mimics the condition seen in human NAFLD and fits with these technical aspects.

Since fructose is included in commercial/fast food and juice beverages and as it was suggested to form most of the NAFLD manifestations noted in humans, fructose was selected as an inducer for metabolic syndrome and NAFL (\geq type 2) in this study. LCN2 is a known positive acute phase protein, which is synthesized in stress conditions, and which may be helpful to distinguish between simple steatosis and NASH.

1.7. Research Hypotheses and Aims

The present study focused on the liver as it plays a pivotal role in inflammation and the homeostasis of lipid, carbohydrate and other metabolisms. NAFLD is a metabolic liver disease with increasing prevalence. The availability of more representative and differentiated NAFLD models could greatly facilitate studies on the pathobiology of different NAFLD types, such as simple steatosis and NASH, as well as investigations on potential interventions to avoid the latest stages of the disease.

Hypotheses

1. Conditions of low physical activity and overnutrition with a high caloric intake of 35% kcal fat could lead to simple steatosis.
2. Chronic feeding of rats with a fructose-enriched diet will lead to NASH which might be similar to the physiological milieu seen in humans.
3. Fructose-caused oxidative stress and inflammation could trigger hepatic LCN2 expression in nutritionally induced rat fatty liver.
4. LCN2 may serve as a biomarker for NASH.

The aims of the present study are

- i. to develop simple steatosis and NASH models
- ii. to compare the features of these models with what is known about the human liver pathology and other NAFLD parameters
- iii. to explore and compare the expression of LCN2 and other parameters in these models, and to assess whether LCN2 may serve as a diagnostic indicator for NASH.
- iv. to investigate the potential mechanism(s) of the production and possible role(s) of LCN2 in currently studied models.

2. MATERIALS AND METHODS

2.1. Materials

2.1.1. Chemicals

The chemicals that were used in this study are listed in Table 2.1.

Table 2.1 List of the chemicals and materials that were used in this study.

Provider	Chemical
Applichem, Darmstadt, Germany	3-[(3-Cholamidopropyl)-dimethylammonio]-1-propanesulfonate (CHAPS), Glycine, Methanol, Glacial acetic acid, Acetonitrile
Carl Roth GmbH & Co. KG, Karlsruhe, Germany	Bromophenol blue, Glycerine, Tris, Sodium chloride, Sodium acetate, Sodium hydroxide
Sigma-Aldrich Chemie, Hamburg, Germany	Urea, Thiourea, DL-Dithiothreitol (DDT), Phenylmethylsulfonyl fluoride (PMSF), HEPES sodium salt, Nile red, Sodium dodecyl sulphate (SDS), Tritin-X 100, Nonidet NP-40
Merck KGaA, Darmstadt, Germany	Phosphatase inhibitor cocktail 1 and 2, Iodoacetamide, Sodium acetate, Ethanol, Formaldehyde, Sodium carbonate, β -mercaptoethanol, Kaiser's glycerol gelatine, Mayer's Hemalum solution, AQUATEX
Bio-Rad, München, Germany	Ampholytes Bio-Lyte [®] 3/10, ReadyStrip [™] Immobilized pH gradient strip (IPG), Phosphate buffered saline (PBS), Bio Rad protein assay kit, Tween 20
Serva Electrophoresis GmbH, Heidelberg, Germany	Bis/acrylamid, 2 mg/mL Albumin bovine Fraction V, Ponceau S
Bio-Rad, USA	Mineral oil
Invitrogen, Ltd., Paisley, UK	Pro-Q [®] Diamond Phosphoprotein Gel Stain Platinum SYBR [®] Green Universal qPCR Master Mix (Applied Biosystems [®]) Reverse Transcriptase (RT) and 1x RT buffer Western blot Transfer and MOPS Running buffers NuPAGE [®] Novex 4-12% Bis-Tris Gels Rainbow [™] coloured-protein marker Percoll-gradient solution
Merial GmbH, Hallbergmoos, Germany	Pentobarbital sodium (Narcoren [®]) anaesthesia

Millipore, MA. USA	Accutase, Leptin, Radioimmunoassay (RIA) kit
Lonza Braine SA, Braine-l'Alleud, Belgien	Penicillin/streptomycin, RPMI
BioAssay Systems, EnzyChrom™ Kit, Hayward, USA	Triglyceride (TG) assay
Bioporto® immunoassay kit, Denmark	LCN2 ELISA
Amersham Biosciences, UK	Ficoll-Paque™ PLUS
Biochrom, Berlin, Germany	Trypan blue

2.1.2. Equipment

The technical equipment (apparatus) and the companies were listed in Table 2.2.

Table 2.2 The technical equipment that were utilized in this study.

Application	Manufacturer
2-DE gel scanner	FLA-8000, Fujifilm Europe, Düsseldorf, Germany
Tissue culture cabinet: clean air	Thermo life science, Lund, Sweden
Microplate reader	Dynatech MRX, Cottbus, Germany
Homogenizer and Tissuelyser	Ultra-Turrax®, Janke & Kunkel IKA, Staufen, Germany
Sonicator	Branson Sonifier 250, Branson, USA
Microplate/Support Base	Applied Biosystems® StepOne system, MicroAmp™, Darmstadt, Germany
Epifluorescence microscope IDO3, Standard 25, Axiovert 200M	Zeiss, Göttingen, Germany
Film processor machine	Konica SRX-101A, Japan
Centrifuge Mikro Rapid	Hettich, Tuttlingen, Germany
Centrifuge K, Rotixa	Sigma, Osterode am Harz, Germany
pH-Meter CG841	Schott, Mainz, Germany
PROTEAN IEF Cell first dimensional IEF	Bio-Rad, Munich, Germany
Protean II xi Cell, 2-DE gel electrophoresis	Bio-Rad, Munich, Germany
Gel dryer	Model 583, Bio-Rad
Western blot apparatus: XCell SureLock® Mini-Cell system	Invitrogen, Ltd., Paisley, UK
Light microscope (with an internal digital camera)	Olympus BX43, Hamburg, Germany (Olympus DP21)

2.1.3. Antibodies

The antibodies that were used for Western blotting (WB) and immunofluorescence (IF) staining are listed in Table 2.3.

Table 2.3 List of the antibodies that were used in this study.

Name	Clone	Species	Company	dilution	Use
HNE	PC	Rabbit	Abcam	1:100	WB
LCN2	MC	Mouse	Novus biologicals	1:250	WB
	PC	Goat	R&D	1:100	IF
GRP-78	PC	Rabbit	Novus Biocompa	1:800	WB
CD14	PC	Rabbit	Antibodies-online	1:700	WB
Casp 9	PC	Rabbit	Chemicon international	1:1200	WB
Cyt c	MC	Mouse	Millipore	1:600	WB
PGC-1 α	PC	Goat	Abcam	1:200	WB
I κ B1 α	MC	Rabbit	Abcam	1:10000	WB
β -actin	MC	Mouse	Sigma-Aldrich	1:5000	WB
MPO	PC	Rabbit	Dako, A0398	1:100	IF
ED1	MC	Mouse	AbD Serotec	1:100	IF
Anti-rabbit-HRP	PC	Swine	Dako	1:1500	WB
Anti-mouse-HRP	PC	Rabbit	Dako	1:1500	WB
AlexaFluor-555-Conjugated anti-goat IgG		Donkey	Invitrogen	1:500	IF
AlexaFluor-488 conjugated anti-mouse or anti-rabbit IgG		Donkey	Invitrogen	1:500	IF

MC: monoclonal, PC: polyclonal, HRP: horseradish peroxidase

2.1.4. Oligonucleotides

The forward and reverse primers for the quantification of the rat mRNA expression of the genes by quantitative Reverse-Transcription Polymerase Chain Reaction (qRT-PCR) listed are shown in Table 2.4.

Table 2.4 List of gene-specific primers used for qRT-PCR analysis.

Name	Forward 5'-3'	Reverse 5'-3'
<i>Lcn2</i>	GGAATATTCACAGCTACCCTC	TTGTTATCCTTGAGGCCAG
<i>Il-8</i>	GTGTCCCCAAGTAATGGAGAA	CGCCTACCATCTTTAAACTGC
<i>α2-m</i>	CTGTCACCTCATCCTGTTGTC	ATCTCCTTCTTCGTGTCCTG
<i>Glut5</i>	TGCAGAGCAACGATGGAGAAA	ACAGCAGCGTCAGGGTGAAG
<i>Tnf-α</i>	AAATGGGCTCCCTCTCATCAGTTC	TCTGCTTGGTGGTTTGTACGAC
<i>Mcp-1</i>	CTCACCTGCTGCTACTCATTCACT	TTCCTTATTGGGGTCAGCAC
<i>Lep-r</i>	GTTCTGGCCATCAATTCCAT	GCCCTCTGGTTGCTTTGTAT
<i>Actb</i>	ACCACCATGTACCCAGGCATT	CCACACAGAGTACTTGCCTCA
<i>Ubc</i>	CACCAAGAAGGTCAAACAGGAA	AAGACACCTCCCCATCAAACC

2.1.5. Software

The following scientific software (Table 2.5) was applied for data acquisition and analysis.

Table 2.5 List of the scientific software that were applied in this study.

Software	Application	Reference
StepOne™ Version 2.0	RT-PCR	Applied Biosystems®, Darmstadt, Germany
GraphPad Prism 5	Statistical analysis	GraphPad Software Inc. California, USA
AxioVision Rel. 4.8	Histo-localization analysis	Carl Zeiss, Jena, Germany
ImageJ 1.46s	Densitometric analysis	NIH, MD, USA
Reference Manager 12 EndNote	Insert the desired References for in-Text citations and format the bibliography at a later time	Thomson Reuters, New York, USA
Delta2D V 4.2	Analysis of 2-DE data	Decodon, Greifswald, Germany

2.2. Methods

2.2.1. *Experimental animals and diets*

Healthy male Sprague-Dawley rats (160-180 g) were used in this study. All animals were purchased from Charles River, Sulzfeld, Germany. On arrival at our facility, the rats were placed immediately in their respective experimental conditions. For house acclimatization, the rats were provided with standard chow diet and tap water for one week *ad libitum*. To facilitate measures of food intake and to promote minimal sedentary movement patterns, the rats were maintained individually in conventional cages in a 12:12 h light-dark cycle in a hygienically controlled room. Ethically, all animals received humane care within the provision of the German Law on the Protection of Animals and the institutional guidelines. All animal experiments were approved by the ethics review board and supervised by the local ethics commission (Application # 33.9-42502-04-10/0152).

2.2.2. *Fructose-containing Lieber-DeCarli diet*

The Lieber-DeCarli (LDC) diet is a nutritionally complete liquid diet that is used widely for modeling (in rodents) the pathological changes seen in human beings (Cohen *et al.* 2009). The standard diet composition for rats on the LDC diet is (in kcal) 35% fat, 17% protein, and 48% carbohydrates (Lieber and Decarli 1994). The carbohydrate source in the LDC diet is maltodextrin, while the amount of calories provided by fat is similar to that found in the typical American diet. As the amount of energy that is provided by 1 g of the LDC diet is known, about 70% kcal fructose was mixed with LDC powder, and this group was named the LDC + high fructose (L-HFr) group. Each gram of both diet categories was calibrated to provide approximately (one) energy unit.

2.2.3. *Induction of nonalcoholic fatty liver in rats*

Animals were randomly allocated (n= 4 per group/ time point) as follows: standard chow pellets (control (Co)) group, liquid Lieber-DeCarli (LDC) group, also called high-fat diet, and LDC + high (70%) fructose (L-HFr) group (Figure 2.1). Apart from the Co group, the animals did not receive additional drinking water as the liquid diets were sufficient (Wang *et al.* 2008). The animals were allowed access to a pre-weighed amount of food for 4 wks or 8 wks. The amounts of the consumed food were recorded

daily, while animal body weights (BW) were measured weekly throughout the study. The animals were deprived of any food 10 h before sacrifice.

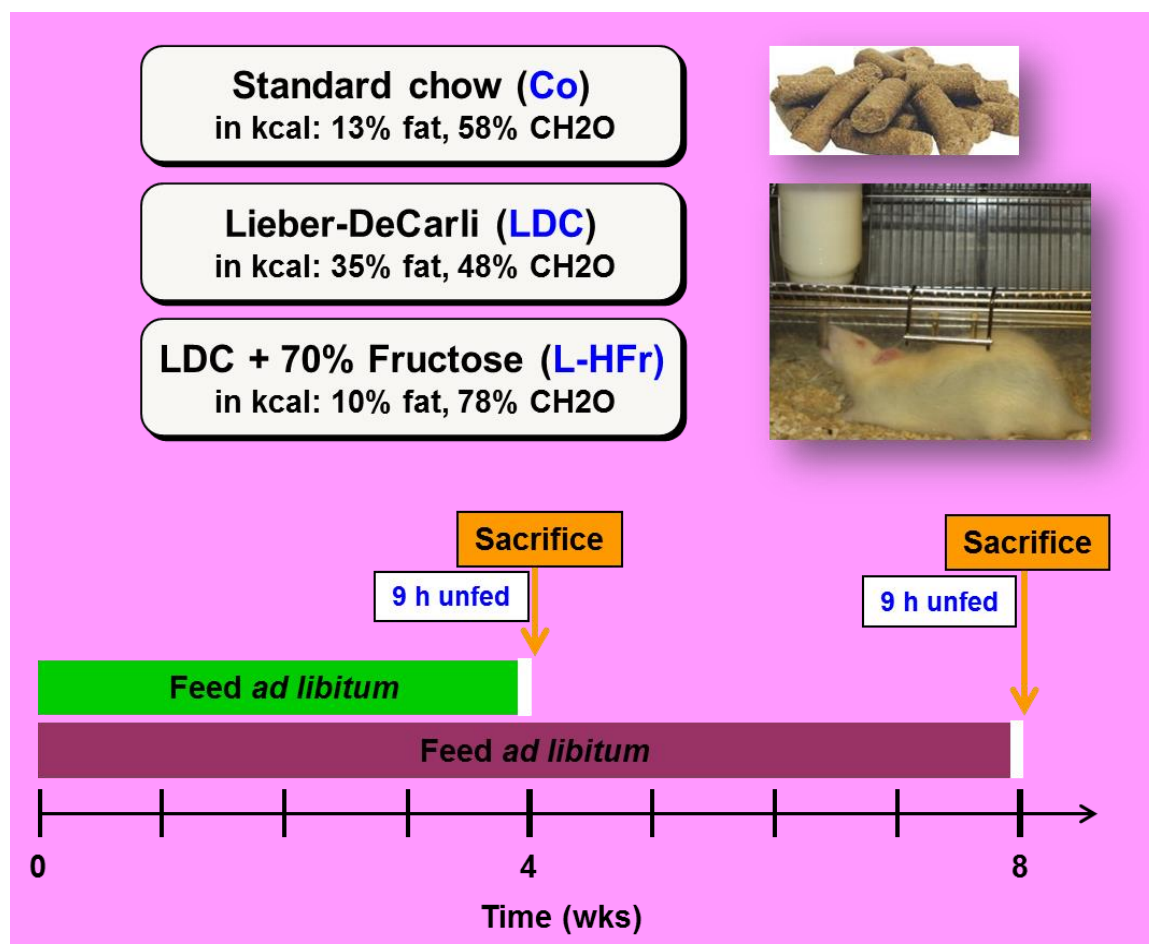


Figure 2.1 Diet categories and feeding periods.

2.2.4. Collection of blood and liver samples

After 4 wks or 8 wks, the animals were weighed and euthanized using sodium pentobarbital (Narcoren[®]) (0.2 mL per 100 g BW *i.p.*). Under deep anesthesia, the rats were subjected to laparotomy, photographed, and blood was withdrawn from the *inferior vena cava* in plain (sera) and heparinized plasma tubes. Subsequently, livers were excised, weighed, photographed, and quickly dipped in physiological saline. Next, three portions of different liver lobes of each animal were immersion-fixed (with 4:1% (v/v) neutral-buffered formaldehyde: glutaraldehyde in isotonic PBS, pH 7.4) for paraffin embedding. Alternatively, liver pieces were snap-frozen in liquid nitrogen and

stored at -80°C until use. Relative liver weights (RLW) were expressed as a percentage of the ratio of absolute liver weight in gram, divided by the total body weight (g) at the time of sacrifice multiplied by 100.

2.2.5. Histological (morphological) staining

2.2.5.1. Oil Red O

2.2.5.1.1. Principle

It is a diazo dye targets to stain the accumulated lipids (within the cells) which include fats, sterols, fat-soluble vitamins, monoglycerides, diglycerides, phospholipids, lipoproteins and others.

2.2.5.1.2. Solutions' preparation

Preparation of Oil Red O stock solution

The Oil Red O stock solution was prepared in a concentration of 5 mg/mL Oil Red O powder/ isopropanol with a magnetic shaking. This solution is stable at RT for about 3 wks.

Preparation of working solution

A 60% working solution was prepared by dilution of the stock solution with $\text{d}_2\text{H}_2\text{O}$. The solution was then double filtrated 1 h at RT.

PBS pH 7.4 buffer: 137 mmol/L sodium chloride, 2.7 mmol/L potassium chloride, 10 mmol/L disodium hydrogen phosphate, 1.76 mmol/L potassium.

2.2.5.1.3. Oil Red O staining procedure

Tissue preparation

To determine cellular lipid accumulation, liver tissue portions were fixed with 4% phosphate-buffered 4:1% formalin/glutaraldehyde for 15-20 minutes (min) at 4°C , washed for 5 min in PBS, and immersed in 10% fresh-buffered sucrose for 2-3 h and in 30% sucrose overnight. The hepatic pieces were embedded in an optimal cutting temperature medium-filled aluminum foil mold, and were successively frozen at -20°C .

Staining recipe

Liver cryosections (5 μm) were prepared from OCT-embedding medium, and stained with filtered Oil Red O working solution for 30 min at RT. Afterwards, the slides were

washed 3 times with ddH_2O , and nuclei were counterstained with hematoxylin (Mayer's Hemalum solution) for 1-2 min. Then, twice washing steps were performed by using tap H_2O ; the slides were immediately mounted with AQUATEX, allowed to dry and finally photographed by light microscope with a build-in camera.

2.2.5.2. Fluorescence-based Nile red staining

Epi-fluorescence microscopy is a technique that is used in the evaluation of fluorochrome-stained samples. As Nile red and immunofluorescence stains are based on the use of fluorescent substances, it is useful to explain the fluorescence principle briefly.

Fluorescence is a special form of luminescence, in which a photon of the same or lower energy is emitted while the molecule is returning to the ground state. A (color) substance that is able to fluoresce is called a fluorochrome. These fluorochromes have often in their structure an aromatic ring group, and they can be used to "mark" or label the desired substance, e.g. an antibody. Fluorescent dyes absorb light at certain wavelengths (λ) e.g. ultraviolet or blue and in turn emit their fluorescence energy at a longer λ , e.g. green or red. This difference in excitation and emission maxima of a fluorescent dye is called Stoke's shift, which represents the basis for fluorescence detection. As each dye has almost a distinct emission spectrum, this prosperity can be exploited for multicolor analysis using several fluorochromes simultaneously.

Fluorescence results only in a very short visible or measurable emission of light quanta, while phosphorescence can gradually release the absorbed energy over time in the visible band after excitation. The electrons return from the excited state (S1) to the original energy state (S0) very fast (10^{-9} sec). On the other hand, the phosphorescence occurs when the emission delays (lags) of min to days to S0 state. The Jablonski diagram (Figure 2.2) shows the number of possible routes by which an excited molecule can return to its ground via unstable triplet states. A rapid return results in fluorescence, while a delayed return leads phosphorescence.

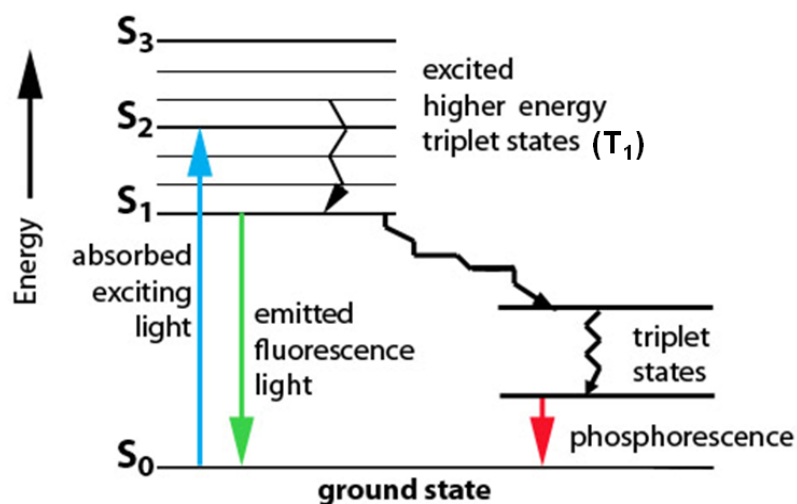


Figure 2.2 Simplified Jablonski diagram. The chain of events that lead to fluorescence and phosphorescence are shown. S₀ is the ground state; T₁ is an excited triplet state, S₁ and S₂ are excited singlet states. Straight lines represent transitions involving photons, while wavy lines represent vibrational or thermal transitions (Nery *et al.* 2010).

2.2.5.2.1. Nile red staining protocol

Fluorescent Nile red dye, 9-diethylamino-5H-benzo[α]phenoxazine-5-one, is an excellent vital and selective stain for the detection of intracellular neutral lipid droplets (e.g. TG) by fluorescence microscopy (Greenspan *et al.* 1985). Nile red does not fluoresce in aqueous or polar solutions; in contrast, it is very soluble in hydrophobic phases and excites at λ 450-560 nm, while the emission is detected at λ = 590 nm.

Hepatic cryosections (5 μ m) were stained with 4,6-diamidino-2-phenylindole (DAPI) (Molecular Probes) for 5 min, washed for 5 min with PBS. A mixture of 750 μ L of 65°C heated-Kaiser's glycerol gelatin, 250 μ L d_0 H₂O and 50 μ L of light-protected Nile red solution was added per 4 slides. Afterwards, sections were cover-slipped and allowed to shortly dry in dark, followed by fluorescence-immunodetection using an epifluorescence microscope. Microphotographs were collected accordingly.

2.2.5.3. Haematoxylin and eosin stain

Morphological changes of the liver were histologically evaluated via Haematoxylin and eosin (HE) stain. The stained liver tissues were examined for inflammation and fat degeneration. Paraffin-embedded hepatic slices of 5 μ m thickness were transversely cut into serial sections by a microtome. Sections were deparaffinized in xylene 2x (3 min), rehydrated through a graded ethanol series (100%, 96%, 80%, & 60%) and

stained automatically with haematoxylin (6 min). Subsequently, the slides were placed for 5 min under running tap water, counterstained for 2 min with eosin and washed with water. The slides were again dehydrated by immersing in ascending ethanol gradients, and finally placed in xylene until mounting. Afterwards, the slides were mounted with xylene-based media and air-dried.

The nuclei were stained blue-purple with hematoxylin, while cell cytoplasm (proteins) were nonspecifically counterstained with pink-red (eosin). A pathologist (Schaefer IM) who had no knowledge about the rats' treatments carried out the histological examination. In addition, the HE stained slides were evaluated by three different scientists by using a light microscope with an internal digital camera.

2.2.5.4. Masson's Trichrome stain

Masson's stain was used for different specific applications such as distinguishing cells from surrounding connective tissue (collagen, fibrosis, and architectural changes of liver sections). Five micrometer liver sections were used for this staining. The procedure was done according to the manufacturer's instructions. The diagnostic criteria of the fibrosis stages applied by the pathologist were according to Desmet & Scheuer (Fibrosis stage 0-4) with stage 0: no fibrosis, stage 1: minimal fibrosis, mild portal connective tissue, stage 2: mild fibrosis increased portal fibrosis with beginning extension into/affection of the hepatic lobule, stage 3: moderate portal connective tissue formation with incomplete and complete septa, and stage 4: hard for grading, numerous septa complete with the transition to cirrhosis.

2.2.6. Biochemical studies

2.2.6.1. Determination of TG content in the liver tissue

Frozen liver samples (ca. 100 mg) were homogenized in ice-cold 2 x PBS by using a TissueLyser. Tissue lipids in each sample were extracted with 2:1 methanol/chloroform, vacuum dried, and re-suspended in 50 μ L (3:2) tert-butanol + TRITON MIX (Triton x-114/ methanol (2:1)). TGs levels were colorimetrically determined using a commercially available kit. Values were normalized to the initial wet weight of liver portion and expressed as g TG/g liver.

2.2.6.2. Biochemical parameters

After an overnight (10 h) fasting, the collected rat heparinized blood was centrifuged at 3,500 xg for 15 min at 4°C. The harvested plasma samples were studied for

glucose, uric acid, urea, total cholesterol, TG, high-density lipoprotein containing cholesterol (HDL-C), and low-density lipoprotein containing cholesterol (LDL-C) concentrations by using the appropriate kits. The activities of liver transaminases (ALT and AST) were also determined in the sera by utilizing the automated systems of the central laboratory of the Department of Clinical Chemistry in University Medical Center Goettingen.

2.2.6.3. Leptin assay

Radioimmunoassay (RIA) is a sensitive technique that quantifies the concentration of certain antigens (proteins) in blood samples. Frozen (-80°C) serum specimens were thawed at RT, and the RIA kit was used for measuring leptin levels according to the manufacturer's protocol.

In brief, 300 µL assay buffer was pipetted to a non-specific binding tube, 200 µL to the reference tube, and 100 µL to the rest of tubes. Next, 100 µL of the standard and the quality controls were added in duplicate. A 100 µL of serum sample was pipetted in duplicate, followed by another 100 µL of ¹²⁵I-Rat Leptin Tracer (HPLC purified) to all tubes. Afterwards, 100 µL of rat leptin antibody was transferred to all tubes except total count tubes and non-specific binding tubes. After vortexing, samples were incubated overnight at 4°C. A 1 mL of cold precipitating reagent was added to all tubes except to the total count tubes. The tubes were vortexed and incubated for 20 min at 4°C, followed by another 20 min centrifugation at 2,500 xg. Note: conversion of rpm into xg: $[xg = (1.12 \times 10^{-5}) (r) (rpm)^2]$, r= radial distance in cm, rpm: rotational velocity of the rotor. Immediately, the supernatant was decanted of all tubes except total count tubes, and the tubes were inverted to remove the excess liquid. To calculate the concentration of leptin in the unknown samples, all tubes were counted in a gamma counter for 1 min. Standard Curve Range: 0.5–50 ng/mL.

2.2.7. qRT-PCR analysis

2.2.8.1. RNA isolation

Liver tissues RNA were isolated by Qiagen RNeasy Mini Kit. Extracted RNA concentrations were spectrophotometrically measured at $\lambda = 260$ nm, and RNA's purity was controlled by the ratio of optical density (OD) OD₂₆₀/OD₂₈₀ nm and its integrity by using 1.2% agarose gel electrophoresis.

2.2.7.2. Reverse transcription

Procedure for SYBRgreen reagent:

Briefly, DNase-treated total cellular RNA (1 µg) was denatured at 65°C for 10 min in a total volume of 10 µL with RNase inhibitor. Thereafter, a master mix consisting of 100 nmol/L of dNTPs, 50 pmol/L of primer oligo(dT)₁₅, 200 units of moloney murine leukemia virus reverse transcriptase (M-MLV RT), 1X RT buffer, and 2.5 mL of 0.1 mol/L dithiothreitol was added to the denatured RNA samples and incubated for reverse transcription at 40°C for 1 h, and 72°C for 10 min to terminate the reaction. Complementary DNA (cDNA) was ready to use after addition of 120 µL de-ionized H₂O.

Procedure for TaqMan reagent:

For this purpose, the protocol contains 150 pmol random primers (pd(N)₆) instead of oligo (dT)₁₅ primers. RT master mix was prepared of 2.5 µL 40 mM dNTP, 5 mL 5x RT buffer, 2.5 µL 0.1 M DTT, 1 mL M-MLV RT enzyme, 0.4 µL RNase inhibitor, and 1.6 µL deionized H₂O. The RT reaction was performed by using 1 µg RNA (10 µL), and 2 µL random primer pd(N)₆ 150 pmol, the mixture was heated 10 min at 65°C. Then, 13 µL RT-mix was added for each sample and the mixture was incubated for 60 min at 42°C. A 120 µL deionized H₂O was added into the mixture.

2.2.7.3. Primer design

Primers for different genes were designed using the program “Primer 3 Input (version 0.4.0)” (Whitehead Institute for Biomedical Research) and the gene bank data (<http://www.ncbi.nlm.nih.gov>). All the primer sets used for real-time PCR are listed in Table 2.1.4. The self-annealing, potential hairpin formation, and self-complementary of the forward-reverse primers were examined. Then, the primers sequences were blasted to check primer’s pair-specificity and localization within the gene. Primers were synthesized by Invitrogen.

2.2.7.4. Thermal cyclers amplification program

As the name suggests, “real-time” quantitative PCR relies on the monitoring of the PCR reaction product as the amplification progresses, with product detection and measurement occurring after each cycle. Detection is by means of fluorescence and a number of techniques can be used with a variety of machines, the two most common methods using either the dye SYBR Green or TaqMan. A 1 µL (6.3 ng) cDNA of each

sample was added to 9 μL mixture of targeted primer-pair and Fast Platinum SYBR® Green Universal Master Mix.

The PCR amplification reactions were carried out in a StepOne system: an initial hold step (95°C for 20 sec), and 40 cycles of two-PCR steps (95°C for 3 sec, 60°C for 30 sec) using specific oligonucleotides (Figure 2.3). All samples were assayed in duplicate in 96-well PCR microplates. The PCR amplification program was followed by dissociation curve protocol for controlling the specificity of the PCR products. The fluorescence intensity of each sample was measured at a particular temperature change to monitor amplification of the target gene. The purity of PCR products was verified by melting curves and gel electrophoresis.

Additionally, predesigned TaqMan assays were used for *Inos* and *Tlr4* analysis, and the protocols were set according to the manufacturer. Briefly, 5 μL of 2x universal PCR MM, 0.5 μL 20x Assay on Demand, 3.5 μL H₂O and 1 μL cDNA were mixed and run for 10 min at 95°C (initial phase), 95°C for 15 sec and 1 min at 60°C for 45 cycles.

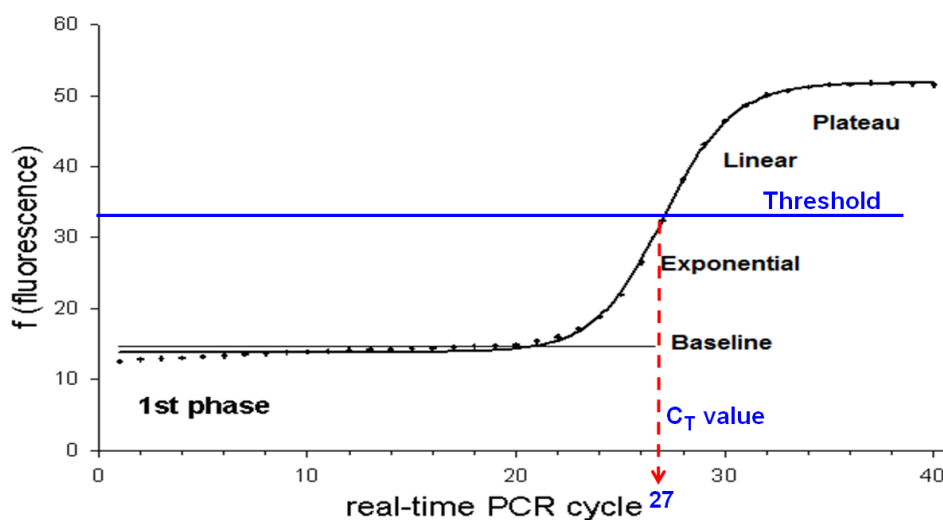


Figure 2.3 qRT-PCR phases. In the initial cycles of PCR, there is no considerable alteration in fluorescence signal. This predefined range of PCR cycles is called the baseline. Exponential (doubling) amplification occurs because all of the reagents are fresh and available, the kinetics of the reaction push the reaction to favoring doubling of amplicon. Linear: as the amplification progresses, some of the reagents are being consumed. The speed of reactions slows down, and the PCR product is no longer being doubled roundly. Plateau: the reactions have halted. The threshold is set in the exponential amplification phase, which is in the logarithmic scale shown linearly. A too low threshold increases the noise, while too high threshold amplifies samples, and thus increase the standard deviation. The C_T value (threshold cycle) is defined as the fractional cycle number at which the fluorescence crosses the fixed threshold; it is inversely correlated to the level of gene expression.

2.2.8. Western immunoblots

2.2.8.1. Protein extraction

Liver samples were protected against proteolytic degradation by placing in ice throughout the experiment. About 150 mg of deep-frozen liver slice of each studied group was washed with pre-cooled PBS (3x) and placed in a reaction tube containing 1 mL total lysis cell buffer (Table 2. 6) for homogenization. Processed specimens were spun at 12,000 rpm for 10 min at 4°C. The supernatants were retrieved, and the pellet was re-suspended again with 1 mL lysis buffer, incubated on ice for 30-60 min, and then sonicated for three strokes by 70% (v/v) by an alcohol- and water-cleaned sonicator for an entire cell disruption. Chilled-centrifugation was performed again.

2.2.8.2. Determination of protein concentration

Whole protein concentration of the collected supernatants was measured by Bradford assay using a Bio-Rad protein assay kit with bovine serum albumin (BSA) as a standard (2 mg/ mL) and an internal control (1:20, 1:40).

2.2.8.3. Principle

The Bradford method ([Bradford 1976](#)) is a colorimetric protein assay, which is based on the absorbance shift of the Coomassie Blue G dye as a result of protein binding. The latter causes color changes from red to blue (maximal absorbance at 595 nm) by protons donation process. The Bradford assay is linear in a range between 2 - 120 µg/mL. Herein, the absorbance at 595 nm is directly proportional to the amount of protein in the sample. A regression curve was derived from a series of standards between 0.03 µg and 1 mg BSA and used to construct an equation for the estimation of the unknown protein concentrations.

Coomassie blue stain was diluted 1:5 with d_4H_2O , and filtrated. The protein extracts as well as the internal control (2 mg/ mL BSA) were diluted with d_4H_2O to 1:20 and 1:40, 5 µL of protein dilution, standard, and control were loaded in duplicate on a microplate, followed by the addition of filtered Coomassie dye solution, and after 5-10 min incubation at RT the plate was read at 595 nm. Finally, the concentrations were calculated by using the regression curve.

Table 2.6 Lysis buffer used for protein extraction in Western blots.

Reagent	Final concentration
Tris-HCl (pH= 7.00)	20 mM
NaCl	150 mM
MgO ₂	1 mM
CaO ₂	1 mM
NP ₄ O	1%
Glycerol	10%

The pre-stained molecular weight marker or the pre-stained PageRuler™ from Fermentas were loaded in a separate lane. The electrophoresis was done at a constant current of 50 mA with maximum voltage set at 100 V for 2 h.

2.2.8.4. Western blots procedure

Western blot method was used to further analyze the protein samples after separation by sodium dodecyl sulphate polyacrylamide gel electrophoresis (SDS-PAGE). The separated proteins were transferred from the gel to a nitrocellulose membrane and analyzed by specific primary antibodies. The primary antibodies are then detected by horseradish peroxidase conjugated secondary antibodies that are directed against the Fc region of the primary antibody. The conjugated peroxidase catalyzes the oxidation of luminol resulting in a chemiluminescence emitting reaction that can be used for the specific detection of the target proteins.

As much as 50 µg of whole lysate from each liver sample was separated by (4-12%) SDS-PAGE. Proteins were then electroblotted onto Hybond-ECL nitrocellulose membranes, and equal loading was monitored in Ponceau S stain. Subsequently, non-specific binding sites on the membranes were blocked at RT for 1.5 h in 5% (w/v) skim milk and 0.1% (v/v) Tween-20 in PBS and incubated with the first antibody overnight on agitated plates at 4°C. Consecutively, the membranes were washed 3 times for 5 min with PBS-T and incubated with appropriate horseradish peroxidase-conjugated secondary antibodies. Immunodetection was performed according to the ECL chemiluminescent solutions A and B Western blotting protocol. Antibodies that were used to study LCN2, inflammation-related proteins and oxidative stress markers

are listed in Table 2.1.3. Immunoreaction signals were viewed with enhanced chemiluminescence using a film processor machine. All Western blot experiments were performed in triplicate. The uniformity of protein loading in each lane was assessed by determining the signal of β -actin as a control-loading protein.

2.2.9. Double immunofluorescent analysis for LCN2 and MPO or ED1

Immunofluorescence was used to detect the localization of the target antigens within liver tissues. Liver cryostatic sections (5 μ m) were air-dried and fixed in methanol/acetone for 9:1 min at -20°C on superfrost slides. After blocking of non-specific binding with serum (according to the species of the secondary antibody) for 1h at RT, the sections were incubated with a solution of the primary antibody anti-LCN2 combined either with ED1 (CD68, a marker for macrophage) or myeloperoxidase (MPO, marker for PMN) overnight at 4°C. In parallel, negative control immunostainings were performed by replacing the primary antibodies with PBS or isotype matching control IgGs (Wojcik *et al.* 2012). Alexa flour-conjugated secondary antibodies were used to detect the primary antibodies (Table 2.1.3). Cells nuclei of the stained sections were remarked by DAPI and the slides were covered with Fluoromount-G and observed using an epifluorescence microscope.

2.2.10. Enzyme-linked immunoadsorbent assay (ELISA) for serum LCN2

2.2.10.1. Principle

This assay employs the quantitative sandwich enzyme immunoassay technique. A microplate is pre-coated with a monoclonal antibody specific for rat LCN2 protein. Serum samples are pipetted into the wells and the immobilized antibody binds LCN2 protein. After washing away any unbound materials, biotinylated rat NGAL antibody specific for rat LCN2 is added. Any unbound antibody-enzyme reagent is washed away, and a substrate solution is added to the wells. The enzymatic reaction yields a blue-colored product that turns yellow when the stop solution is added. The intensity of the color measured by a colorimetric method is directly proportional to the amount of protein bound in the initial step.

2.2.10.2. Reagent preparation

The reagents box was brought at RT. All reagents/working solutions that are necessary for the ELISA were prepared prior to assay procedure as all samples

should be pipetted within 15 min. The following instructions were recommended by the manufacturer:

Wash solution: dilute the 25x Wash Solution Conc. by pouring the total contents of the bottle (40 mL) into a 1L graduated cylinder and add distilled or de-ionized water to a final volume of 1 L. Mix thoroughly and store at 2-8°C till use. *Sample diluent:* dilute the 5x sample diluent conc. by pouring the total contents of the bottle (50 mL) into a 250 mL graduated cylinder and add distilled or deionized water to a final volume of 250 mL. Mix thoroughly and store at 2-8°C for use. *Ready to use reagents:* Rat NGAL calibrators (conc. 0 - 400 pg/mL), biotinylated rat NGAL antibody, HRP-streptavidin, TMB substrate, and stop solution. Negative controls were prepared by using 100 µL of sample diluent per well in duplicate (0 µL serum samples was added).

2.2.10.3. Assay procedure

All specimens were assayed in duplicates. This procedure consists of five steps excluding the 96-microwells plate washing. In the 1st step, 100 µL volumes of each calibrator, diluted non-hemolytic samples, and the internal controls were pipetted into their corresponding positions in the microwells. To synchronize the reaction in each well, all reagents were pipetted using a multi-channel pipette. Wells were covered and incubated for 60 min at RT on a shaking platform set at 200/min. The contents of the microwells were pushed out and washed three times with 300 µL diluted wash solution. Next, 100 µL of biotinylated rat NGAL antibody was dispended into each microwell. The wells were again masked and incubated for 60 min on a shaking platform set at 200/min. After washing, 100 µL of HRP-streptavidin was dispended into each microwell and incubated for 60 min on a shaking platform set at 200/min. Next, the plate was washed three times. Stepwise, 100 µL of TMB substrate was pipetted into each microwell. The wells were covered and incubated for exactly 10 min at RT in the dark. Finally, to stop the enzymatic reaction, 100 µL stop solution was added to each well, maintaining the same pipetting sequence as above and mixed by gentle shaking for 20 sec. Optical density of each well was determined within 20 min by using a microplate reader at 450 nm.

2.2.11. Two-dimensional gel electrophoresis (2-DE)

2.2.11.1. Protein extraction and determination

Protein extraction for the 2-DE method was similar to the procedure which is mentioned in Section 2.2.8.1. However, the lysis buffer for 2-DE is different (7 M urea, 2 M thiourea, 4% (w/v) CHAPS, 2% (v/v) ampholytes, 1% (w/v) DTT, 10 mM PMSF, and 1% (v/v) phosphatase inhibitor cocktail 2 and 3). The concentration of the isolated proteins was measured as described in Section 2.2.8.2 and 2.2.8.3.

2.2.11.2. First dimensional gel electrophoresis

The separation of the proteins based on their charge and mass can be achieved by 2-DE gels according to the protocol of Gorg *et al.* (Gorg *et al.* 2000). A150 µg tissue-extracted total protein plus reswelling buffer (0.2% (v/v) ampholytes, 15 mM DTT and 370 mM bromophenol blue plus to 0.91 mL lysis buffer) up to 330 µL was centrifuged at 4°C, 12,000 rpm for 10 min. The resultant supernatant was used to passively rehydrate 17 cm immobilized pH gradient (IPG) strip with a nonlinear pH range of 3-10 (ReadyStrip™) at RT for 1 h. The IPG strips were then macerated in reswelling tray with 2 mL low viscosity mineral oil for each to prevent the evaporation process, followed by incubation for 14 h at RT. Subsequently, strips were soaked in 2 mL mineral oil and applied in Protean IEF Cell at 20°C and 32,000 Vh. The proteins were separated in the first dimension according to their isoelectric points (isoelectric focusing (IEF)).

2.2.11.3. Gel preparation for 2-DE

The SDS-PAGE was used to separate proteins according to their molecular weight (MW) (Laemmli 1970), i.e. the polyacrylamide matrix acts as a molecular sieve. The anionic detergent SDS is used to denature the proteins by disrupting the non-covalent bonds so interactions can be prevented, and the use of the reducing agent β-mercaptoethanol in the sample buffer leads to the dissociation of subunits of the multimeric proteins. SDS negatively charges the unfolded proteins, which makes them to migrate to the positive electrode (anode) in the electrophoretic gel. Usually, 12% acrylamide gels were used and a 4% stacking gel is cast onto the resolving gel, leads to a decrease in sample spread (Table 2.12). PROTEAN II xi XL Vertical Electrophoresis Cells were used for gel formation.

Table 2.12 The composition of the phase 1 and 2 gels.

Reagents	Stacking (4%) 4 gels	Resolving (12%) 4 gels
1.5 M Tris/HCl	1.5 mL, pH 6.8	38.5 mL pH 6.8
30%Bis/Acrylamid	1.56 mL	64.2 mL
10% (w/v) SDS	60 μ L	2.2 mL
10% (w/v) Ammonium persulfate	60 μ L	770 μ L
TEMED	6 μ L	51 μ L
$_{\text{dd}}\text{H}_2\text{O}$	8.8 μ L	49.3 mL

2.2.11.4. Second dimensional gel electrophoresis

IPG strips were placed in two equilibration buffers contain 6 M urea, 0.15 M Tris/HCl pH 8.8, 2% (w/v) SDS, 30% (v/v) glycerin, and 15 mM DTT + 0.25% bromophenol blue or 40 g/L Iodoacetamide + 0.25% bromophenol blue for 30 min each. Softened IPG strips were lengthwise compressed into a vertical loose 4% gel phase after getting rid of excess oil. A 5 μ L pre-stained molecular marker-wetted filter paper was aligned on the left side of the strip. 1x electrophoresis buffer was diluted from (1 liter 5x concentration: 0.025 M Tris (pH 8.3), 0.192 M glycine, and 2% (w/v) SDS) was used in the second dimensional SDS-PAGE protein separation based on molecular weight for 18-20 h at 4°C and 90 V through a 12% stacking gel in Bio-Rad Protean II xi Cell. As a result, the similar IP proteins bands were further separated according to their molecular weights in individual spots on the gel slabs.

2.2.11.5. Phospho- and silver-staining of proteins

After 30 min fixation of the 2-DE gels with 50% (v/v) methanol + 12% (v/v) glacial acetic acid), the gels were washed 3x with $_{\text{dd}}\text{H}_2\text{O}$. The gels were then phospho-stained in the dark by overnight incubation with Pro-Q[®] Diamond Phosphoprotein gel stain according to the manufacturer's directions. Next, the gels were de-stained for 30 min (3x) using 20% (v/v) acetonitrile and 5% (v/v) 50 mM sodium acetate, pH 4. The stained gels were finally washed 3x with $_{\text{dd}}\text{H}_2\text{O}$ and scanned (Fla 5100) at $\lambda = 532$ nm.

Silver staining is a popular and sensitive protein staining method, with a detection range of 1-10 ng (Wise and Lin 1991). For protein silver staining using the modified method of Blum *et al.* (Blum *et al.* 1987), the gels were washed in graded ethanol for 30 min. Next, they were sensitized with freshly-prepared 100 mL/gel of 0.8 mM

sodium thiosulfate for 1 min followed by rinsing with three changes of ddH_2O for a total of 1 min. The gel slabs were submerged in freshly prepared 12 mmol silver nitrate and 0.026% formaldehyde for 20 min shaking at RT. After three ddH_2O washes; the protein color was developed using developing buffer (sodium carbonate 6%, formaldehyde 0.0185% of 37% formaldehyde stock, and sodium thiosulfate 16 μM) with intensive shaking. The silver-stained gels were stored in 5% (v/v) glacial acetic acid, scanned and finally dried with vacuum gel dryer for 1.5 h at 80° C for further storage and analysis.

2.2.11.6. Analysis of protein spots in the 2-DE polyacrylamide

The two dimensional gel electrophoresis was developed to analyze the final level of gene expression based on resultant proteins (O'farrell *et al.* 1977). Densitometric analysis was accomplished using the Delta2D software V4.2. Gel images of controls and the experimental groups were warped and aligned to correct for differences in protein separation and migration between gels. Protein spots were detected automatically and verified manually using the dual view of the Delta2D software. After background subtraction, the measured intensity of each protein spot was normalized as a percentage to the total intensity of all integrated protein spots of the scanned images of polyacrylamide gel (Luhn *et al.* 2003). The definition for differential expression of proteins was set to at least 1.5-fold increase or decrease in spot intensity that was significant compared to control at least at $P < 0.05$.

2.2.12. In vitro studies

2.2.12.1. Primary liver cell isolation and culturing

2.2.12.1.1. Animal preparation

Rat hepatocytes (HCs) were isolated from livers of male Sprague-Dawley rats (240 g) based on two-step enzymatic (collagenase) perfusion, a method which was firstly described by Seglen (Seglen 1973). Animals were anesthetized with Narcoren® 50% of BW (240 g), and were rested on their backs using clamps/pins. The abdominal region was disinfected with 70% ethanol. Using a large 1.3 mm diameter cannula; the portal vein was punctured and connected longitudinally via sterile tubing to the pump system.

2.2.12.1.2. Liver perfusion

The liver was initially exsanguinated in non-recirculating mode via the portal vein *in situ* at a rate of 10 mL/min with 200 mL CO₂-enriched calcium-deprived sterile Krebs–Ringer buffer (KRB, Table 2.14) pH 7.4 containing 0.25 mM EGTA until liver becomes bloodless. By perfusion with the calcium-free solution, calcium ions were eluted from the desmosomes, resulting in a large cell yield with minimum cell damage. For a sacrifice of the experimental animal, the diaphragm muscle was opened.

Components of the extracellular matrix of the rat liver were enzymatically digested by a perfusion medium (buffer II) for 7-12 min at 37°C with ~ 150 bar carbogen in a firstly non-recirculating mode until the perfusion system filled with buffer II, and then under recirculating conditions for 15 min by cannulating the *inferior vena cava* with soft a tube to the pump system. Glisson's capsule was carefully torn away, and the liver tissues were manually disrupted to yield a crude cell suspension. The suspension of the cells was filtered by pouring over a beaker covered by a nylon mesh filter (pore size 79 µm). HCs and other cells entered through the pores, while undigested connective tissues and remainder aggregates were retained (Figure 2.4). Nonparenchymal cells and cell debris were removed by thrice centrifugation in total (1,200 rpm, 2 min, RT) with cold wash with buffer III (pH 7.4, 120 mM NaCl, 4.83 mM KCl, 1.2 mM MgSO₄·7H₂O, 1.2 mM KH₂PO₄, 20 mM HEPES, and 0.4% BSA). The pellet was re-suspended with Percoll-gradient solution. Subsequently, the cells were re-suspended in culture media and were chamber counted (Neubauer hemocytometer). The final cell pellet predominantly contains HCs (90%, as originally described) (Ates M *et al.* 2012). HCs were 85-90% viable. This procedure was ethically approved (Ramadori *et al.* 1990).

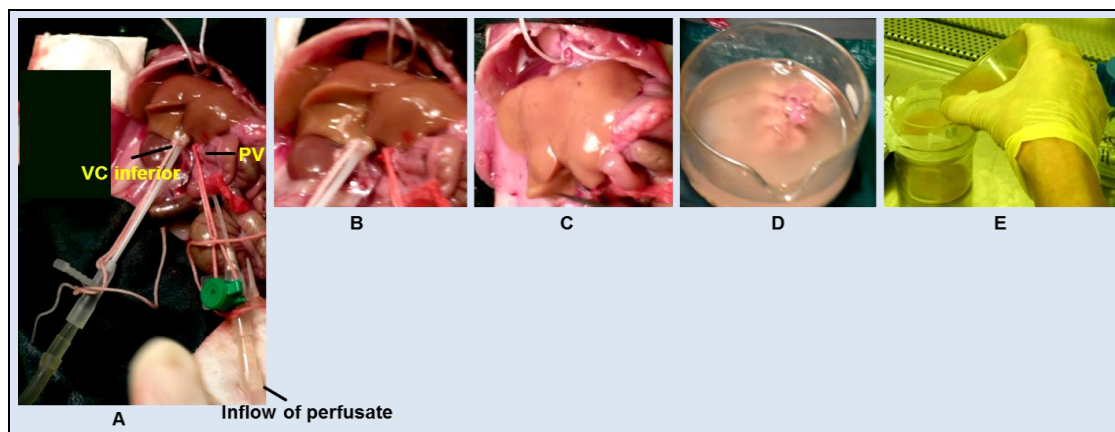


Figure 2.4 The status of rat liver during HC isolation. A-B. Blood was flushed from the liver. C. The liver was softened as a result of collagenase treatment. D. The liver was excised and washed in PBS. E. The liver was crushed and filtered.

Table 2.14 Buffer I: Pre-perfusion, Ca-free KRB + EGTA pH (7.4) KRB.

Molar	Mass/ 1L
24 mM NaHCO ₃	2.016 g/L
120 mM NaCl	7.020 g/L
4.83 mM KCl	360 mg/L
1.2 mM MgSO ₄ ·7H ₂ O	296 mg/L
1.2 mM KH ₂ PO ₄	163 mg/L

Buffer II: Collagenase-containing medium *pH (7.4)*

2.2.12.1.3. HCs treatment

Isolated primary HCs (1 million/ mL) were grown in large culture plates (9 cm) in M199 supplemented with 1.5% (v/v) penicillin-streptomycin, 4% (v/v) FCS and 1 nM swine insulin at 37°C in a 5% CO₂, 95% air- humidified incubator for 40 h. Afterwards, the cells were fasted for 4 h by replacing the culture medium with glucose-free medium plus other supplementary constituents. Thereafter, the isolated HCs were treated with either 20 mM glucose (glu) or equimolar fructose (fru) in M199 medium. Next, the medium was aspirated out and replaced with PBS. Subsequently, the cells were harvested and lysed kinetically at 0, 3, 6, 12, and 24 h for RNA and protein studies either by Qiagen reagents or Western blot lysis buffer (Section 2.2.9.1). Concurrently,

culture medium of each sample was also collected for protein evaluation. All treatments were carried out in duplicate.

2.3. Statistical analysis

Data were processed using the GraphPad Prism 5 software and were described as mean \pm standard error of the mean (SEM). Statistical significance was calculated by one-way analysis of variance (ANOVA) (Dunnett's post-hoc test) to examine the statistical significance in experimental groups versus controls. For statistical analysis of RT-PCR results, the comparative C_T method was used to determine the amount of target gene transcripts, normalized to an endogenous reference (housekeeping gene transcript, β -actin and ubiquitin c) and relative to a calibrator (arithmetic formula; $2^{-\Delta\Delta C_t}$). For 2-DE data, ANOVA cluster analysis and T test were used. The null hypothesis was rejected when $P < 0.05$.

3. RESULTS

Part I: Animal Model

3.1. Animal phenotypes and biophysical parameters

3.1.1. L-HFr fed rats exhibited increases of food intake

The rats were treated with standard chow (Co), liquid Lieber De-Carli (LDC) or LDC plus 70% fructose (L-HFr) diet for 4 wks or 8 wks. Average basal food intake (at wk 0) was 25.2 ± 0.5 kcal/100g BW/day for all animals. The food intake of the control rats slightly declined at wk 4 (23.5 ± 0.1) and wk 8 (21.2 ± 0.1). There was no noticeable difference in the food intake between the Co and the LDC group. Instead, a significant increase of food intake was observed in the L-HFr group at wk 4 (33.5 ± 0.7 kcal/100g BW/day) and wk 8 (29.0 ± 0.2 kcal/100g BW/day) (Figure 3.1A).

3.1.2. Variations in the body and liver weights

The phenotypes of the animals were studied to observe the effect of the diets on the BW gain and liver weight (LW). The BW of the Co group was 160-180 g at wk 0 and increased up to 393 ± 5 g at wk 4 and 489 ± 7 g at wk 8. The rats of the Co and the LDC group had a comparable BW and gained more BW than the animals in the L-HFr group during the study.

Despite markedly higher total caloric intake in the high fructose-challenged rats, the absolute BW was significantly diminished at wk 4 (300 ± 7 g; $P < 0.001$) and at wk 8 (420 ± 16 g; $P < 0.001$). This implies that the BW of L-HFr treated rats was reduced by 30% and 15% relative to the corresponding age-matched control rats (Figure 3.1B). However, these animals remained behaviorally normal and showed no signs of stress.

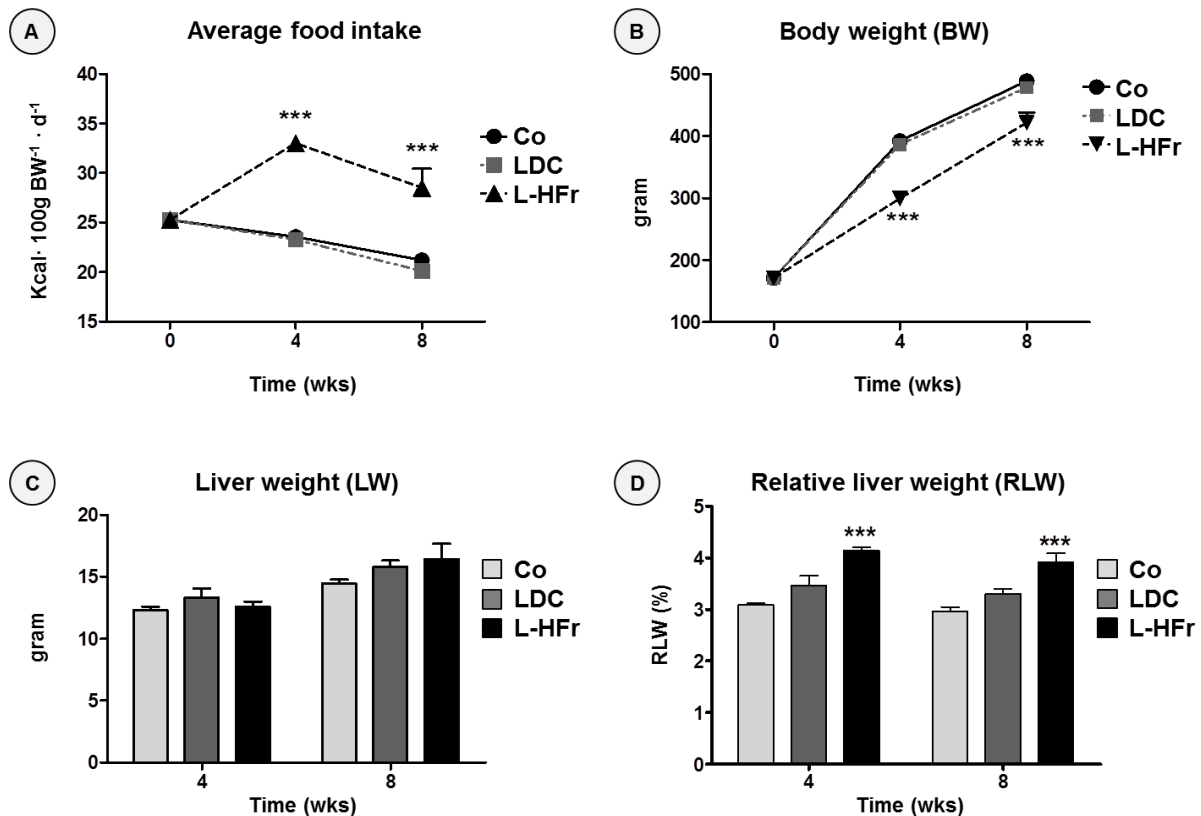


Figure 3.1 Phenotypes of the animals. Linear graphs show the average of caloric daily intake of the animals (A) at wk 0, 4 and 8 of treatment (food intake expressed as kcal · g BW⁻¹ · d⁻¹) and animal body weight (B). Bar blots show liver weight (C) and relative liver weight (D). Data are presented as mean ± SEM of four rats per group in correspondence to time points (wks). ** Indicates statistically significant difference $P < 0.01$, *** $P < 0.001$. Standard chow pellet (Co), a freshly prepared liquid LDC: Lieber DeCarli (LDC), and LDC combined with 70% fructose (L-HFr).

In general, the LW of both animal groups was moderately higher than that of littermate controls (Figure 3.1C). LW of the Co group was 12.3 ± 3 g at wk 4 and 14.5 ± 0.3 g at wk 8, while in the LDC group it was 13.1 ± 0.7 at wk 4 and 15.7 ± 0.5 g at wk 8. In addition, the LW under the L-HFr regimen was 12.6 ± 0.4 g and 16.4 ± 1.0 g at wk 4 and 8, respectively.

Consequently, RLW ($LW \cdot g \cdot BW^{-1} \cdot 100\%$) was high in both experimental groups compared to controls. The LDC-fed animals had slightly higher RLW ($3.5 \pm 0.2\%$, and $3.3 \pm 0.1\%$) compared with that of the fed animals standard Co ($3.1 \pm 0.1\%$, $3.0 \pm 0.1\%$) at wk 4 and 8, respectively. Yet, the RLW of L-HFr fed rats was the highest ($4.5 \pm 0.1\%$ at wk 4 and $4.0 \pm 0.4\%$ at wk 8) during the observation period ($P < 0.001$) (Figure 3.1D).

3.2. Fatty liver developed in the LDC and the L-HFr group

As the contents of the livers in the groups are different, the LW is imprecise. Thus, size (scale) of the liver and its general appearance were additionally evaluated. The Co-fed animals exhibited normal liver size and morphology at both time points. In the LDC reared rats, liver size was insignificantly larger, while the liver was somewhat lighter than the liver colors observed in the Co group (scale, Figure 3.2). Of note, the L-HFr fed rats presented hepatomegaly as well as yellowish, greasy and soft livers compared to other groups at both time points (Figure 3.2). In the L-HFr fed rats, visceral fat deposition in the abdominal cavity was noticeably higher

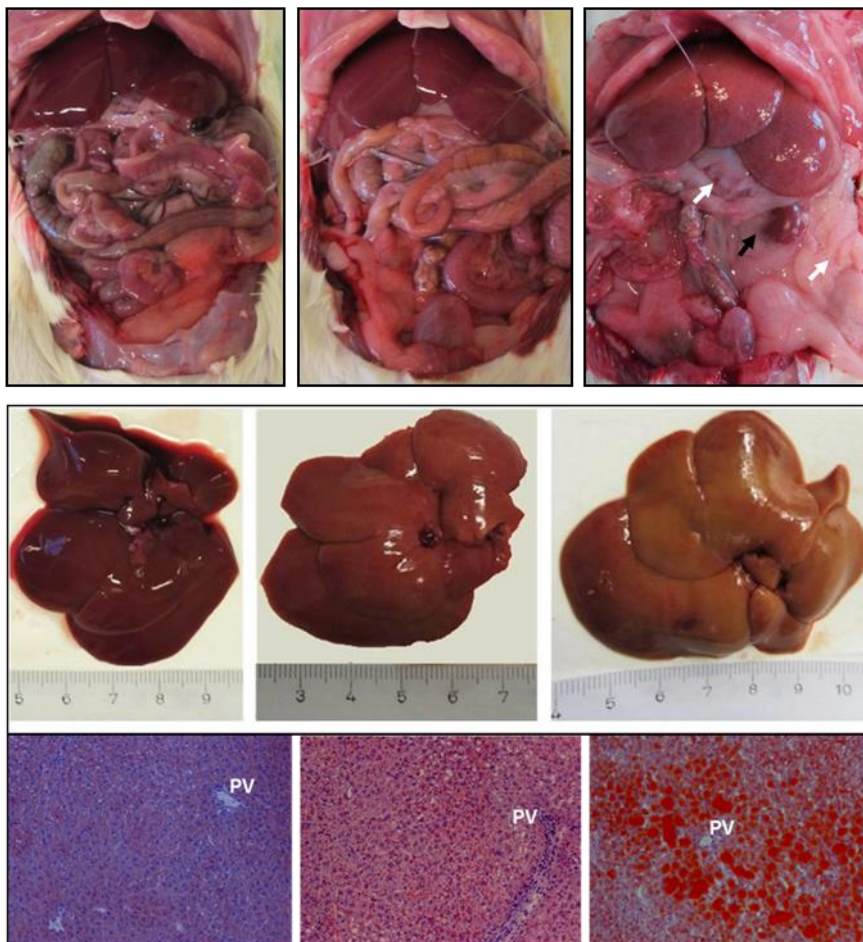


Figure 3.2 An overview of the rat liver and visceral adipose tissue after laparotomy. Co: grossly, liver color is brown, and the surface is smooth, microscopic: normal liver, no fat droplets; LDC: grossly, liver color is light brown; L-HFr: liver is enlarged and greasy, and it has a pale yellow appearance. In addition, more visceral fat (perirenal black *arrow* and mesenteric white *arrow* areas) can be seen in L-HFr fed animals. Since there was no difference in the general appearance of the livers of the same group at both time points, only wk 4 is presented above.

Furthermore, the histological manifestations of the liver tissue were microscopically assessed by Oil Red O, Nile red, HE, and Masson's Trichrome staining.

3.2.1. Hepatic lipid partitioning in the animal groups

Lipid distribution in the liver varied among the animal groups. Oil Red O, a specific lipid staining, revealed no lipid accumulation in control livers (Figure 3.3). In LDC fed rats, fat microvesicles were observed primarily in the HCs of the portal triad at wk 4. Microvesicular and occasionally macrovesicular steatosis were evidenced in the LDC group at wk 8 (Figure 3.4). The uniform liver change in the L-HFr group was consistent with fatty metamorphosis (change) with large fat vesicles in the HCs of zone I and II at both time points.

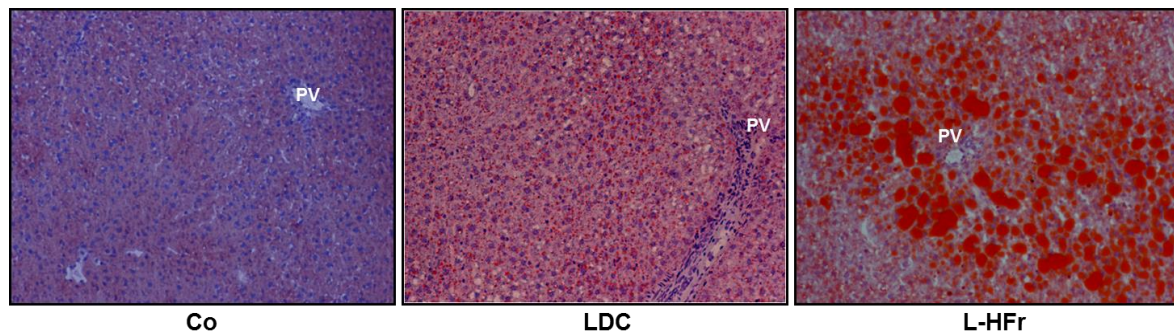


Figure 3.3 Representative micrographs illustrate lipid deposition. Cryo-liver sections were stained with Oil-Red O at wk 4. The red color represents the accumulated lipid droplets in the HCs, while the blue color represents the hematoxylin-stained nuclei. A massive lipid accumulation is visualized in the portal area towards the central vein in the L-HFr group. PV: portal vein, HCs: hepatocytes. Magnification x100.

The liver sections were stained with TG-specific Nile red dye for further confirmation. The LDC as well as the L-HFr diet induced hepatosteatorosis with different degrees compared to the control group. Different sizes of fat droplets can be seen in the livers of the L-HFr fed group (Figure 3.4).

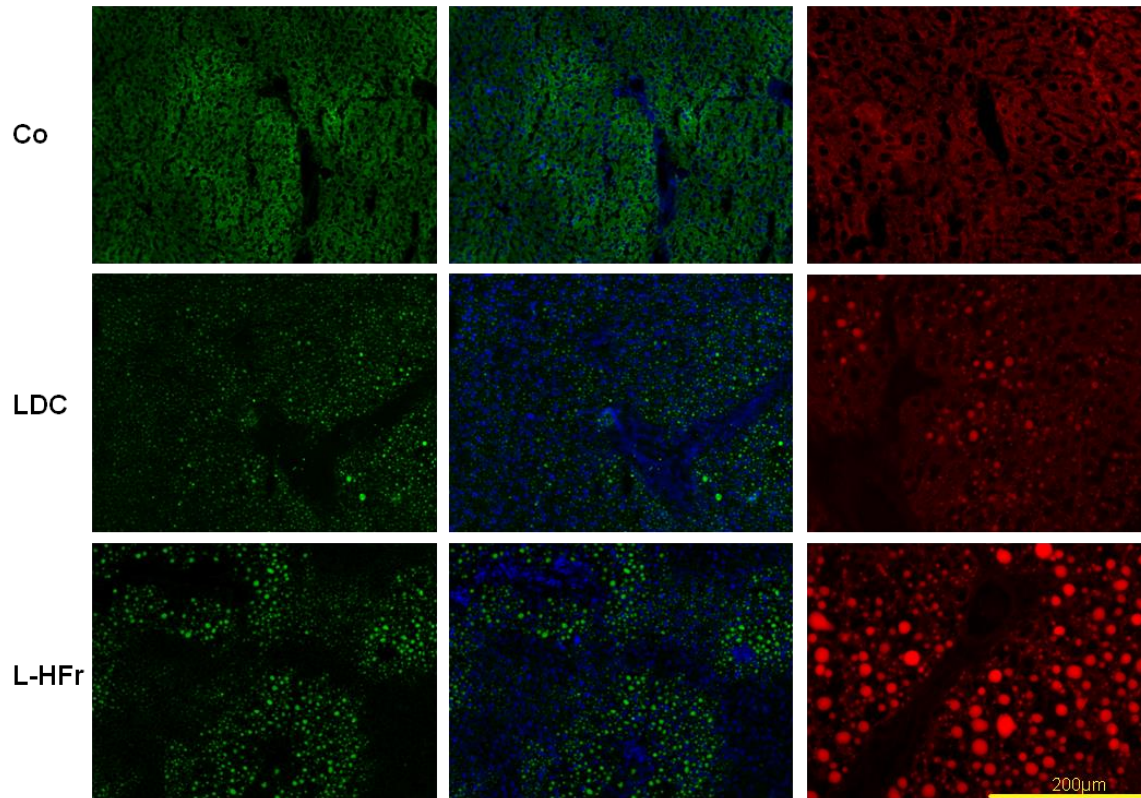


Figure 3.4 Photomicrographs of Nile red stained liver sections. The staining demonstrates the TG retention in the HCs of the LDC and the L-HFr group. Intracellular accumulated fat was exhibited in green or red small vesicles (LDC group) and almost large vesicles (L-HFr group). Since there is no difference in the morphology of Nile red staining between the time points, the presented pictures were collected at wk 8. The rats were fed with standard chow (Co), liquid Lieber-DeCarli diet (LDC) or LDC + 70% kcal fructose (L-HFr). The magnification of left and middle columns is x100, whereas in the right one it is x200. The nuclei were stained with DAPI and they appear Blue.

3.1.2. HE staining manifested macrosteatosis, HCs ballooning, and moderate inflammation in the L-HFr group

Histopathological examination of the liver tissue in each animal group was mostly consistent. Control (chow-fed) rats showed normal hepatic architecture and there was no sign of steatosis, inflammation or fibrosis. The livers of rats fed with liquid LDC diet showed admixture of micro- and/or macrovesicular steatosis commonly observed in periportal areas at wk 4 (Figure 3.5A) and wk 8 (Figure 3.5B), respectively. Instead, livers of L-HFr treated rats were distinguishable from those of rats fed with chow or LDC diet. Hallmarks of NASH included extremely panacinar/ panlobular steatosis (covering the total surface of the hepatic lobule) and moderate inflammation (grade 2) noticed mainly in zone I of the L-HFr group at both time points.

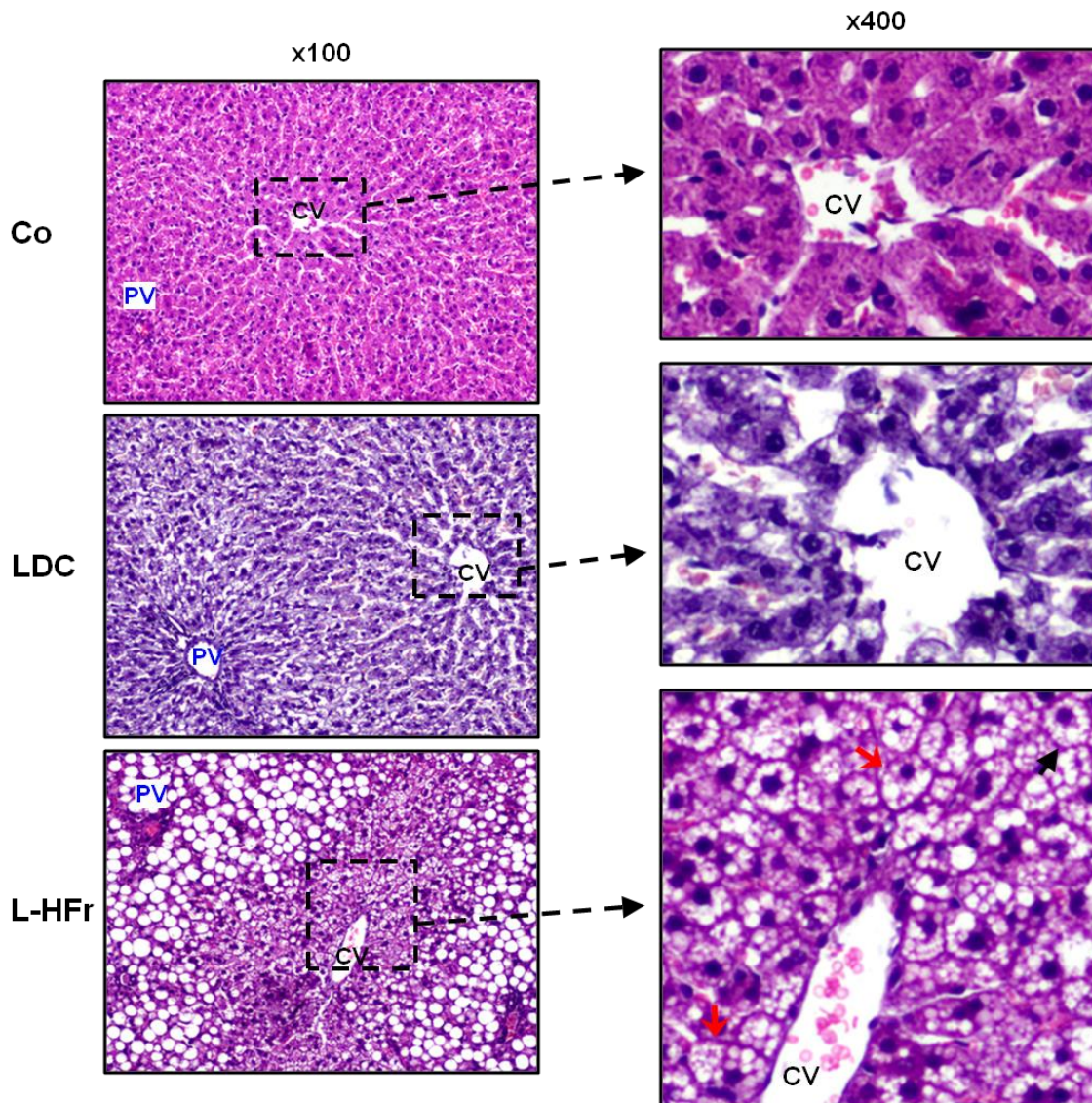


Figure 3.5A HE-stained livers at wk 4. The rats were fed with standard chow (Co), liquid Lieber-DeCarli diet (LDC) or LDC + 70% kcal fructose (L-HFr). The left column represents x100 overview and the right column represents x400 magnification. Microvesicular steatosis is present in the periportal area (zone I) of the livers of the LDC group. Pronounced macrovesicular steatosis in zone I and II is observed in the L-HFr group. The right column focuses on the perivenular area which shows mostly intact HCs in Co and LDC. In contrast, HCs ballooning surrounds the CV area. Red arrows point to ballooned HCs, the black arrow shows foamy HCs. CV: central vein, PV: portal vein. The white clear vacuoles contained lipid. However, since histological fixation caused it to be dissolved only empty/clear spaces can be seen.

Pronounced macrovesicular fat degeneration indicating that the cytoplasm of the hepatocyte is occupied by a single large fat droplet that displaces the nucleus to the periphery (eccentric nucleus) was the major feature under the L-HFr regimen. At wk 8, however, the percentage of fat-laden HCs was lesser than at wk 4 in the L-HFr group. Moreover, ballooned HCs were seen in centrilobular areas, along with a loss of structural integrity and vascular architecture at both time points. The perivenular HCs

revealed a foamy fatty change characterized by striking cell swelling with additional massive infiltration of small fat droplets throughout the cytoplasm. The nuclei in these cells are almost centrally located.

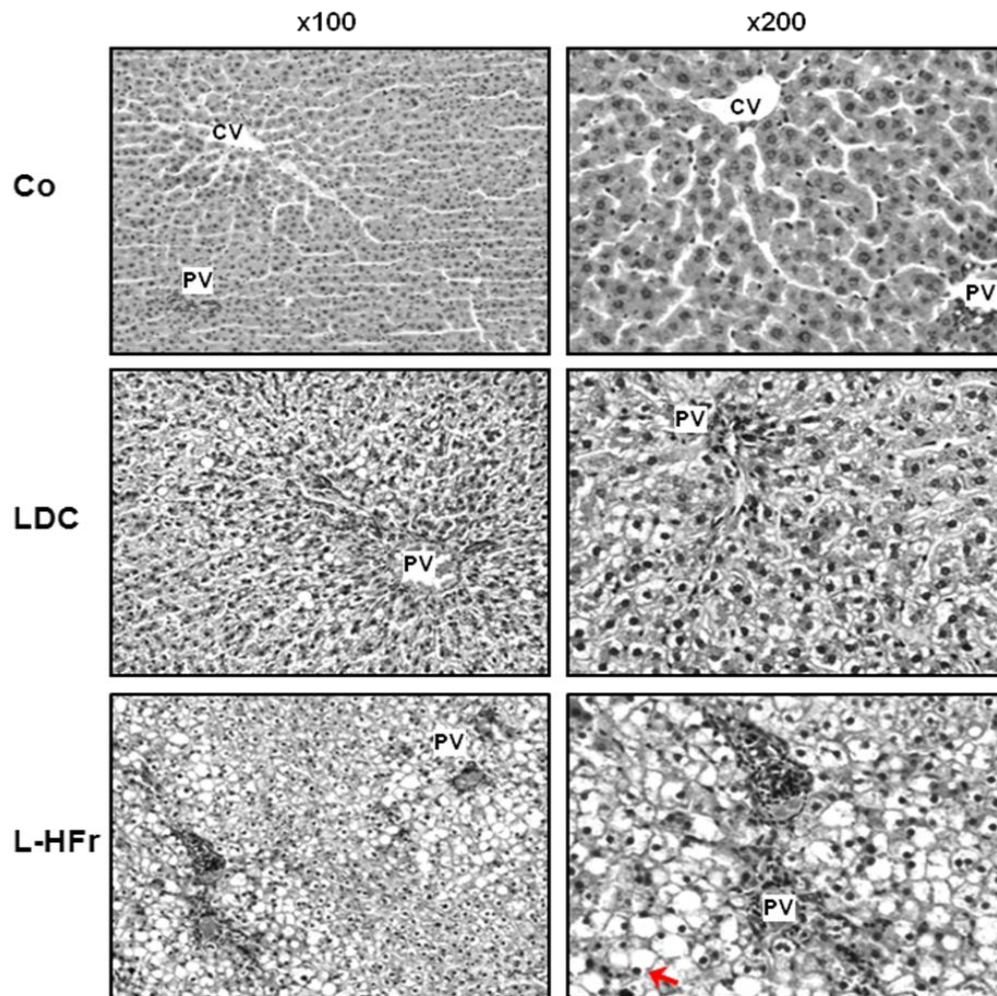


Figure 3.5B Photomicrographs of HE staining of wk 8 hepatic tissue. Normal liver features are presented in the Co group, admixture of macro and micro steatosis can be evidenced in the LDC group. Pronounced panacinar/panlobular steatosis seen in the L-HFr group with moderate inflammation. Rats were reared on Co: chow (control), LDC: Lieber-DeCarli, or L-HFr: LDC + high fructose (70%) diet. Left column x100, right column x200 magnification.

Percentage of fat-loaded HCs was histologically evaluated by a pathologist and three different scientists (Figure 3.5C).

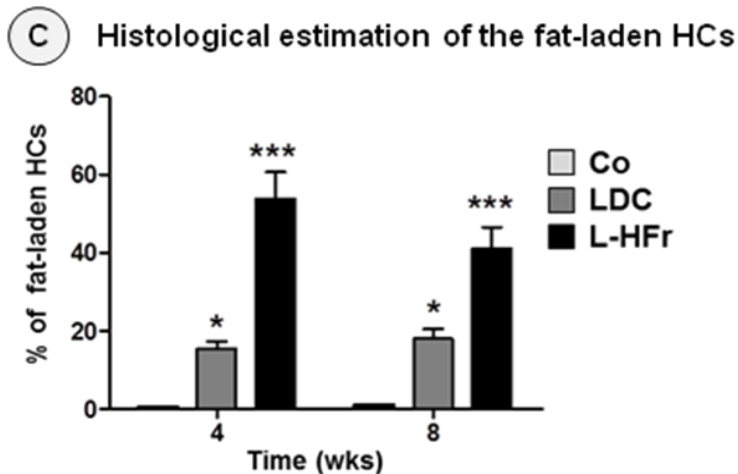


Figure 3.5C Percentage of fat-laden HCs. The evaluation was microscopically performed on the HE-stained liver slices * $P < 0.05$, *** $P < 0.001$ vs. Co. Data were presented as mean \pm SEM of four rats per group. Rats were fed for 4 wks or 8 wks with standard chow (Co), liquid Lieber-DeCarli diet (LDC) or LDC + 70% kcal fructose (L-HFr). HCs: hepatocytes.

3.2.3. Stages of liver fibrosis in the experimental groups

No fibrosis was seen in the control and the LDC group at wk 4. In addition, at wk 8 the control group showed the same liver features seen at wk 4, while the LDC group exhibited stage 1 fibrosis (minimal fibrosis, mild portal connective tissue) at wk 8. The L-HFr regimen resulted in progressively fibrosing livers: stage 1 fibrosis at wk 4, and stage 2 (mild fibrosis, increased portal fibrosis with beginning extension into/affection of the hepatic lobule) at wk 8 (Figure 3.6). In addition, the liver architecture was somewhat impaired in the L-HFr animal model. The slides were classified according to Desmet & Scheuer (stages of fibrosis 0-4, grade of inflammation 0-4) by a pathologist.

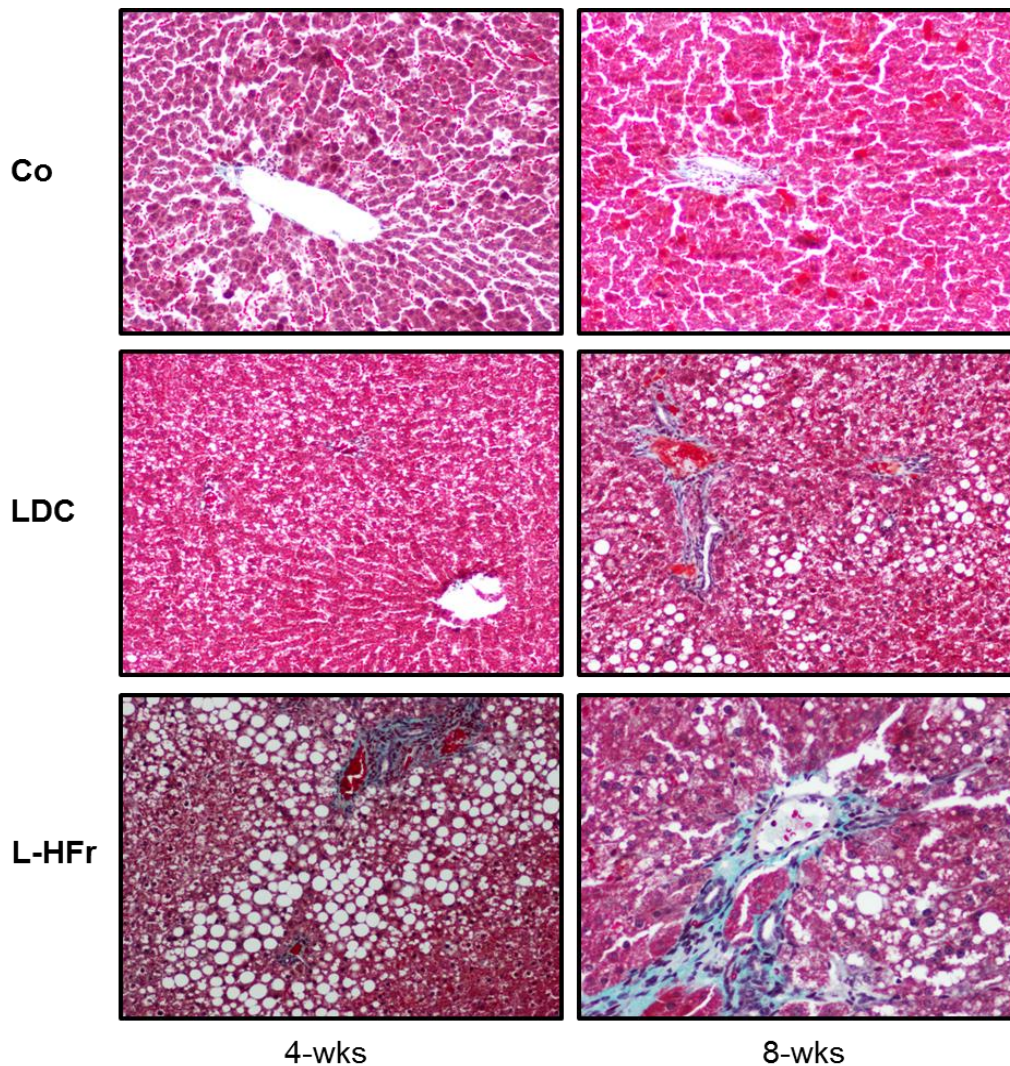


Figure 3.6 Masson's Trichrome stained liver slices. At wk 4 (left column), both the Co and the LDC group showed no fibrosis (stage 0), while the L-HFr group showed stage 1 (minimal, mild portal connective tissue). At wk 8 (right column), the hepatic features were the same as at wk 4 in the Co group, the LDC group showed stage 1 fibrosis, whereas the L-HFr animal model had stage 2 (mild fibrosis, increased portal fibrosis with beginning extension into/affection of the hepatic lobule). The rats were fed with standard chow (Co), liquid Lieber-DeCarli diet (LDC) or LDC + high (70% kcal) fructose (L-HFr) regimen. Magnification (x100).

3. 3. Biochemical Studies

3.3.1. Hepatic TG content

Intrahepatic TG loading was further measured. In the control liver tissues, 1.4 ± 0.1 g TG was assessed in 1 g at wk 4. This value was slightly higher (1.8 ± 0.1 g TG/g liver) at wk 8 in the same group. In agreement with the histological assessment, the LDC diet induced an approximately 1.8-fold increase in hepatic TG content respective to chow

diet. Moreover, a three-fold increase of TG content was found in the livers of the L-HFr fed rats at wk 4 and a two-fold increase at wk 8 (Figure 3.7).

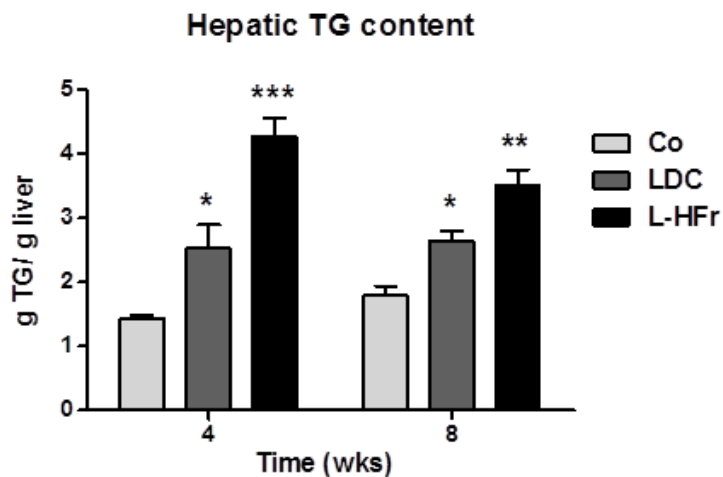


Figure 3.7 Triglyceride content in the rat liver. Data are expressed as mean \pm SEM of four animals/group per time point. The rats were fed with standard chow (Co), Lieber-DeCarli (LDC), or LDC plus high fructose (L-HFr) diet. The food was removed 10 h before the sacrifice. * $P<0.05$, ** $P<0.01$, *** $P<0.001$ vs. Co.

3.3.2. Plasma biochemical profiles differed markedly in the L-HFr model

The LDC diet resulted in significantly increased fasting TG concentration in the plasma compared with littermate controls at wk 4, but not at wk 8. Although the levels of fasting glucose, total cholesterol and ALT and AST were numerically higher in the LDC group than in the control group, the difference was not statistically significant (Table 3.1). The L-HFr diet resulted in increased levels of blood TG and glucose compared to controls (Table 3.1). Consistently, the concentration of total plasma cholesterol was moderately higher in the L-HFr animal model compared to the age-matched control group. Moreover, the plasma level of HDL-C (the “good” cholesterol) was diminished in the L-HFr rat group after 8 wks ($P<0.001$) (Table 3.1). The LDL cholesterol levels remained unchanged in all groups (data not shown). In addition, the L-HFr diet was associated with a two-fold increase in plasma uric acid concentration at wk 8 ($P<0.01$). Serum ALT and AST activities were significantly increased in the L-HFr model ($P<0.05$) at both studied time points (Table 3.1).

Table 3.1 Data of plasma biochemistry of the rats during 8 wks of feeding.

Parameter	Time point/ Group	Co	LDC	L-HFr
ALT (U/l)	4 wks	41 ± 8	43 ± 3	69 ± 7 *
	8 wks	55 ± 8	48 ± 4	80 ± 8 *
AST (U/l)	4 wks	67 ± 5	74 ± 2	136 ± 8 **
	8 wks	90 ± 7	117 ± 13	166 ± 10 **
Glucose (mg/dl)	4 wks	152 ± 12	182 ± 5	243 ± 4**
	8 wks	210 ± 7	244 ± 5	292 ± 6 ***
TG (mg/dl)	4 wks	26 ± 5	74 ± 8*	75 ± 13 *
	8 wks	44 ± 13	62 ± 15	127 ± 21 *
Cholesterol (mg/dl)	4 wks	55 ± 2	58 ± 4	58 ± 3
	8 wks	47 ± 4	52 ± 4	53 ± 5
HDL-C (mg/dl)	4 wks	49 ± 1	43 ± 2	46 ± 1
	8 wks	44 ± 1	45 ± 3	32 ± 2 ***
Uric acid (mg/dl)	4 wks	0.6 ± 0.0	0.9 ± 0.2	0.5 ± 0.0
	8 wks	1.1 ± 0.0	0.5 ± 0.1	2.2 ± 0.3 **

All animals were overnight fasted before sacrifice. The hallmarks of metabolic syndrome were induced in the L-HFr group. The animals were fed with: Co: chow (control), LDC: Lieber-DeCarli liquid diet, or L-HFr: LDC + 70% kcal fructose. * $P < 0.05$, ** $P < 0.01$, *** $P < 0.001$ compared with control group: Data are expressed as mean ± SEM of four rats per group.

3.3.3. Changes in serum leptin levels

Leptin is a 16-kDa protein hormone made by fat tissue that plays a key role in regulating energy intake, satiety and expenditure, including appetite and hunger, BW changes (Friedman and Halaas 1998). It is encoded by the *ob* gene. Sugar consumption elevates fasting leptin concentrations and the increases are associated with BW changes (Rezvani *et al.* 2013). The leptin also augments the release of proinflammatory cytokines (TNF- α and MCP-1) in mice (Chatterjee *et al.* 2013). The diurnal pattern of leptin is disrupted by fasting, and its concentration decreases dramatically in response to overnight fasting (Weigle *et al.* 1997).

Fasting leptin levels were measured in serum samples using RIA. Obviously, leptin concentrations at wk 8 were higher compared to wk 4 in all groups (Figure 3.8). At wk 4, the leptin level in the control group was 1.8 ng/mL and in the LDC group, 3.0 ± 0.2 ng/mL. Interestingly, the fructose-enriched diet elevated leptin levels up to 5.1 ng/mL (2.8-fold) compared to age-matched controls ($P < 0.01$). At wk 8, the leptin serum level in the Co group was 3.7 ± 0.9 , and in the LDC group 5.7 ± 2.1 ng/mL. Although in the normal situation of the blood leptin should decrease during fasting, the L-HFr regimen caused a 3.3-time increase of fasting leptin level compared to control rats ($P < 0.01$) (Figure 3.8).

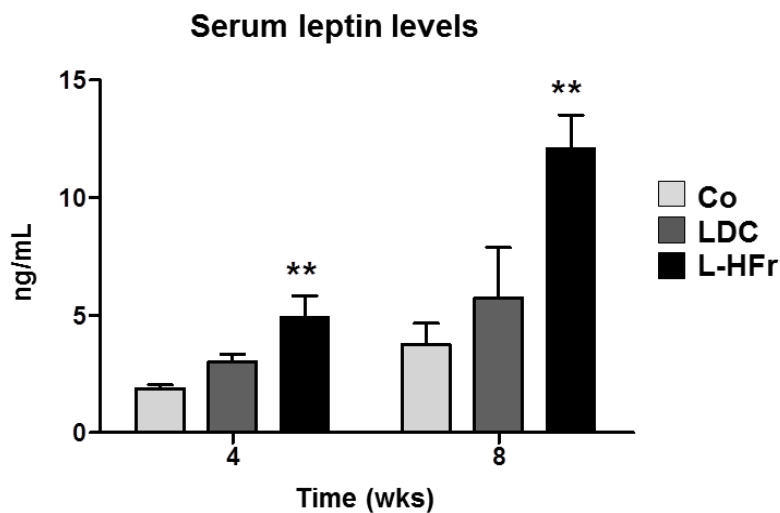


Figure 3.8 Fasting serum leptin levels. The values (ng/mL) were expressed as mean SEM of four rats per group. The rats were fed with Co: control, LDC: Lieber DeCarli diet or L-HFr: LDC + high (70% kcal) fructose for 4 or 8 wks. ** $P < 0.01$ vs. Co.

Part II: Lipocalin-2

3.4. Changes of hepatic inflammation- and metabolism-related genes

3.4.1. mRNA transcript of *Lcn2* increased significantly in the L-HFr group

To explore whether both animal models of nonalcoholic induced fatty liver (LDC and L-HFr) will noticeably express *Lcn2* in the liver tissue, qRT-PCR was used. Interestingly, the mRNA specific transcript of *Lcn2* was not significantly changed in the livers of LDC-fed rats at wk 4 and wk 8 compared to corresponding control rats. Alternatively, a significant increase of hepatic *Lcn2* expression was detectable in the L-HFr category at

wk 4 (90 ± 11 fold; $P < 0.001$) and at wk 8 (507 ± 28 fold; $P < 0.001$) (Figure 3.9). The extent of *Lcn2* mRNA in the L-HFr group was the highest among the other studied genes.

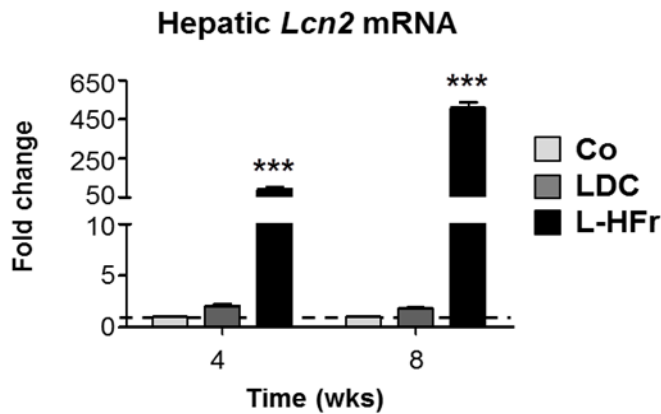


Figure 3.9 Bar plot shows relative expression of *Lcn2* in the liver. Each bar represents the mean \pm SEM of four rats/group at the 4th and 8th wk. * Indicates statistically significant difference (***) $P < 0.001$. The animals were nourished with standard chow pellet (Co), a freshly prepared liquid Lieber DeCarli (LDC) or LDC combined with 70% fructose (L-HFr).

3.4.2. Expression of inflammation-related genes in the liver samples

The following inflammation-related genes were measured in this study at wk 4 and 8: interleukin-8 (*Il-8*), a potent activator of polymorphonuclear neutrophils (PMN); *Mcp-1* which recruits monocytes and granulocytes; $\alpha 2$ -*m*, a positive acute phase protein in human and rat; *Tnf- α* , a pro-inflammatory cytokine; *Inos*, involved in innate immunity and oxidative conditions; and *Tlr4*, a pathogen recognition receptor. The regulation of these genes did not significantly differ between the LDC and the Co group at both time points. Conversely, in the L-HFr group, the mRNA expressions of *Il-8* (30-fold), *Mcp-1* (4.9-fold), $\alpha 2$ -*m* (9.4-fold), *Tnf- α* (4.5-fold), *Inos* (5.6-fold) and *Tlr4* (7.1-fold) were significantly augmented at wk 4 (Figure 3.10 A-F). Noticeably, upregulations were also found of *Il-8* (13-fold), *Mcp-1* (3.6-fold) and $\alpha 2$ -*m* (5.7-fold) in the L-HFr group at wk 8 (Figure 3.10A-C). At this time point, however, no significant changes in *Tnf- α* , *Inos* and *Tlr4* expression were found in the same group (Figure 3.10D-F).

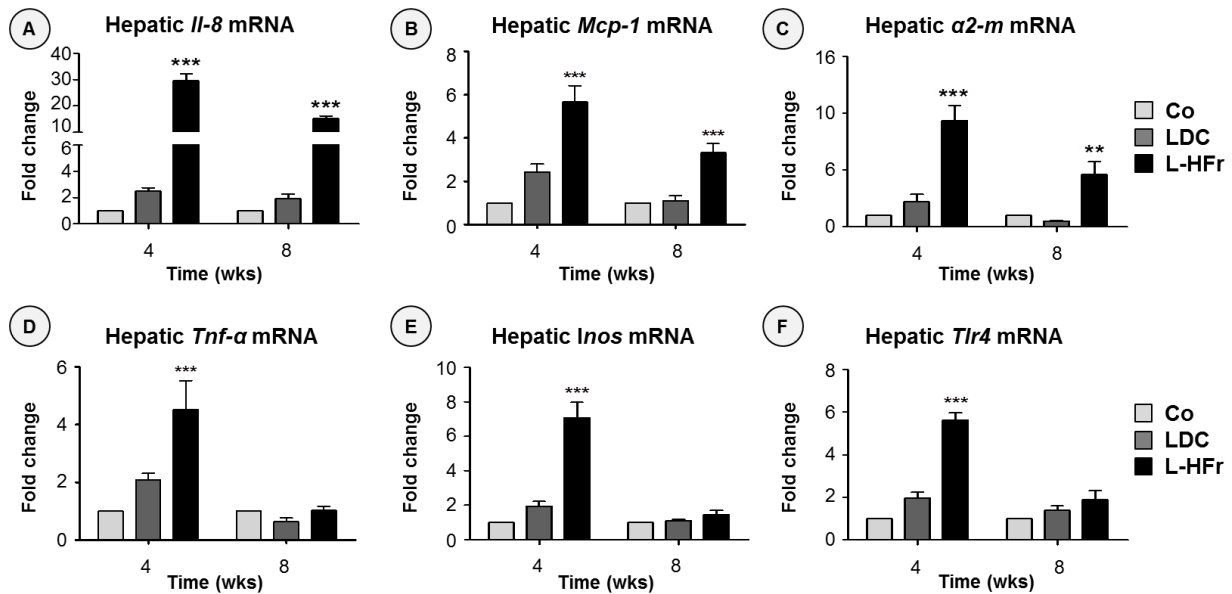


Figure 3.10 Changes of specific mRNA transcription in the liver. Each bar represents as mean \pm SEM of four rats/group at wk 4 and wk 8. Data were normalized by ubiquitin C (Ubc). β -actin (Actb) was additionally used as a reference housekeeping gene. Standard chow pellets (Co), a freshly prepared liquid LDC: Lieber DeCarli (LDC), and LDC combined with 70% fructose (L-HFr). * Indicates statistically significant difference (***) $P < 0.001$.

3.4.3. Hepatic *Glut5* and *Lep-r* transcripts were elevated in the L-HFr regimen

Under the LDC regimen, both levels of *Glut5* (the major fructose transporter) and *Lep-r* (leptin receptor) mRNA expression remained almost at the level of the controls. In contrast, *Glut5* mRNA was considerably enhanced at wk 4 (seven-fold) and wk 8 (six-fold) in the L-HFr-challenged rats compared to controls (Figure 3.11G). Concomitantly, hepatic *Lep-r* specific transcripts were substantially raised 9.2-fold (wk 4) and six-fold (wk 8) in L-HFr fed animals (Figure 3.11H).

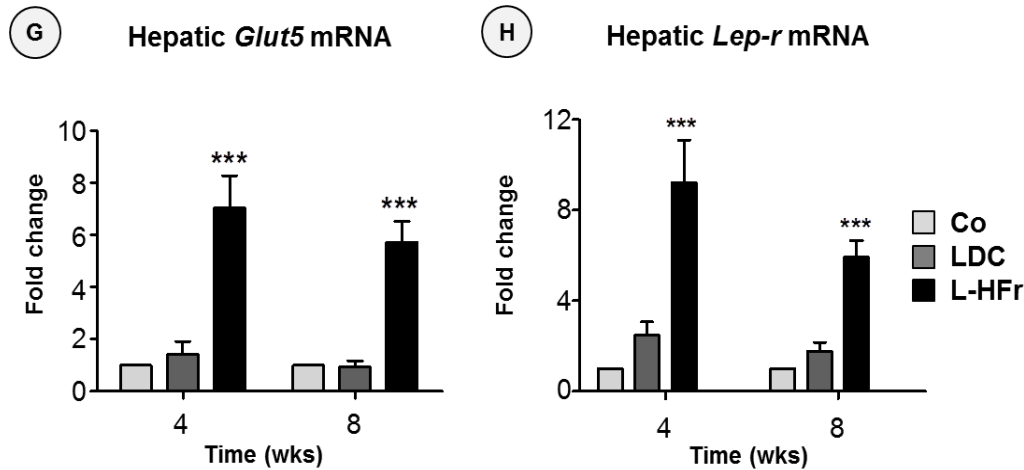


Figure 3.11 Modulations of *Glut5* and *Lep-r* mRNA in the liver. The rats were fed chow pellets (Co), a freshly prepared liquid LDC: Lieber DeCarli (LDC) or LDC combined with 70% fructose (L-HFr). * Indicates statistically significant difference (***) $P < 0.001$.

3.5. Changes of the hepatic LCN2 expression at protein levels

L-HFr treated animals showed an increase of LCN2 expression in the liver. Western blots were used to detect the amount of hepatic LCN2 protein. The expression of LCN2 protein was almost similar in the LDC and the control group. Along with an increased *Lcn2* mRNA expression in the L-HFr group, the expression of LCN2 protein in the total liver homogenates was clearly upregulated (Figure 3.12). Prominently, the maximal increase of hepatic LCN2 protein was at wk 8.

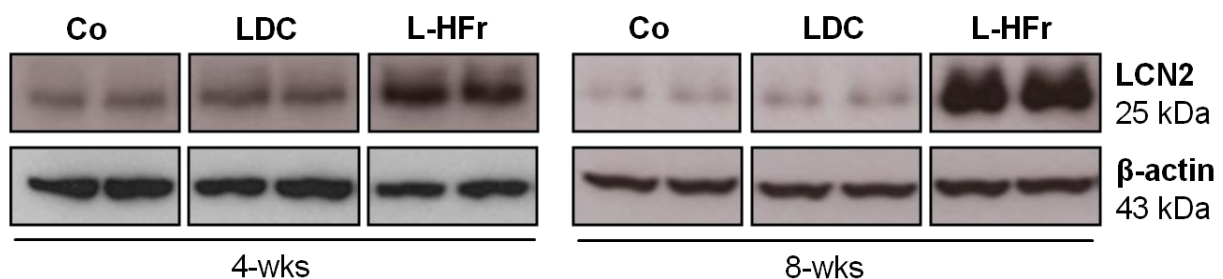


Figure 3.12 Changes in LCN2 protein expression in the rat liver. Representative immunoblots for LCN2 proteins. The animals were fed with standard chow (Co), Lieber-DeCarli (LDC), or LDC plus 70% fructose (L-HFr).

3.6. Immunohistochemical detection of LCN2, MPO and ED1 in rat liver

Immunofluorescence staining proved the tissue specific LCN2 localization. The positivity of LCN2 in the liver was restricted to MPO⁺ cells (Figure 3.13, left-panel). Only a few LCN2⁺ cells were observed in the normal (healthy) liver tissues. The LDC fed animals presented a similar view as seen in controls, but some LCN2 signals were observed in MPO⁺ cells in the periportal area mainly at wk 8 of the study. Interestingly, the highest LCN2 positivity was detected in the MPO⁺ PMN in the livers of the L-HFr group. A possible overlapping between anti-MPO and anti-ED1 was examined by double-immunostaining. The positivity of each marker was entirely separated (data not shown), indicating that MPO is a PMN-restricted marker.

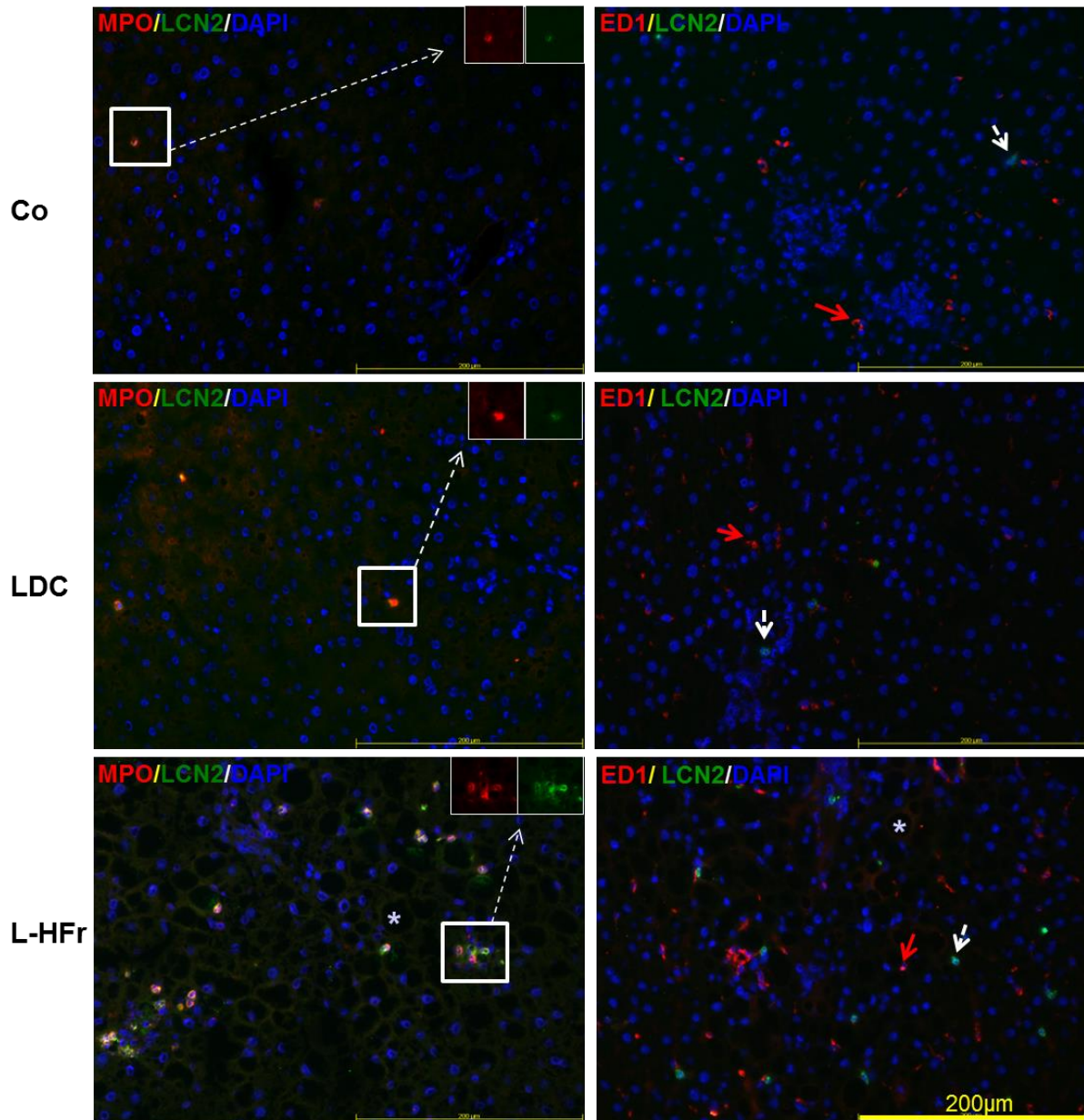


Figure 3.13 Immunolocalization of hepatic LCN2. The LCN2 was double-stained with MPO (a marker for PMN, left-panel) and ED1 (a marker for macrophages, right-panel) at wk 4. A co-localization of LCN2 and MPO can be detected in the liver sections. The blue color indicates the nuclei stained with DAPI. The black cavities (vesicles) that were marked by star (*) in the L-HFr micrographs resulted from washing, off of the fat from the HCs during the fixation step. The red *arrows* in the right panel show ED1⁺ cells, while the white *arrow* shows the LCN2⁺ cells. Scale bar = 200 µm. MPO: myeloperoxidase, PMN: polymorphonuclear neutrophils, ED1: ectodysplasin (CD68), Co: chow diet, LDC: Lieber-DeCarli liquid diet, and L-HFr: LDC + 70% fructose.

3.7. Serum levels of LCN2

Serum LCN2 was detected by ELISA. At wk 8, the concentration of serum LCN2 tended to be higher than the concentration at wk 4 in all groups (Figure 3.14A). The LDC group showed a mild increase in serum LCN2 when compared to controls. Conversely, the concentration of LCN2 in bloodstream revealed by ELISA was clearly augmented in the fructose fed animals (Figure 3.12A). At wk 4, the L-HFr fed rats evidenced a two-fold ($P<0.05$) enhancement in the level of serum LCN2, and a more than 2.2-fold ($P<0.05$) increase at wk 8 in the LCN2 magnitudes. The increase of circulatory LCN2 protein was further confirmed by Western blots (Figure 3.14B).

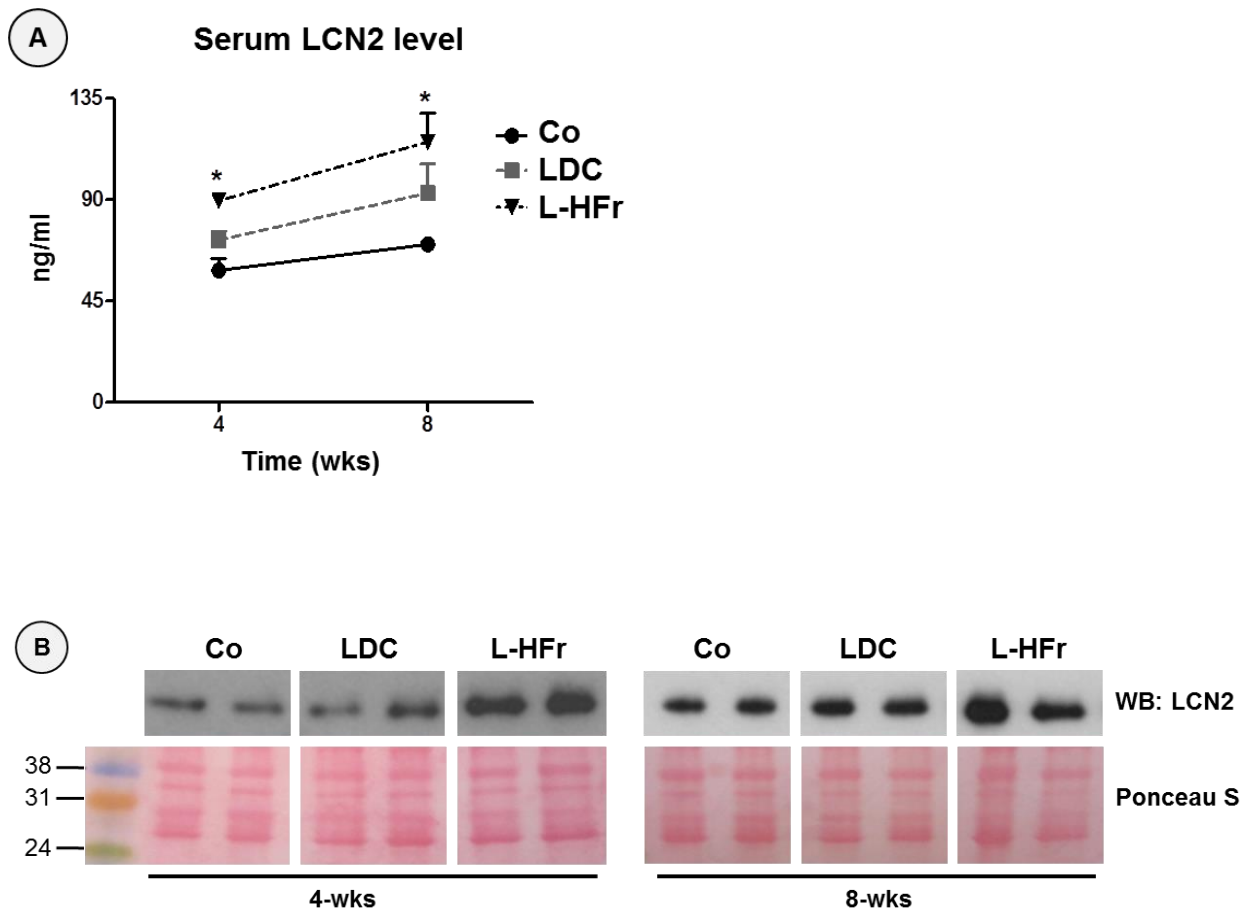


Figure 3.14 Upregulation of systemic LCN2 levels was seen in the L-HFr group. Serum LCN2 data (A), values on y-axis were expressed in ng/mL. (B) Representative autoradiographies from Western blots determination and the corresponding Ponceau stained membranes of two animals per group are shown. Co: Chow diet, LDC: Lieber DeCarli, and L-HFr: LDC + 70% fructose. * $P<0.05$ vs. Co.

3.8. Modulations of hepatic expression of inflammation-related proteins

Concurrently, the fructose-enriched diets evidently stimulated the protein expression of CD14, a multifunctional protein involved in TLR4 signal transduction and apoptosis, and MAPK (ERK), is activated by phosphorylation in response to stress and coordinates pro-apoptotic functions. Markedly, hepatic I κ B α 1 protein expression was considerably attenuated in the L-HFr group at wk 8 (Figure 3.15).

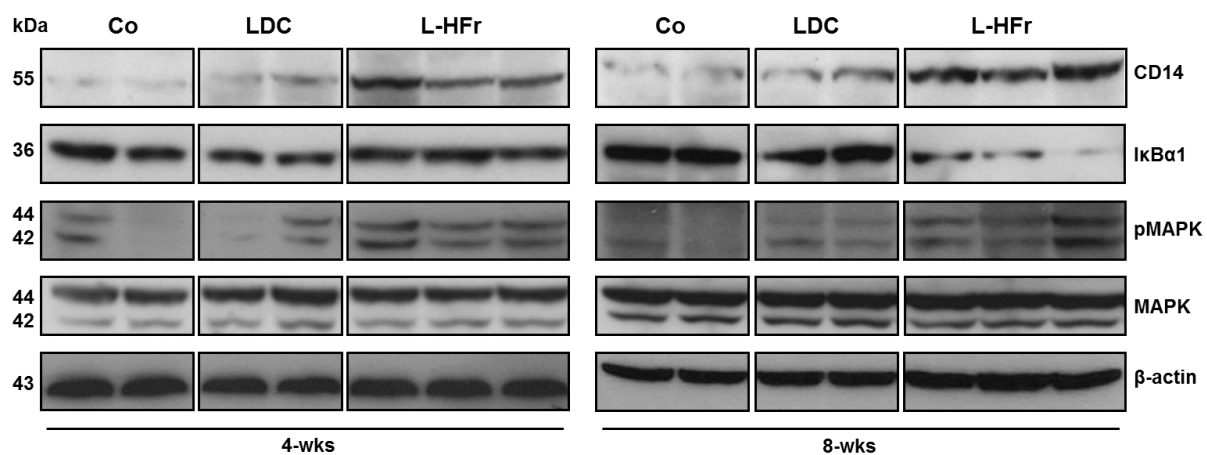


Figure 3.15 Changes in the expression of liver inflammation-related proteins. Representative immunoblots for inflammation-related proteins in the liver. Co: Chow diet, LDC: liquid Lieber-DeCarli diet, and L-HFr: LDC + 70% fructose.

3.9. Metabolism and oxidative stress related indicators

To study whether chronic dietary fructose impairs mitochondrial and/or endoplasmic reticulum functions, Western blots were performed on hepatic casp 9, the initial casp in the mitochondrial apoptotic cascade in response of ROS, and GRP78 a molecular chaperone correlates with endoplasmic reticulum stress. It regulates the unfolded protein response and 4-HNE, a specific end product of lipid peroxidation.

In contrast to the Co and the LDC diet, the L-HFr diet induced casp 9, GRP78, and 4-HNE at both time points (Figure 3.16). However, Cyt *c* protein, required for mitochondrial function and apoptosis, was maximally increased at wk 8. Additionally, it has been known that PGC-1 α plays a crucial role in the mitochondrial biogenesis (Zhou *et al.* 2012). In the present study, the data showed that the L-HFr diet clearly

diminished the hepatic PGC-1 α protein expression at wk 8 (Figure 3.16). This result was inversely correlated to the patterns of liver LCN2 protein.

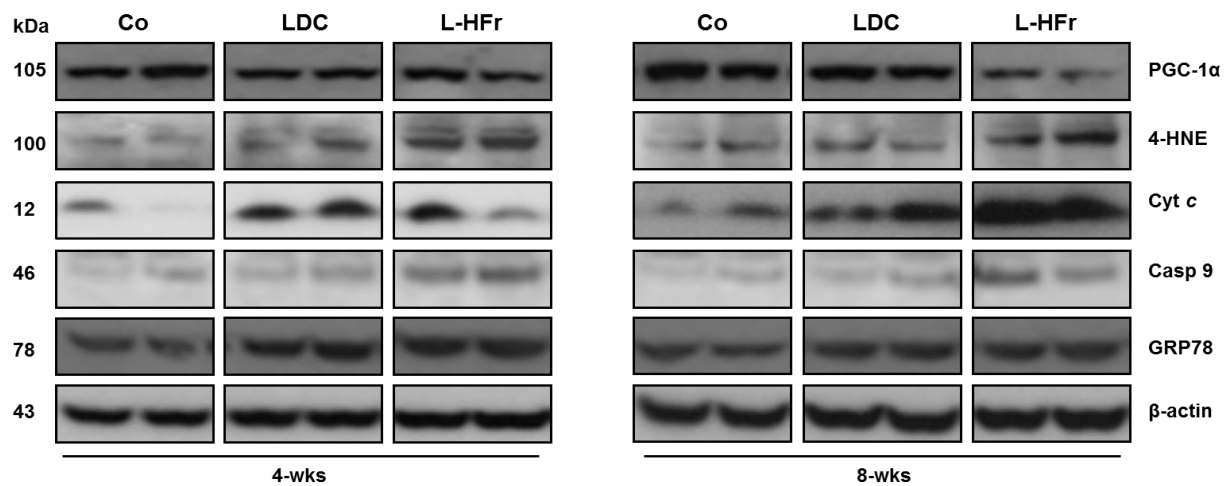


Figure 3.16 Changes in oxidative stress related proteins in the liver. Co: Chow diet, LDC: Lieber DeCarli, and L-HFr: LDC + 70% fructose. Representative immunoblots were shown per group.

3.10. 2-DE data analysis

To screen other possible biomarkers, four animals per group were used for hepatic 2-DE analysis. Phospho- and silver-staining were performed (Figure 3.17). However, no significant regulated protein spot was found in the region between 20 and 37 kDa.

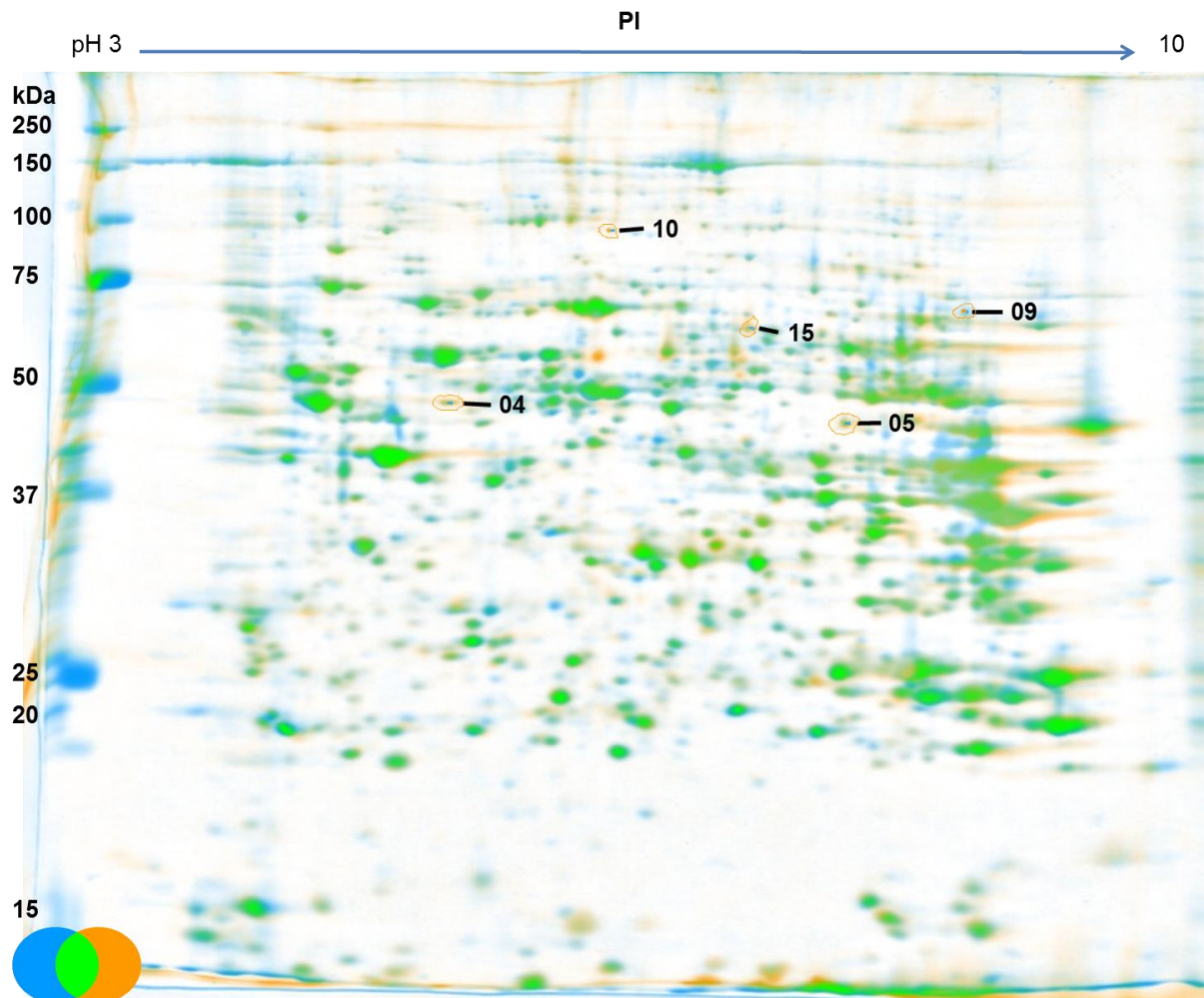


Figure 3.17 Representation of two gel images warped by the software Delta2D. The digitized images of the master gel (Blue) and the L-HFr group (orange) after a silver-nitrate staining of total liver homogenate were placed one above the other by Delta2D. Green color shows the overlapping spots.

3.10.1. Proteins with significantly altered amount

For investigation of proteins modulated by treatment of rats with L-HFr diet, tissue extracts were prepared from treated and untreated rats and separated by 2-DE. One phosphoprotein (spot label 2) was significantly higher phosphorylated on treatment of rats with HFr-diet.

On comparative computational analysis of images of silver-stained 2-DE gels, five spots revealed changes in relative intensity. Significant differences ($P < 0.05$) in protein intensity were observed between L-HFr and control or LDC rats for all spots. Four proteins significantly displayed more intense staining in the L-HFr-group (Figure 3.18). Intensity of one spot was significantly lower in the same group compared to the control or LDC group.

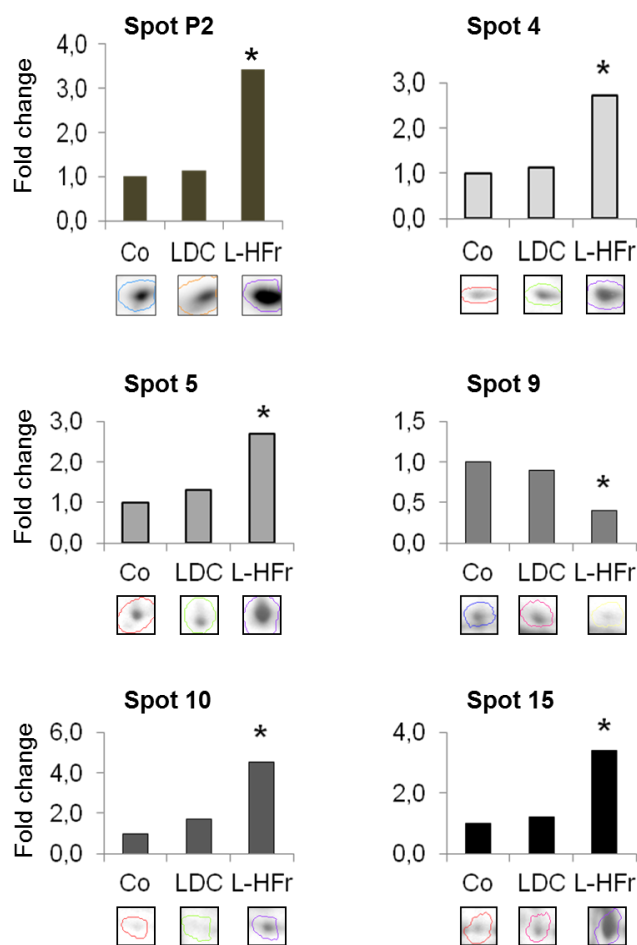


Figure 3.18 Representative protein spots of phospho and silver stained 2-DE gels. Total protein hepatic lysate from Co, LDC or L-HFr fed rats was separated by 2-DE and then stained by phospho and silver stain. Encircled differentially regulated protein spots were identified using Delta 2D software. The figure shows exemplary protein spots from 2-DE gels of each experimental group. In addition, Delta 2D software was used for densitometric analysis as illustrated in the bar chart as fold change ($*P < 0.05$). Co: control, LDC: Lieber-DeCarli, L-HFr: LDC + 70% kcal fructose diet for 4 wks.

3.11. Expression of LCN2 *in vitro*

3.12.1. Expression of LCN2 in isolated rat HCs was upregulated by fructose

The rat primary HCs were isolated and cultured kinetically in M199 containing either 20 mM glucose or fructose for 0, 3, 6, 12, and 24 h. After 6 h and 12 h, *Lcn2* specific transcripts were more pronounced in fructose-incubated HCs than glucose-incubated HCs at the corresponding time points (Figure 3.19).

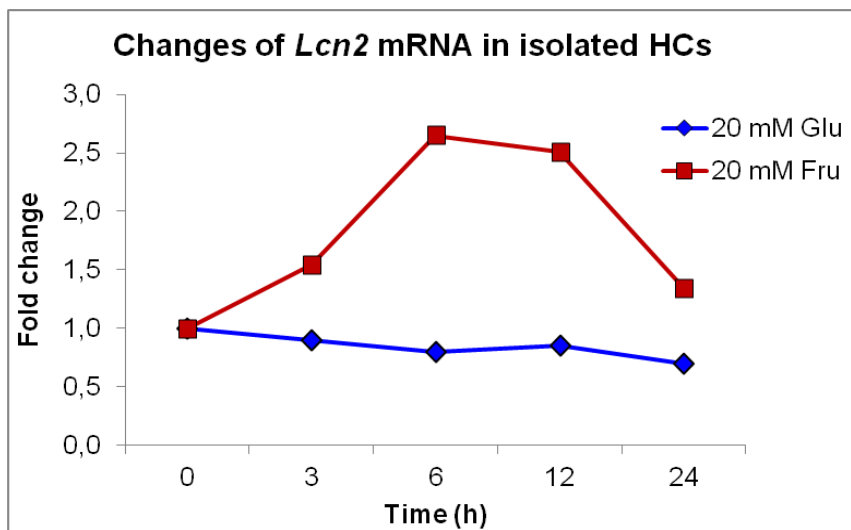


Figure 3.19 Changes of *Lcn2* expression in the isolated primary HCs. The rat cultured cells were kinetically incubated in either 20 mM glucose (Glu) or equimolar fructose (Fru) containing M199 medium for 0, 3, 6, 12 h. HCs: hepatocytes.

The RT-PCR data were confirmed by Western blots (Figure 3.20). The time effect of the 20 mM dose of glucose on LCN2 expression in the HCs was minimal. Instead, in the first 3 h of fructose treatment the LCN2 expression evidently elevated upwards to 12 h. All time points of fructose treatment showed a clear increase in expression of LCN2 compared to that found in equimolar glucose treatment.

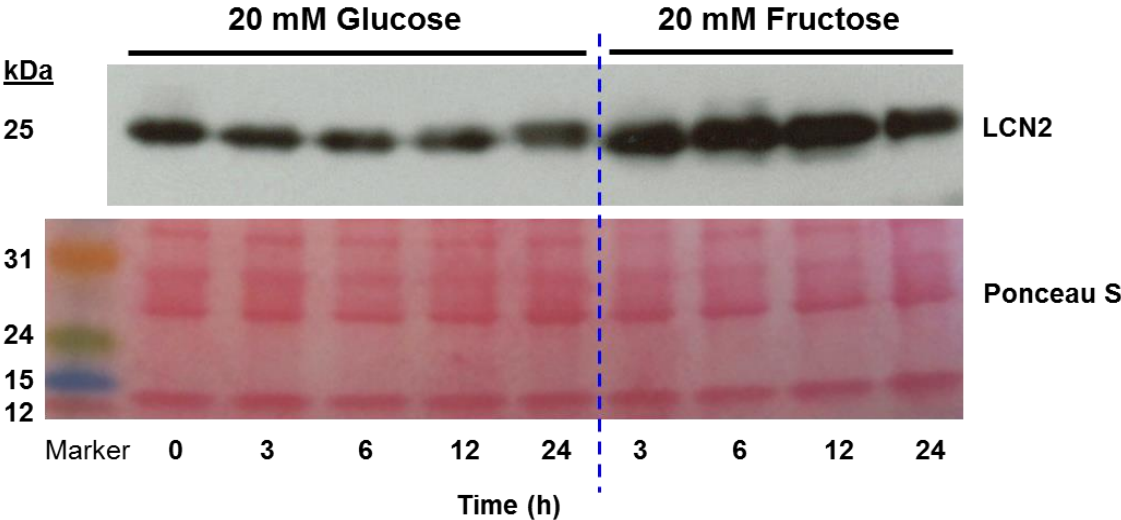


Figure 3.20A Changes of LCN2 protein expression in cultured HCs. The rat cells were kinetically treated with either 20 mM glucose or equimolar fructose containing M199 medium for 0, 3, 6, 12 h. HCs: hepatocytes.

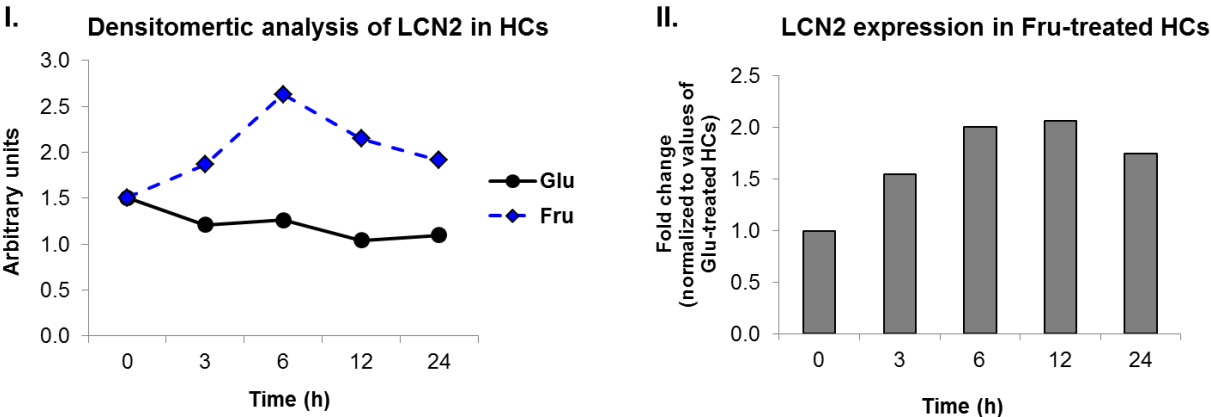


Figure 3.20B Densitometric analysis (I) and fold change (II) LCN2 expression. The HCs were kinetically treated with either 20 mM glucose or equimolar fructose containing M199 medium for 0, 3, 6, 12 h. HCs: hepatocytes.

4. DISCUSSION

In the present study, the experimental *animals* were fed with a Co, LDC or L-HFr diet for 4 wks or 8 wks. The LDC and the L-HFr animal model developed fatty liver. The LDC diet induced simple steatosis, while L-HFr induced NASH and metabolic syndrome in the rats broadly as reflected in the pathophysiology of human NASH. A significant upregulation of LCN2 expression in the liver and serum was observed in the L-HFr induced NASH group. Indeed, LCN2 serves as a serological marker for diagnosis NASH in this animal model. Since LCN2 expression is influenced by inflammatory and other stressful conditions, its specificity is not yet well defined. The localization, the regulation and the role of LCN2 are still controversially discussed in the literature. However, in the present models the LCN2 positivity in the liver tissue was detected in PMN.

4.1. Animal phenotypes and NAFLD

Male Sprague-Dawley rats were used in this study due to their calmness and easy handling. In contrast to genetically identical inbred mice, the genetic polymorphism in these rats can be used to show the diversity of the responsiveness which appears in the population as a result of the genetic variety (Kacew and Festing 1996). Since sex hormones (e.g. estrogen) in the female animal increase fat deposition, LDL-C levels and obesity (Brown *et al.* 2010), and thus may interfere with the diet effects, male rats were preferred in this study. The other existing animal models were mostly genetically-modified ones, e.g. *ob/ob*, *db/db*, and ZF *fa/fa*, which do not mimic human conditions (Charlton *et al.* 2011). For instance, most features of steatohepatitis could be reproduced, but without features of the metabolic syndrome (ZF *fa/fa*) or vice versa (*ob/ob* and *db/db*) (Charlton *et al.* 2011; Takahashi *et al.* 2012). Another disadvantage of existing animal models is feeding the rats with a diet lacking choline and methionine, which creates a nutritional deficiency that is not common in patients with NASH but to which rodents are selectively sensitive (Lieber *et al.* 2004). Therefore, presence of a representative NAFLD animal models is of crucial impact, not only to elucidate the pathogenesis of simple steatosis to NASH, but also to investigate the therapeutic effects of various agents (Takahashi *et al.* 2012).

The LDC diet (36% kcal fat) is a nutritionally complete liquid diet widely used for modeling (in rodents) the pathological NAFLD changes manifested in humans (Bertola *et al.* 2013; Cohen *et al.* 2009). In these studies, the LDC diet resulted histologically in a simple hepatic steatosis (without inflammation), and no significant increases of serum TG concentration and activities of ALT and AST compared to chow diet (Lieber *et al.* 2004). Indeed, these features of the LDC animal model were exhibited in the current study. Hence, the LDC diet developed a typical simple steatosis in the rat liver.

Fructose is included in commercial/fast food as well as juice beverages, and it is consumed frequently. It was shown in several animal experiments that a diet rich in fructose (e.g., up to 60% of the daily caloric intake) may lead to the development of NAFLD in rodents but may also result in the development of IR, dyslipidemia and oxidative stress (Spruss *et al.* 2012). Since the amount of uptake varies in human beings, several studies use different percentages of fructose (e.g. 30% kcal (Spruss *et al.* 2012) and 60% kcal (Haring and Harris 2011)) to investigate its effects on NAFLD and other metabolic disorders. Moreover, it has been reported that the onset of fructose-induced NAFLD is associated with intestinal bacterial overgrowth and/or increased intestinal permeability (Spruss *et al.* 2009). This facilitates the influx of LPS via portal blood and subsequent inflammation in the fatty liver (Spruss *et al.* 2012). Based on these studies, the L-HFr diet was selected to develop a NASH model and to investigate whether LCN2 could serve as a diagnostic biomarker.

In the current study, there were no significant differences between the control and LDC groups regarding the total calorie consumption and initial as well as final BW. On the contrary, the highest food intake was observed in the L-HFr group. Unexpectedly, the BW of the L-HFr fed rats was reduced by 30% and 15% at wk 4 and wk 8, respectively, compared to age-matched controls. However, the rats of this group possibly restore their BW if they are fed for longer. These findings were also described by Bruggeman *et al.* in their experiment where female rats were nourished with a high-fructose diet containing 10% kcal fat, 20% protein, 60% fructose, 10% corn (Bruggeman *et al.* 2011). The paradoxical correlation between food consumption and BW of the animals could be related to the hepatic inflammation seen in the L-HFr regimen especially at wk 4. In fact, the most pronounced elevation

of hepatic inflammatory mediators, such as *Il-8*, *Mcp-1*, *α2-m* and *Tnf-α*, was found at this time point.

Up to 56% of NALFD patients present obesity and hepatomegaly at the time of physical examination (De Lusong *et al.* 2008; Paschos and Paletas 2009). Although the L-HFr fed rats showed a significant decrease in their BW compared to the Co group, visceral fat deposition and obvious hepatomegaly were observed in this group. Furthermore, the LW:BW ratio was significantly increased in the L-HFr fed rats similar to the findings of Bruggeman *et al.* (Bruggeman *et al.* 2011). Taken together, rats of the L-HFr group showed physical features comparable to human patients with NAFLD.

4.2. The effect of the diets on the histopathological manifestations of NAFLD

The LDC diet induced simple steatosis (NAFL type 1), while the L-HFr diet developed the typical criteria of hepatic lesions of NASH (NAFL type ≥ 2), namely extreme steatosis and moderate inflammation (grade 2) noticed mainly in zone I, whereas ongoing fibrosis was reproduced at both time points. Most importantly, NASH criteria (Angulo 2002; Tilg 2004) includes also a hepatocellular ballooning in the centrilobular areas. The presence of ballooned HCs is generally regarded to be a form of apoptosis (Tilg 2004; Yip and Burt 2006) and is associated with steatohepatitis, regardless whether its etiology was alcoholic or nonalcoholic (Lackner *et al.* 2008). According to the literature, these features are typical for human NASH (Charlton *et al.* 2011). Indeed, under the L-HFr regimen, hepatocellular ballooning was often seen in the area surrounding the central vein.

Although the pathogenesis of NASH has not yet been fully elucidated, a popular mechanism is the "two-hit" theory, in which the first hit is the accumulation of fatty acids in the liver (Lieber *et al.* 2004). One major promoting factor of this first hit is IR, which is present in most patients with NASH (Chitturi *et al.* 2002a). The second hit is the lipid peroxidation due to the oxidative stress produced by different factors, such as mitochondrial abnormalities, CYP2E1 induction, and endotoxins (Angulo and Lindor 2001). The 4-HNE adducts, by-products of lipid peroxidation, are also known to stimulate collagen (fibrosis) production (Houglum *et al.* 1990). In the present study, the fructose-supplemented diet induced more deleterious effects to the liver than the

LDC diet. Overall, the presence of ballooned HCs implies the development of NASH in the L-HFr group. Hence, the L-HFr regimen reproduces the key features of human NASH.

4.3. Metabolic syndrome and serum transaminase

Accompanied with NASH, the hallmarks of metabolic syndrome, e.g. an elevation of fasting plasma glucose, high TGs and low HDL-C levels, were found in humans (Adiels *et al.* 2006; Papakonstantinou *et al.* 2013). In contrast to the ZF *fa/fa* rat model (Charlton *et al.* 2011) and the LDC diet used in the current study, these features were indeed present in the L-HFr fed rats. Thus, this animal model is similar to the clinical pathophysiology of human NAFLD.

After intestinal uptake, fructose is typically extracted from the blood stream by the HCs, independent of insulin exertion and the phosphofructokinase regulation step. Next, within the liver the acquired fructose is metabolized to glucose, fatty acids or lactate (Tappy and Le 2010). A significant upregulation of hepatic *Glut5* (fructose transporter) gene expression was observed in the L-HFr nourished animals, which correlated with the accumulated fat in the liver. It has been stated that high fructose intake is associated with increased plasma TGs, most probably caused by an upregulation of hepatic *de novo* lipogenesis and TGs secretion, and a decreased clearance of VLDL-TG (Johnson *et al.* 2007). At this point, the L-HFr fed rats promoted the onset of massive hepatic steatosis mainly in zone I and II in this experiment.

Circulating ALT and AST are known indicators of liver damage and present in very low concentrations in the circulation of healthy individuals (Yuzer *et al.* 2009). On contrast, most of the patients with simple steatosis are usually clinically asymptomatic, whereas their serum transaminase levels may be elevated, most frequently serum ALT (Ekstedt *et al.* 2006; Yu and Keeffe 2003). It was also reported that a low normal ALT value does not guarantee freedom from underlying steatohepatitis, especially when there is advanced fibrosis (Mofrad *et al.* 2003). In fact, the activities of serum ALT and AST in the LDC regimen were mildly higher than the control but not significantly so. This finding is also not uncommon in the human disease, for which a significant increase in ALT activity has been reported in less

than one-third of the patients (Diehl *et al.* 1988; Lieber *et al.* 2004). In fact, the L-HFr group showed a significant increase in the serum transaminase activities as found in most human cases with NASH (Francque *et al.* 2012). Thus, a reliable predictor to differentiate between the simple steatosis and NASH is still required.

The L-HFr diet induced a substantial elevation of fasting leptin levels. It has been stated that fructose promotes leptin resistance in rodents and humans (Gray *et al.* 2013; Shapiro *et al.* 2008), whereby the leptin action was suppressed and did not induce satiation (fullness). In this context, there are two popular mouse models of a spontaneous mutation in the leptin *ob/ob* or its receptor *db/db* gene. The *ob/ob* mice are hyperphagic (eat extensively), inactive and extremely obese. The *db/db* mice show normal or elevated levels of leptin but are resistant to the effects of leptin (Takahashi *et al.* 2012). This possibly explains the increased food consumption noted in the L-HFr group compared to the Co or the LDC groups.

The advantage of *ob/ob* and *db/db* mice is that the phenotype of these mice simulates the human condition of the metabolic syndrome in many aspects except physiological leptin levels and/or action (Nagarajan *et al.* 2012; Takahashi *et al.* 2012). While both models develop spontaneous hepatic steatosis, it does not progress spontaneously to steatohepatitis or fibrosis (Takahashi *et al.* 2012). Leptin is not only a critical regulator of BW and appetite, but its role as a proinflammatory mediator has also gained attention in NASH (Chatterjee *et al.* 2013). In NASH patients serum leptin levels are increased compared with gender and BMI matched controls (Chitturi *et al.* 2002b). Furthermore, serum leptin levels were independently associated with the amount of steatosis and inflammation but not with fibrosis (Chitturi *et al.* 2002b). Together, key features of the metabolic syndrome and elevated serum transaminase activities under the L-HFr regimen are similar to pathological conditions seen in humans.

4.4. LCN2 expression in the liver and serum of L-HFr fed rats

It has been reported that the expression of LCN2 is influenced by pro-inflammatory factors (Fujino *et al.* 2006). In addition, the studies showed that LCN2 has emerged as a potential link between obesity, inflammation, and obesity-associated metabolic dysfunction such as IR (Wang *et al.* 2007).

The expression of hepatic LCN2 was significantly increased at gene as well as protein levels accompanied by elevated serum level in the L-HFr regimen compared to the Co or the LDC group at wk 4 and wk 8, respectively. As the LDC group showed primarily simple steatosis, it can be considered as a control for the L-HFr induced NASH group. While the LDC as well as the L-HFr models showed fatty liver, the significant expression of LCN2 in the liver and serum was seen in the L-HFr model. Thus, LCN2 is a biomarker for NASH in the present study.

Studies of NAFLD in humans have limitations. This is due to the fact that progression of simple steatosis to NASH takes years, and the ethical limitations in administering drugs to or collecting liver tissues from patients (Takahashi *et al.* 2012). The tools widely used for assessment of NAFLD cannot classify the stage of the disease (Tarasow *et al.* 2002). Biopsy studies show that progression of NASH to fibrosis occurs in approximately 40% of patients, but most of these patients do not show clinical or biochemical deterioration (Lall *et al.* 2008). Also, routine liver function tests, such as serum ALT activity, cannot guarantee absence of underlying steatohepatitis (Mofrad *et al.* 2003). Thus, there is a need for a reliable noninvasive biomarker to monitor the shift from simple steatosis (benign and readily reversible form (Hubscher 2004)) to NASH (a progressing form). In this study, the increased systemic LCN2 level in the L-HFr group could be shown. However, specificity of the LCN2 as a diagnostic indicator is low unless other causes of liver inflammation can be excluded.

The following factors that induce liver inflammation should be considered: γ -irradiation, turpentine oil toxins, medical drugs (Patel and Sanyal 2013) and autoimmune cholangiopathies. The general goal in the treatment of NASH is to correct risk factors with exercise and appropriate diet and to avoid drugs such as tamoxifen and steroids which exacerbate liver disease (Lall *et al.* 2008).

4.5. Localization and possible role of LCN2 in the liver

As most experimental models that studied LCN2 were with *Lcn2*KO mice, no focus was placed on the localization of this protein in the liver. Hence, the pathological significance of the localization of LCN2 in the liver needs clarification. In the present study, a double-immunofluorescence staining was performed to detect LCN2 co-localization with MPO⁺ and/or ED1⁺ cells in the liver tissues. This immunostaining

demonstrated hepatic LCN2 positivity in MPO⁺ neutrophil granulocytes and confirms previous findings in the literature (Sultan *et al.* 2013).

One study that defines the localization of LCN2 in mice fatty liver found LCN2-expressing HCs were localized around the inflammatory cell clusters (Semba *et al.* 2013). However, immunoperoxidase staining with a single antibody was used to detect hepatic LCN2 positivity in this study (Semba *et al.* 2013). Thus, exact localization of LCN2 in the liver will be rather difficult. Similarly, another study detected LCN2 positivity in HCs of liver sections using the same method (Borkham-Kamphorst *et al.* 2011) (Appendix Table 1).

The studies (Borkham-Kamphorst *et al.* 2011; Sultan *et al.* 2013; Sultan *et al.* 2012) that found increased *Lcn2* expression by various stimuli in primary rat HCs used the cell isolation method according to Seglen (Seglen 1973). It has been reported that unlike LCN2 expression in cultured HSC, freshly isolated HCs do not express LCN2. Upon culturing, however, the respective mRNA and protein levels increased dramatically in time-dependent fashion (Borkham-Kamphorst *et al.* 2011) probably owing to the fact that conventional monolayers of cultured HCs develop autocrine TGF- β -mediated apoptosis (Gressner *et al.* 1997). However, Seglen's method was discussed as a method of HCs enrichment, as the purity of the HCs is 90%, thus it is not an absolutely pure method (Ates M *et al.* 2012; Wojcik *et al.*, 2012). Primary rat HCs were isolated and treated with 20 mM glucose or fructose in the current study. Fructose-treated HCs significantly expressed LCN2. In comparison to *in vivo* studies, where *Lcn2* mRNA expression in liver showed a 90-fold and 507-fold increase at wk 4 and wk 8, respectively, the *Lcn2* gene expression was maximally 2.5-fold higher than in controls of the cultured HCs.

Although it was able to detect the expression of the hepatic LCN2 in the L-HFr-fed rats by WB in this study, the immunofluorescence staining did not show LCN2⁺ HCs in rat's liver. In addition, there were no significant changes in the proteins in the range of 20-37 kDa by using 2-DE analysis. These findings indicate that LCN2 (25 kDa) is most probably expressed by a minority of liver cells than in HCs. Indeed, it was previously shown that a macrophage-specific protein was not detectable in liver total homogenates by using 2-DE. In contrast, this protein was clearly detectable in protein extracts from a macrophage cell line using the same method (Wojcik *et al.* 2012).

The sensitivity of WB is higher than normal 2-DE ([Kumar *et al.* 2013](#); [Wise and Lin 1991](#)). Since most proteins of total liver homogenates are from HCs, the percentage of proteins from PMN may be beyond the sensitivity of 2-DE detection. This implies that other cell type (most probably PMN) rather than HCs could be the responsible cells for *Lcn2* expression *in vivo* as confirmed by the results of the immunofluorescence staining presented in this study.

The likelihood that changes in the concentration of hepatic fructose and its metabolites after intake could potentiate lipid peroxidation, alterations of endoplasmic reticulum and mitochondrial functions was assessed by 4-HNE adducts, GRP78, casp 9, Cyt *c* and PGC-1 α . The expression of 4-HNE adducts was markedly higher in L-HFr fed rats than in controls. This result is similar to findings of other studies in rodent models of diet induced NAFLD ([Armutcu *et al.* 2005](#)), suggesting that the formation of ROS in the L-HFr group was markedly enhanced or ROS were less efficiently quenched. The hepatic oxidative stress in fructose-induced fatty liver is not caused by sulfur amino acid insufficiency ([Kunde *et al.* 2011](#)). Augmentations of GRP78, casp 9 and Cyt *c* expression were also noticed in L-HFr fed rats, suggesting that these rats, compared with the LDC or chow-fed rats, were facing elevated oxidative stress conditions. Additionally, 4-HNE chemotactically recruits PMN into the stressed liver (Figure 4.1).

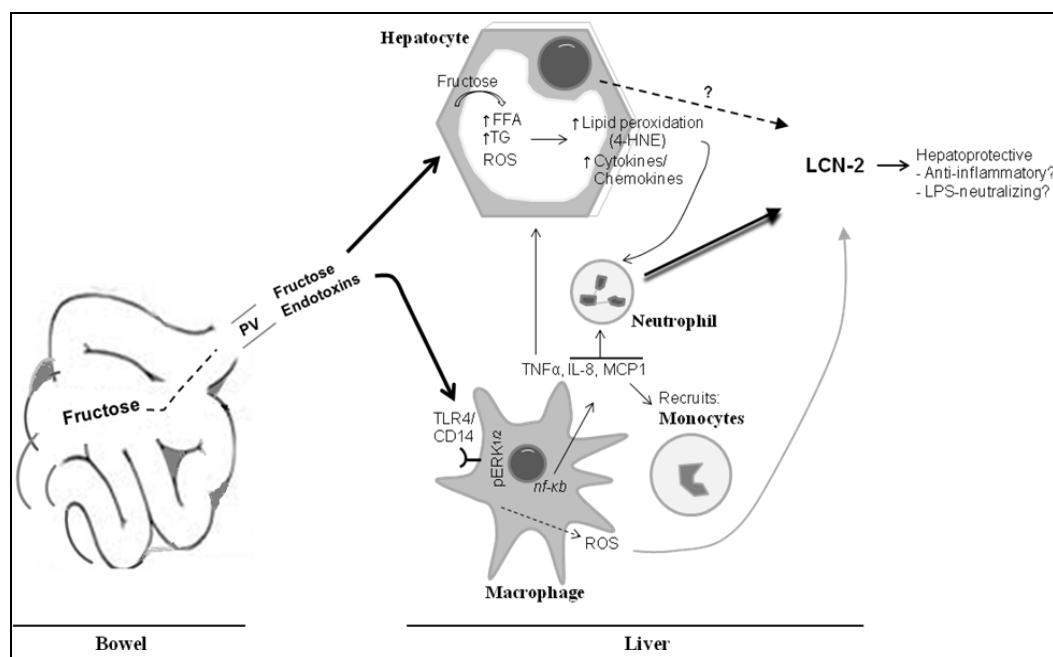


Figure 4.1 Hypothetical model of the mechanism of hepatic LCN2 production in L-HFr. Ingested fructose is delivered into the liver via portal vein. Once inside the liver, hepatocytes transformed fructose into FFAs and TGs. As a result of fat accumulation in hepatocytes, lipid peroxidation end products (e.g. 4-HNE), iNOS and other cytokines/chemokines will be produced, which could recruit PMN to the liver. In addition, chronic fructose consumption facilitates the influx of endotoxins (LPS) into the liver. Endotoxins stimulate KCs which, in turn, release ROS and cytokines. This results in recruitment of more PMN and monocytes to the liver. Further studies are needed to investigate whether LCN2 could act as hepatoprotective protein. KCs: Kupffer cells, PMN: polymorphonuclear neutrophils, PV: portal vein.

Although the cleaved casp 9 and the release of Cyto *c* were not measured in the current study, an important mitochondrial-biogenic protein (PGC-1 α) was explored. It was regarded that PGC-1 α expression in the liver is normally increased during fasting in response to glucagon (Herzig *et al.* 2001), and it also plays a central role in the regulation of cellular energy metabolism (Liang and Ward 2006) and mitochondrial function (Holmstrom *et al.* 2012). Interestingly, the protein expression of PGC-1 α was predominantly at wk 8 in livers from the L-HFr group. This was consistent with hepatocellular ballooning, providing further evidence for a decreased mitochondrial function. Taken together, these results indicated that chronic fructose-enriched diet altered, at least partially, mitochondrial and endoplasmic reticulum functions and induced cellular apoptosis and stress conditions. These conditions were associated with the significant increase in LCN2 expression.

It has been emphasized that fructose consumption is also correlated with elevated LPS levels in the liver, which can trigger the release of proinflammatory cytokines

when bound to CD14/TLR4 which are present in immune cells (Baker *et al.* 2011). Recognition of LPS by the CD14/TLR4/MD-2 complex activates intracellular signaling pathways involving MAPK, resulting in the production of proinflammatory cytokines and chemokines (Lin *et al.* 2004). It is known that chronic endotoxin that induces TLR4 activation can also induce liver fibrosis (Paik *et al.* 2003). Indeed, upregulated levels of hepatic TLR4, CD14 and p/ERK1/2 in L-HFr regimen were found at wk 4. In addition, the L-HFr diet potentiated stronger fibrosis - as observed by Masson's Trichrome staining - than the LDC and the Co diet. The multifunctional CD14, however, was also elevated in livers of the L-HFr group at wk 8. CD14, in addition to its important role in inflammation and innate immunity, promotes cell survival and antagonizes programmed cell death "apoptosis" (Heidenreich 1999). Overall, these findings, indirectly, suggest that the influx of endotoxins from the bowel into the liver via the portal vein could also be involved in the modulation of liver inflammation in L-HFr-treated rats by TLR4-dependent manner (Anurag and Anuradha 2002) (Figure 4.1).

Actually, several *Lcn2* knockout mouse models have been used to study the role of LCN2 in the liver. However, the data are controversial regarding whether LCN2 plays a role in recruiting the inflammatory cells to the site of injury and exacerbating the local inflammation (Pedersen *et al.* 2001), and regarding its role as an anti-inflammatory and protective protein (Zhang *et al.* 2008). In addition, the role of LCN2 in glucose metabolism and IR also remains contradictory (Guo *et al.* 2010; Jun *et al.* 2011). However, in the current study LCN2 is elevated in fructose-induced steatohepatitis, and thus it is a marker for hepatic inflammation. Functional studies are needed to evaluate, whether LCN2 upregulation might have a hepato-protective function.

4.6. Conclusion

Both of the applied diets induced NAFLD. While the LDC diet led to a simple steatosis, the L-HFr diet resulted in NASH. Fructose supplementation appears to worsen liver pathology. The key features of the metabolic syndrome and NASH with progressive fibrosis represent an animal model broadly similar to the typical conditions in human NASH. These findings highlight the impact of dietary composition in the development of NAFLD. The fructose diet upregulates hepatic

LCN2 gene expression in fructose-induced NASH. This correlates with increased indicators of inflammation, oxidative stress, and mitochondrial dysfunction. As the hallmarks of human pathophysiology were reproduced in this novel study, serum LCN2 could be emerging as a useful new biomarker to discriminate between simple steatosis and NASH. Evidently, an interaction exists between the metabolic impetus and inflammatory processes in the animals. The diet described in this study provides a useful model for further LCN2 studies in depth and the development of new insights for preventing NASH.

5. Outlook

The high-fructose induced NASH model may be used in further studies on the role of LCN2 in apoptosis. In addition, this model could be extended to study whether LCN2 are involved in liver protection, e.g. as a LPS-neutralizing factor. With this fructose rat model, additional biomarkers with higher specificity should be investigated. Since the present study highlights the controversial role of LCN2 in inflammation and insulin resistance, further studies should investigate this issue. Similarly, as the LCN2 localization remains controversial its significance deserves to be investigated. Translating the findings of the present model into human samples will reveal valuable insights into the pathogenesis of NASH in humans.

6. References

- Abdelmalek MF, Suzuki A, Guy C, Unalp-Arida A, Colvin R, Johnson RJ, Diehl AM (2010): Increased fructose consumption is associated with fibrosis severity in patients with nonalcoholic fatty liver disease. *Hepatology* 51:1961-71
- Adams LA, Angulo P (2005): Recent concepts in non-alcoholic fatty liver disease. *Diabet Med* 22:1129-33
- Adams LA, Lymp JF, St Sauver J, Sanderson SO, Lindor KD, Feldstein A, Angulo P (2005): The natural history of nonalcoholic fatty liver disease: a population-based cohort study. *Gastroenterology* 129:113-21
- Adiels M, Olofsson SO, Taskinen MR, Boren J (2006): Diabetic dyslipidaemia. *Curr Opin Lipidol* 17:238-46
- Akar F, Uludag O, Aydin A, Aytakin YA, Elbeg S, Tuzcu M, Sahin K (2012): High-fructose corn syrup causes vascular dysfunction associated with metabolic disturbance in rats: protective effect of resveratrol. *Food Chem Toxicol* 50:2135-41
- Alpini G, McGill JM, Larusso NF (2002): The pathobiology of biliary epithelia. *Hepatology* 35:1256-68
- Angulo P (2002): Nonalcoholic fatty liver disease. *N Engl J Med* 346:1221-31
- Angulo P (2007): Obesity and nonalcoholic fatty liver disease. *Nutr Rev* 65:S57-63
- Angulo P, Lindor KD (2001): Insulin resistance and mitochondrial abnormalities in NASH: a cool look into a burning issue. *Gastroenterology* 120:1281-5
- Anurag P, Anuradha CV (2002): Metformin improves lipid metabolism and attenuates lipid peroxidation in high fructose-fed rats. *Diabetes Obes Metab* 4:36-42
- Armutcu F, Coskun O, Gurel A, Kanter M, Can M, Ucar F, Unalacak M (2005): Thymosin alpha 1 attenuates lipid peroxidation and improves fructose-induced steatohepatitis in rats. *Clin Biochem* 38:540-7
- Arteel GE (2003): Oxidants and antioxidants in alcohol-induced liver disease. *Gastroenterology* 124:778-90
- Ates M, Pinarlı Fa, Kaplanoğlu Gt, Tiryaki M, Mercan S, Erdoğan D, Büyük G, Firat Z, Eyerci N, Topaloğlu O, *et al.* (2012): A Modified Method for Isolation of Rat Hepatocyte: Saving Time, Increases Viability. *Niche* 1:8-11
- Attar BM, Van Thiel DH (2013): Current concepts and management approaches in nonalcoholic Fatty liver disease. *ScientificWorldJournal* 2013:481893
- Bacon BR, Farahvash MJ, Janney CG, Neuschwander-Tetri BA (1994): Nonalcoholic steatohepatitis: an expanded clinical entity. *Gastroenterology* 107:1103-9
- Baker RG, Hayden MS, Ghosh S (2011): NF-kappaB, inflammation, and metabolic disease. *Cell Metab* 13:11-22
- Bantle JP (2009): Dietary fructose and metabolic syndrome and diabetes. *J Nutr* 139:1263S-1268S
- Barrows BR, Parks EJ (2006): Contributions of different fatty acid sources to very low-density lipoprotein-triacylglycerol in the fasted and fed states. *J Clin Endocrinol Metab* 91:1446-52
- Baumgardner JN, Shankar K, Hennings L, Badger TM, Ronis MJ (2008): A new model for nonalcoholic steatohepatitis in the rat utilizing total enteral nutrition to overfeed a high-polyunsaturated fat diet. *Am J Physiol Gastrointest Liver Physiol* 294:G27-38
- Bedogni G, Miglioli L, Masutti F, Tiribelli C, Marchesini G, Bellentani S (2005): Prevalence of and risk factors for nonalcoholic fatty liver disease: the Dionysos nutrition and liver study. *Hepatology* 42:44-52
- Berger T, Togawa A, Duncan GS, Elia AJ, You-Ten A, Wakeham A, Fong HE, Cheung CC, Mak TW (2006): Lipocalin 2-deficient mice exhibit increased sensitivity to *Escherichia coli* infection but not to ischemia-reperfusion injury. *Proc Natl Acad Sci U S A* 103:1834-9
- Bergheim I, Weber S, Vos M, Kramer S, Volynets V, Kaserouni S, McClain CJ, Bischoff SC (2008): Antibiotics protect against fructose-induced hepatic lipid accumulation in mice: role of endotoxin. *J Hepatol* 48:983-92
- Bertola A, Mathews S, Ki SH, Wang H, Gao B (2013): Mouse model of chronic and binge ethanol feeding (the NIAAA model). *Nat Protoc* 8:627-37

- Blum H, Beier DH, Gross HJ (1987): Improved silver staining of plant proteins, RNA and DNA in polyacrylamide gels. *Electrophoresis* **8**:93
- Borkham-Kamphorst E, Drews F, Weiskirchen R (2011): Induction of lipocalin-2 expression in acute and chronic experimental liver injury moderated by pro-inflammatory cytokines interleukin-1beta through nuclear factor-kappaB activation. *Liver Int* **31**:656-65
- Bradford MM (1976): A rapid and sensitive method for the quantitation of microgram quantities of protein utilizing the principle of protein-dye binding. *Anal Biochem* **72**:248-54
- Bravo AA, Sheth SG, Chopra S (2001): Liver biopsy. *N Engl J Med* **344**:495-500
- Brown LM, Gent L, Davis K, Clegg DJ (2010): Metabolic impact of sex hormones on obesity. *Brain Res* **1350**:77-85
- Bruggeman EC, Li C, Ross AP, Doherty JM, Williams BF, Frantz KJ, Parent MB (2011): A high fructose diet does not affect amphetamine self-administration or spatial water maze learning and memory in female rats. *Pharmacol Biochem Behav* **99**:356-64
- Brun P, Castagliuolo I, Di Leo V, Buda A, Pinzani M, Palu G, Martines D (2007): Increased intestinal permeability in obese mice: new evidence in the pathogenesis of nonalcoholic steatohepatitis. *Am J Physiol Gastrointest Liver Physiol* **292**:G518-25
- Brunt EM, Neuschwander-Tetri BA, Oliver D, Wehmeier KR, Bacon BR (2004): Nonalcoholic steatohepatitis: histologic features and clinical correlations with 30 blinded biopsy specimens. *Hum Pathol* **35**:1070-82
- Bugianesi E, McCullough AJ, Marchesini G (2005): Insulin resistance: a metabolic pathway to chronic liver disease. *Hepatology* **42**:987-1000
- Cadranel JF, Rufat P, Degos F (2000): Practices of liver biopsy in France: results of a prospective nationwide survey. For the Group of Epidemiology of the French Association for the Study of the Liver (AFEF). *Hepatology* **32**:477-81
- Cani PD, Bibiloni R, Knauf C, Waget A, Neyrinck AM, Delzenne NM, Burcelin R (2008): Changes in gut microbiota control metabolic endotoxemia-induced inflammation in high-fat diet-induced obesity and diabetes in mice. *Diabetes* **57**:1470-81
- Carniel-Haggai M, Cederbaum AI, Nieto N (2005): A high-fat diet leads to the progression of non-alcoholic fatty liver disease in obese rats. *FASEB J* **19**:136-8
- Celton-Morizur S, Merlen G, Couton D, Desdouets C (2010): Polyploidy and liver proliferation: central role of insulin signaling. *Cell Cycle* **9**:460-6
- Charlton M, Krishnan A, Viker K, Sanderson S, Cazanave S, McConico A, Masuoko H, Gores G (2011): Fast food diet mouse: novel small animal model of NASH with ballooning, progressive fibrosis, and high physiological fidelity to the human condition. *Am J Physiol Gastrointest Liver Physiol* **301**:G825-34
- Charlton M, Sreekumar R, Rasmussen D, Lindor K, Nair KS (2002): Apolipoprotein synthesis in nonalcoholic steatohepatitis. *Hepatology* **35**:898-904
- Chatterjee S, Ganini D, Tokar EJ, Kumar A, Das S, Corbett J, Kadiiska MB, Waalkes MP, Diehl AM, Mason RP (2013): Leptin is key to peroxynitrite-mediated oxidative stress and Kupffer cell activation in experimental non-alcoholic steatohepatitis. *J Hepatol* **58**:778-84
- Chen X, Cushman SW, Pannell LK, Hess S (2005): Quantitative proteomic analysis of the secretory proteins from rat adipose cells using a 2D liquid chromatography-MS/MS approach. *J Proteome Res* **4**:570-7
- Chitturi S, Abeygunasekera S, Farrell GC, Holmes-Walker J, Hui JM, Fung C, Karim R, Lin R, Samarasinghe D, Liddle C, *et al.* (2002a): NASH and insulin resistance: Insulin hypersecretion and specific association with the insulin resistance syndrome. *Hepatology* **35**:373-9
- Chitturi S, Farrell G, Frost L, Kriketos A, Lin R, Fung C, Liddle C, Samarasinghe D, George J (2002b): Serum leptin in NASH correlates with hepatic steatosis but not fibrosis: a manifestation of lipotoxicity? *Hepatology* **36**:403-9
- Cohen JJ, Roychowdhury S, Dibello PM, Jacobsen DW, Nagy LE (2009): Exogenous thioredoxin prevents ethanol-induced oxidative damage and apoptosis in mouse liver. *Hepatology* **49**:1709-17

- Commerford SR, Ferniza JB, Bizeau ME, Thresher JS, Willis WT, Pagliassotti MJ (2002): Diets enriched in sucrose or fat increase gluconeogenesis and G-6-Pase but not basal glucose production in rats. *Am J Physiol Endocrinol Metab* 283:E545-55
- Cowland JB, Borregaard N (1997): Molecular characterization and pattern of tissue expression of the gene for neutrophil gelatinase-associated lipocalin from humans. *Genomics* 45:17-23
- Cowland JB, Muta T, Borregaard N (2006): IL-1beta-specific up-regulation of neutrophil gelatinase-associated lipocalin is controlled by IkappaB-zeta. *J Immunol* 176:5559-66
- Cummings LE (1988): Commercial foodservice considerations in providing consumer-driven nutrition program elements. Part I. Consumer health objectives and associated employee education needs. *Cater Health* 1:51-71
- Daly ME, Vale C, Walker M, Alberti KG, Mathers JC (1997): Dietary carbohydrates and insulin sensitivity: a review of the evidence and clinical implications. *Am J Clin Nutr* 66:1072-85
- Day CP (2002): Pathogenesis of steatohepatitis. *Best Pract Res Clin Gastroenterol* 16:663-78
- Day CP, James OF (1998): Steatohepatitis: a tale of two "hits"? *Gastroenterology* 114:842-5
- De Lusong MA, Labio E, Daez L, Gloria V (2008): Non-alcoholic fatty liver disease in the Philippines: comparable with other nations? *World J Gastroenterol* 14:913-7
- De Villiers WJ, Song Z, Nasser MS, Deaciuc IV, McClain CJ (2007): 4-Hydroxynonenal-induced apoptosis in rat hepatic stellate cells: mechanistic approach. *J Gastroenterol Hepatol* 22:414-22
- Devireddy LR, Teodoro JG, Richard FA, Green MR (2001): Induction of apoptosis by a secreted lipocalin that is transcriptionally regulated by IL-3 deprivation. *Science* 293:829-34
- Dey A, Cederbaum AI (2006): Alcohol and oxidative liver injury. *Hepatology* 43:S63-74
- Diehl AM, Goodman Z, Ishak KG (1988): Alcohollike liver disease in nonalcoholics. A clinical and histologic comparison with alcohol-induced liver injury. *Gastroenterology* 95:1056-62
- Donnelly KL, Smith CI, Schwarzenberg SJ, Jessurun J, Boldt MD, Parks EJ (2005): Sources of fatty acids stored in liver and secreted via lipoproteins in patients with nonalcoholic fatty liver disease. *J Clin Invest* 115:1343-51
- Douard V, Ferraris RP (2008): Regulation of the fructose transporter GLUT5 in health and disease. *Am J Physiol Endocrinol Metab* 295:E227-37
- Dufour J-F, Clavien P-A (2005): *Signaling Pathways in Liver Diseases*. Springer Berlin:8
- Edmison J, Mccullough AJ (2007): Pathogenesis of non-alcoholic steatohepatitis: human data. *Clin Liver Dis* 11:75-104, ix
- Ekstedt M, Franzen LE, Holmqvist M, Bendtsen P, Mathiesen UL, Bodemar G, Kechagias S (2009): Alcohol consumption is associated with progression of hepatic fibrosis in non-alcoholic fatty liver disease. *Scand J Gastroenterol* 44:366-74
- Ekstedt M, Franzen LE, Mathiesen UL, Thorelius L, Holmqvist M, Bodemar G, Kechagias S (2006): Long-term follow-up of patients with NAFLD and elevated liver enzymes. *Hepatology* 44:865-73
- Elliott SS, Keim NL, Stern JS, Teff K, Havel PJ (2002): Fructose, weight gain, and the insulin resistance syndrome. *Am J Clin Nutr* 76:911-22
- Flo TH, Smith KD, Sato S, Rodriguez DJ, Holmes MA, Strong RK, Akira S, Aderem A (2004): Lipocalin 2 mediates an innate immune response to bacterial infection by sequestering iron. *Nature* 432:917-21
- Flower DR (1996): The lipocalin protein family: structure and function. *Biochem J* 318 (Pt 1):1-14
- Francq SM, Verrijken A, Mertens I, Hubens G, Van Marck E, Pelckmans P, Michielsen P, Van Gaal L (2012): Noninvasive assessment of nonalcoholic fatty liver disease in obese or overweight patients. *Clin Gastroenterol Hepatol* 10:1162-8; quiz e87
- Friedman JM, Halaas JL (1998): Leptin and the regulation of body weight in mammals. *Nature* 395:763-70
- Fujino RS, Tanaka K, Morimatsu M, Tamura K, Kogo H, Hara T (2006): Spermatogonial cell-mediated activation of an IkappaBzeta-independent nuclear factor-kappaB pathway in Sertoli cells induces transcription of the lipocalin-2 gene. *Mol Endocrinol* 20:904-15
- Garg A, Misra A (2002): Hepatic steatosis, insulin resistance, and adipose tissue disorders. *J Clin Endocrinol Metab* 87:3019-22

- Gary-Bobo M, Elachouri G, Gallas JF, Janiak P, Marini P, Ravinet-Trillou C, Chabbert M, Cruccioli N, Pfersdorff C, Roque C, *et al.* (2007): Rimonabant reduces obesity-associated hepatic steatosis and features of metabolic syndrome in obese Zucker fa/fa rats. *Hepatology* 46:122-9
- Gorg A, Obermaier C, Boguth G, Harder A, Scheibe B, Wildgruber R, Weiss W (2000): The current state of two-dimensional electrophoresis with immobilized pH gradients. *Electrophoresis* 21:1037-53
- Grattagliano I, Vendemiale G, Caraceni P, Domenicali M, Nardo B, Cavallari A, Trevisani F, Bernardi M, Altomare E (2000): Starvation impairs antioxidant defense in fatty livers of rats fed a choline-deficient diet. *J Nutr* 130:2131-6
- Gray B, Steyn F, Davies PS, Vitetta L (2013): Omega-3 fatty acids: a review of the effects on adiponectin and leptin and potential implications for obesity management. *Eur J Clin Nutr*:(in press)
- Greenspan P, Mayer EP, Fowler SD (1985): Nile red: a selective fluorescent stain for intracellular lipid droplets. *J Cell Biol* 100:965-73
- Gregory SH, Wing EJ (2002): Neutrophil-Kupffer cell interaction: a critical component of host defenses to systemic bacterial infections. *J Leukoc Biol* 72:239-48
- Gressner AM, Lahme B, Mannherz HG, Polzar B (1997): TGF-beta-mediated hepatocellular apoptosis by rat and human hepatoma cells and primary rat hepatocytes. *J Hepatol* 26:1079-92
- Guo H, Jin D, Zhang Y, Wright W, Bazuine M, Brockman DA, Bernlohr DA, Chen X (2010): Lipocalin-2 deficiency impairs thermogenesis and potentiates diet-induced insulin resistance in mice. *Diabetes* 59:1376-85
- Haring SJ, Harris RB (2011): The relation between dietary fructose, dietary fat and leptin responsiveness in rats. *Physiol Behav* 104:914-22
- Heidenreich S (1999): Monocyte CD14: a multifunctional receptor engaged in apoptosis from both sides. *J Leukoc Biol* 65:737-43
- Henson PM, Hume DA (2006): Apoptotic cell removal in development and tissue homeostasis. *Trends Immunol* 27:244-50
- Herzig S, Long F, Jhala US, Hedrick S, Quinn R, Bauer A, Rudolph D, Schutz G, Yoon C, Puigserver P, *et al.* (2001): CREB regulates hepatic gluconeogenesis through the coactivator PGC-1. *Nature* 413:179-83
- Holmstrom MH, Iglesias-Gutierrez E, Zierath JR, Garcia-Roves PM (2012): Tissue-specific control of mitochondrial respiration in obesity-related insulin resistance and diabetes. *Am J Physiol Endocrinol Metab* 302:E731-9
- Houglum K, Filip M, Witztum JL, Chojkier M (1990): Malondialdehyde and 4-hydroxynonenal protein adducts in plasma and liver of rats with iron overload. *J Clin Invest* 86:1991-8
- Hubscher SG (2004): Role of liver biopsy in the assessment of non-alcoholic fatty liver disease. *Eur J Gastroenterol Hepatol* 16:1107-15
- Ito M, Suzuki J, Tsujioka S, Sasaki M, Gomori A, Shirakura T, Hirose H, Ito M, Ishihara A, Iwaasa H, *et al.* (2007): Longitudinal analysis of murine steatohepatitis model induced by chronic exposure to high-fat diet. *Hepatology* 37:50-7
- Jin D, Guo H, Bu SY, Zhang Y, Hannaford J, Mashek DG, Chen X (2011): Lipocalin 2 is a selective modulator of peroxisome proliferator-activated receptor-gamma activation and function in lipid homeostasis and energy expenditure. *FASEB J* 25:754-64
- Johnson RJ, Segal MS, Sautin Y, Nakagawa T, Feig DI, Kang DH, Gersch MS, Benner S, Sanchez-Lozada LG (2007): Potential role of sugar (fructose) in the epidemic of hypertension, obesity and the metabolic syndrome, diabetes, kidney disease, and cardiovascular disease. *Am J Clin Nutr* 86:899-906
- Jun LS, Siddall CP, Rosen ED (2011): A minor role for lipocalin 2 in high-fat diet-induced glucose intolerance. *Am J Physiol Endocrinol Metab* 301:E825-35
- Kacew S, Festing MF (1996): Role of rat strain in the differential sensitivity to pharmaceutical agents and naturally occurring substances. *J Toxicol Environ Health* 47:1-30
- Kahn CR (1978): Insulin resistance, insulin insensitivity, and insulin unresponsiveness: a necessary distinction. *Metabolism* 27:1893-902

- Kasim-Karakas SE, Vriend H, Almario R, Chow LC, Goodman MN (1996): Effects of dietary carbohydrates on glucose and lipid metabolism in golden Syrian hamsters. *J Lab Clin Med* 128:208-13
- Kleiner DE, Brunt EM, Van Natta M, Behling C, Contos MJ, Cummings OW, Ferrell LD, Liu YC, Torbenson MS, Unalp-Arida A, *et al.* (2005): Design and validation of a histological scoring system for nonalcoholic fatty liver disease. *Hepatology* 41:1313-21
- Kmiec Z (2001): Cooperation of liver cells in health and disease. *Adv Anat Embryol Cell Biol* 161:III-XIII, 1-151
- Kumar S, Zheng H, Sangweme DT, Mahajan B, Kozakai Y, Pham PT, Morin MJ, Locke E, Kumar N (2013): A chemiluminescent-western blot assay for quantitative detection of *Plasmodium falciparum* circumsporozoite protein. *J Immunol Methods* 390:99-105
- Kunde SS, Roede JR, Vos MB, Orr ML, Go YM, Park Y, Ziegler TR, Jones DP (2011): Hepatic oxidative stress in fructose-induced fatty liver is not caused by sulfur amino acid insufficiency. *Nutrients* 3:987-1002
- Lackner C, Gogg-Kamerer M, Zatloukal K, Stumptner C, Brunt EM, Denk H (2008): Ballooned hepatocytes in steatohepatitis: the value of keratin immunohistochemistry for diagnosis. *J Hepatol* 48:821-8
- Laemmli UK (1970): Cleavage of structural proteins during the assembly of the head of bacteriophage T4. *Nature* 227:680-5
- Lall CG, Aisen AM, Bansal N, Sandrasegaran K (2008): Nonalcoholic fatty liver disease. *AJR Am J Roentgenol* 190:993-1002
- Langelueddecke C, Roussa E, Fenton RA, Thevenod F (2013): Expression and Function of the Lipocalin-2 (24p3/NGAL) Receptor in Rodent and Human Intestinal Epithelia. *PLoS One* 8:e71586
- Law IK, Xu A, Lam KS, Berger T, Mak TW, Vanhoutte PM, Liu JT, Sweeney G, Zhou M, Yang B, *et al.* (2010): Lipocalin-2 deficiency attenuates insulin resistance associated with aging and obesity. *Diabetes* 59:872-82
- Le KA, Bortolotti M (2008): Role of dietary carbohydrates and macronutrients in the pathogenesis of nonalcoholic fatty liver disease. *Curr Opin Clin Nutr Metab Care* 11:477-82
- Lechner M, Wojnar P, Redl B (2001): Human tear lipocalin acts as an oxidative-stress-induced scavenger of potentially harmful lipid peroxidation products in a cell culture system. *Biochem J* 356:129-35
- Leclercq IA, Farrell GC, Schriemer R, Robertson GR (2002): Leptin is essential for the hepatic fibrogenic response to chronic liver injury. *J Hepatol* 37:206-13
- Lee SO (2008): [Physiologic and pathologic experimental models for studying cholangiocytes]. *Korean J Hepatol* 14:139-49
- Liang H, Ward WF (2006): PGC-1alpha: a key regulator of energy metabolism. *Adv Physiol Educ* 30:145-51
- Lieber CS, Decarli LM (1994): Animal models of chronic ethanol toxicity. *Methods Enzymol* 233:585-94
- Lieber CS, Leo MA, Mak KM, Xu Y, Cao Q, Ren C, Ponomarenko A, Decarli LM (2004): Model of nonalcoholic steatohepatitis. *Am J Clin Nutr* 79:502-9
- Lin SM, Frevert CW, Kajikawa O, Wurfel MM, Ballman K, Mongovin S, Wong VA, Selk A, Martin TR (2004): Differential regulation of membrane CD14 expression and endotoxin-tolerance in alveolar macrophages. *Am J Respir Cell Mol Biol* 31:162-70
- Liu Q, Nilsen-Hamilton M (1995): Identification of a new acute phase protein. *J Biol Chem* 270:22565-70
- Lu GD, Shen HM, Chung MC, Ong CN (2007): Critical role of oxidative stress and sustained JNK activation in aloe-emodin-mediated apoptotic cell death in human hepatoma cells. *Carcinogenesis* 28:1937-45
- Luhn S, Berth M, Hecker M, Bernhardt J (2003): Using standard positions and image fusion to create proteome maps from collections of two-dimensional gel electrophoresis images. *Proteomics* 3:1117-27
- Malato Y, Naqvi S, Schurmann N, Ng R, Wang B, Zape J, Kay MA, Grimm D, Willenbring H (2011): Fate tracing of mature hepatocytes in mouse liver homeostasis and regeneration. *J Clin Invest* 121:4850-60

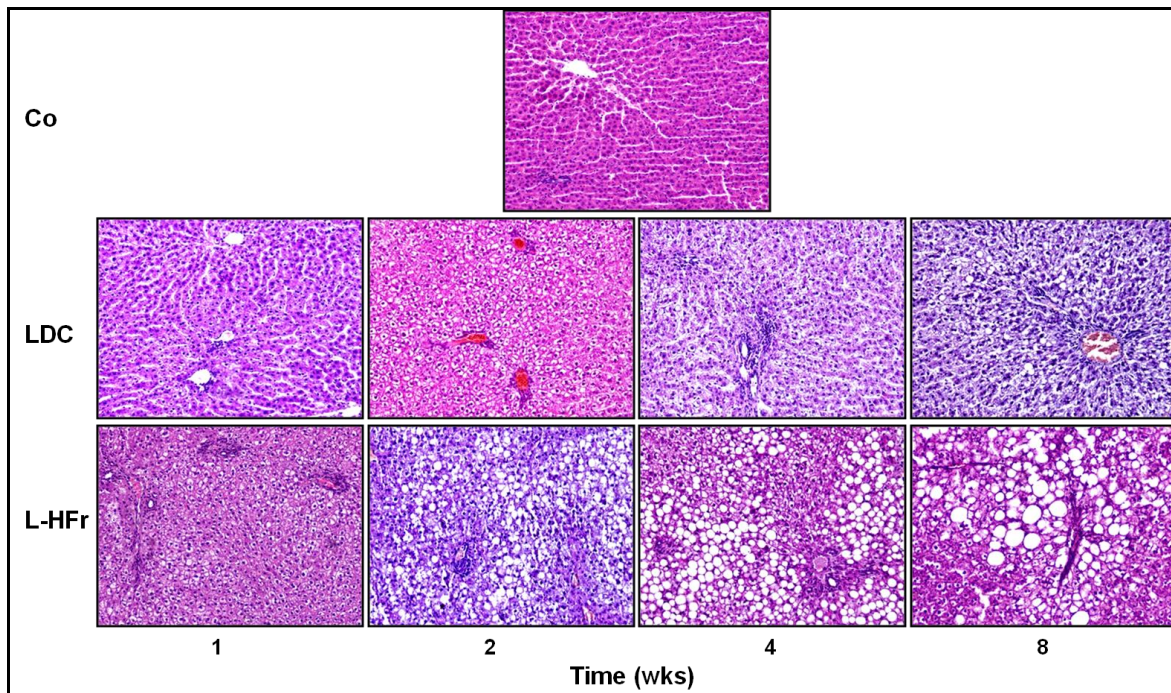
- Marchesini G, Babini M (2006): Nonalcoholic fatty liver disease and the metabolic syndrome. *Minerva Cardioangiolog* 54:229-39
- Marchesini G, Brizi M, Bianchi G, Tomassetti S, Bugianesi E, Lenzi M, Mccullough AJ, Natale S, Forlani G, Melchionda N (2001): Nonalcoholic fatty liver disease: a feature of the metabolic syndrome. *Diabetes* 50:1844-50
- Marchesini G, Bugianesi E, Forlani G, Cerrelli F, Lenzi M, Manini R, Natale S, Vanni E, Villanova N, Melchionda N, *et al.* (2003): Nonalcoholic fatty liver, steatohepatitis, and the metabolic syndrome. *Hepatology* 37:917-23
- Mauss S, Berg T, Rockstroh J, Sarrazin C, Wedemeyer H (2012): *Hepatology*. Flying Publisher, Germany:p427
- Mccullough AJ (2004): The clinical features, diagnosis and natural history of nonalcoholic fatty liver disease. *Clin Liver Dis* 8:521-33, viii
- Merat S, Malekzadeh R, Sohrabi MR, Sotoudeh M, Rakhshani N, Sohrabpour AA, Naserimoghadam S (2003): Probuocol in the treatment of non-alcoholic steatohepatitis: a double-blind randomized controlled study. *J Hepatol* 38:414-8
- Miele L, Valenza V, La Torre G, Montalto M, Cammarota G, Ricci R, Masciana R, Forgione A, Gabrieli ML, Perotti G, *et al.* (2009): Increased intestinal permeability and tight junction alterations in nonalcoholic fatty liver disease. *Hepatology* 49:1877-87
- Mishra J, Ma Q, Kelly C, Mitsnefes M, Mori K, Barasch J, Devarajan P (2006): Kidney NGAL is a novel early marker of acute injury following transplantation. *Pediatr Nephrol* 21:856-63
- Mofrad P, Contos MJ, Haque M, Sargeant C, Fisher RA, Luketic VA, Sterling RK, Shiffman ML, Stravitz RT, Sanyal AJ (2003): Clinical and histologic spectrum of nonalcoholic fatty liver disease associated with normal ALT values. *Hepatology* 37:1286-92
- Nagarajan P, Mahesh Kumar MJ, Venkatesan R, Majundar SS, Juyal RC (2012): Genetically modified mouse models for the study of nonalcoholic fatty liver disease. *World J Gastroenterol* 18:1141-53
- Neel JV (1999): The "thrifty genotype" in 1998. *Nutr Rev* 57:S2-9
- Nery ALP, Liegel RM, Fernandez C (2010): Fluorescence and Chemiluminescence: Teaching Basic Principles by Simple Demonstration Experiments. *Chemical Education Journal* 13:22
- O'farrell PZ, Goodman HM, O'farrell PH (1977): High resolution two-dimensional electrophoresis of basic as well as acidic proteins. *Cell* 12:1133-41
- Ong JP, Younossi ZM (2007): Epidemiology and natural history of NAFLD and NASH. *Clin Liver Dis* 11:1-16, vii
- Paik YH, Schwabe RF, Bataller R, Russo MP, Jobin C, Brenner DA (2003): Toll-like receptor 4 mediates inflammatory signaling by bacterial lipopolysaccharide in human hepatic stellate cells. *Hepatology* 37:1043-55
- Papakonstantinou E, Lambadiari V, Dimitriadis G, Zampelas A (2013): Metabolic Syndrome and Cardiometabolic Risk Factors. *Curr Vasc Pharmacol*
- Paschos P, Paletas K (2009): Non alcoholic fatty liver disease and metabolic syndrome. *Hippokratia* 13:9-19
- Patel V, Sanyal AJ (2013): Drug-induced steatohepatitis. *Clin Liver Dis* 17:533-46
- Pedersen BK, Steensberg A, Fischer C, Keller C, Ostrowski K, Schjerling P (2001): Exercise and cytokines with particular focus on muscle-derived IL-6. *Exerc Immunol Rev* 7:18-31
- Ploeg RJ, D'alessandro AM, Knechtle SJ, Stegall MD, Pirsch JD, Hoffmann RM, Sasaki T, Sollinger HW, Belzer FO, Kalayoglu M (1993): Risk factors for primary dysfunction after liver transplantation--a multivariate analysis. *Transplantation* 55:807-13
- Podrini C, Borghesan M, Greco A, Paziienza V, Mazzoccoli G, Vinciguerra M (2013): Redox homeostasis and epigenetics in non-alcoholic fatty liver disease (NAFLD). *Curr Pharm Des* 19:2737-46
- Quinn MT, Linner JG, Siemsen D, Dratz EA, Buescher ES, Jesaitis AJ (1995): Immunocytochemical detection of lipid peroxidation in phagosomes of human neutrophils: correlation with expression of flavocytochrome b. *J Leukoc Biol* 57:415-21

- Quinn SF, Gosink BB (1985): Characteristic sonographic signs of hepatic fatty infiltration. *AJR Am J Roentgenol* 145:753-5
- Ramadori G, Moebius U, Dienes HP, Meuer S, Meyer Zum Buschenfelde KH (1990): Lymphocytes from hepatic inflammatory infiltrate kill rat hepatocytes in primary culture. Comparison with peripheral blood lymphocytes. *Virchows Arch B Cell Pathol Incl Mol Pathol* 59:263-70
- Rezvani R, Cianflone K, Mcgahan JP, Berglund L, Bremer AA, Keim NL, Griffen SC, Havel PJ, Stanhope KL (2013): Effects of sugar-sweetened beverages on plasma acylation stimulating protein, leptin, and adiponectin: Relationships with Metabolic Outcomes. *Obesity (Silver Spring)*
- Ribeiro PS, Cortez-Pinto H, Sola S, Castro RE, Ramalho RM, Baptista A, Moura MC, Camilo ME, Rodrigues CM (2004): Hepatocyte apoptosis, expression of death receptors, and activation of NF-kappaB in the liver of nonalcoholic and alcoholic steatohepatitis patients. *Am J Gastroenterol* 99:1708-17
- Saadeh S, Younossi ZM, Remer EM, Gramlich T, Ong JP, Hurley M, Mullen KD, Cooper JN, Sheridan MJ (2002): The utility of radiological imaging in nonalcoholic fatty liver disease. *Gastroenterology* 123:745-50
- Saile B, Matthes N, Knittel T, Ramadori G (1999): Transforming growth factor beta and tumor necrosis factor alpha inhibit both apoptosis and proliferation of activated rat hepatic stellate cells. *Hepatology* 30:196-202
- Sandrin L, Fourquet B, Hasquenoph JM, Yon S, Fournier C, Mal F, Christidis C, Ziol M, Poulet B, Kazemi F, *et al.* (2003): Transient elastography: a new noninvasive method for assessment of hepatic fibrosis. *Ultrasound Med Biol* 29:1705-13
- Sanyal AJ (2011): NASH: A global health problem. *Hepatology* 41:670-4
- Seeley RR, Stephens TD, Tate P (2008): *Anatomy and Physiology*, 8th Edition:901
- Seglen PO (1973): Preparation of rat liver cells. 3. Enzymatic requirements for tissue dispersion. *Exp Cell Res* 82:391-8
- Semba T, Nishimura M, Nishimura S, Ohara O, Ishige T, Ohno S, Nonaka K, Sogawa K, Satoh M, Sawai S, *et al.* (2013): The FLS (fatty liver Shionogi) mouse reveals local expressions of lipocalin-2, CXCL1 and CXCL9 in the liver with non-alcoholic steatohepatitis. *BMC Gastroenterol* 13:120
- Shapiro A, Mu W, Roncal C, Cheng KY, Johnson RJ, Scarpace PJ (2008): Fructose-induced leptin resistance exacerbates weight gain in response to subsequent high-fat feeding. *Am J Physiol Regul Integr Comp Physiol* 295:R1370-5
- Shiri-Sverdlov R, Wouters K, Van Gorp PJ, Gijbels MJ, Noel B, Buffat L, Staels B, Maeda N, Van Bilsen M, Hofker MH (2006): Early diet-induced non-alcoholic steatohepatitis in APOE2 knock-in mice and its prevention by fibrates. *J Hepatol* 44:732-41
- Spruss A, Kanuri G, Stahl C, Bischoff SC, Bergheim I (2012): Metformin protects against the development of fructose-induced steatosis in mice: role of the intestinal barrier function. *Lab Invest* 92:1020-32
- Spruss A, Kanuri G, Wagnerberger S, Haub S, Bischoff SC, Bergheim I (2009): Toll-like receptor 4 is involved in the development of fructose-induced hepatic steatosis in mice. *Hepatology* 50:1094-104
- Sultan S, Cameron S, Ahmad S, Malik IA, Schultze FC, Hielscher R, Rave-Frank M, Hess CF, Ramadori G, Christiansen H (2013): Serum Lipocalin2 is a potential biomarker of liver irradiation damage. *Liver Int* 33:459-68
- Sultan S, Pascucci M, Ahmad S, Malik IA, Bianchi A, Ramadori P, Ahmad G, Ramadori G (2012): LIPOCALIN-2 is a major acute-phase protein in a rat and mouse model of sterile abscess. *Shock* 37:191-6
- Tabibian JH, Masyuk AI, Masyuk TV, O'hara SP, Larusso NF (2013): Physiology of cholangiocytes. *Compr Physiol* 3:541-65
- Takahashi Y, Soejima Y, Fukusato T (2012): Animal models of nonalcoholic fatty liver disease/nonalcoholic steatohepatitis. *World J Gastroenterol* 18:2300-8
- Tappy L, Le KA (2010): Metabolic effects of fructose and the worldwide increase in obesity. *Physiol Rev* 90:23-46

- Tarasow E, Siergiejczyk L, Panasiuk A, Kubas B, Dzienis W, Prokopowicz D, Walecki J (2002): MR proton spectroscopy in liver examinations of healthy individuals in vivo. *Med Sci Monit* **8**:MT36-40
- Tilg H (2004): Nicht-alkoholische Steatohepatitis. *J Gastroenterol Hepatol* **2** (3):5-10
- Tordjman J, Guerre-Millo M, Clement K (2008): Adipose tissue inflammation and liver pathology in human obesity. *Diabetes Metab* **34**:658-63
- Torres DM, Harrison SA (2008): Diagnosis and therapy of nonalcoholic steatohepatitis. *Gastroenterology* **134**:1682-98
- Trauner M, Arrese M, Wagner M (2010): Fatty liver and lipotoxicity. *Biochim Biophys Acta* **1801**:299-310
- Tygstrup N, Winkler K, Mellemegaard K, Andreassen M (1962): Determination of the hepatic arterial blood flow and oxygen supply in man by clamping the hepatic artery during surgery. *J Clin Invest* **41**:447-54
- Van Den Berghe G (1986): Fructose: metabolism and short-term effects on carbohydrate and purine metabolic pathways. *Prog Biochem Pharmacol* **21**:1-32
- Vanni E, Bugianesi E, Kotronen A, De Minicis S, Yki-Jarvinen H, Svegliati-Baroni G (2010): From the metabolic syndrome to NAFLD or vice versa? *Dig Liver Dis* **42**:320-30
- Velayudham A, Dolganiuc A, Ellis M, Petrasek J, Kodys K, Mandrekar P, Szabo G (2009): VSL#3 probiotic treatment attenuates fibrosis without changes in steatohepatitis in a diet-induced nonalcoholic steatohepatitis model in mice. *Hepatology* **49**:989-97
- Volynets V, Spruss A, Kanuri G, Wagnerberger S, Bischoff SC, Bergheim I (2010): Protective effect of bile acids on the onset of fructose-induced hepatic steatosis in mice. *J Lipid Res* **51**:3414-24
- Wang Y, Ausman LM, Russell RM, Greenberg AS, Wang XD (2008): Increased apoptosis in high-fat diet-induced nonalcoholic steatohepatitis in rats is associated with c-Jun NH2-terminal kinase activation and elevated proapoptotic Bax. *J Nutr* **138**:1866-71
- Wang Y, Lam KS, Kraegen EW, Sweeney G, Zhang J, Tso AW, Chow WS, Wat NM, Xu JY, Hoo RL, *et al.* (2007): Lipocalin-2 is an inflammatory marker closely associated with obesity, insulin resistance, and hyperglycemia in humans. *Clin Chem* **53**:34-41
- Weigle DS, Duell PB, Connor WE, Steiner RA, Soules MR, Kuijper JL (1997): Effect of fasting, refeeding, and dietary fat restriction on plasma leptin levels. *J Clin Endocrinol Metab* **82**:561-5
- Wiernsperger N, Geloën A, Rapin JR (2010): Fructose and cardiometabolic disorders: the controversy will, and must, continue. *Clinics (Sao Paulo)* **65**:729-38
- Wise C, Pihanathanond M, Perry BF, Alpini G, Mcneal M, Glaser SS (2008): Mechanisms of biliary carcinogenesis and growth. *World J Gastroenterol* **14**:2986-9
- Wise GE, Lin F (1991): Transfer of silver-stained proteins from polyacrylamide gels to polyvinylidene difluoride membranes. *J Biochem Biophys Methods* **22**:223-31
- Wisse E (1974): Kupffer cell reactions in rat liver under various conditions as observed in the electron microscope. *J Ultrastruct Res* **46**:499-520
- Wojcik M, Ramadori P, Blaschke M, Sultan S, Khan S, Malik IA, Naz N, Martius G, Ramadori G, Schultze FC (2012): Immunodetection of cyclooxygenase-2 (COX-2) is restricted to tissue macrophages in normal rat liver and to recruited mononuclear phagocytes in liver injury and cholangiocarcinoma. *Histochem Cell Biol* **137**:217-33
- Wu D, Cederbaum AI (2001): Removal of glutathione produces apoptosis and necrosis in HepG2 cells overexpressing CYP2E1. *Alcohol Clin Exp Res* **25**:619-28
- Yang J, Goetz D, Li JY, Wang W, Mori K, Setlik D, Du T, Erdjument-Bromage H, Tempst P, Strong R, *et al.* (2002): An iron delivery pathway mediated by a lipocalin. *Mol Cell* **10**:1045-56
- Yip WW, Burt AD (2006): Alcoholic liver disease. *Semin Diagn Pathol* **23**:149-60
- Yu AS, Keeffe EB (2003): Elevated AST or ALT to nonalcoholic fatty liver disease: accurate predictor of disease prevalence? *Am J Gastroenterol* **98**:955-6
- Yuzer H, Yuzbasioglu MF, Ciralik H, Kurutas EB, Ozkan OV, Bulbuloglu E, Atli Y, Erdogan O, Kale IT (2009): Effects of intravenous anesthetics on renal ischemia/reperfusion injury. *Ren Fail* **31**:290-6
- Zhang J, Wu Y, Zhang Y, Leroith D, Bernlohr DA, Chen X (2008): The role of lipocalin 2 in the regulation of inflammation in adipocytes and macrophages. *Mol Endocrinol* **22**:1416-26

-
- Zhou L, Yu X, Meng Q, Li H, Niu C, Jiang Y, Cai Y, Li M, Li Q, An C, *et al.* (2012): Resistin reduces mitochondria and induces hepatic steatosis in mice by the protein kinase C/protein kinase G/p65/PPAR gamma coactivator 1 alpha pathway. *Hepatology*
- Zimmet P, Alberti KG, Shaw J (2001): Global and societal implications of the diabetes epidemic. *Nature* 414:782-7

Appendix



Appendix Figure 1 Kinetic HE staining for rat liver sections on 1, 2, 4, 8 wks. The whole experiment was designed as 1, 2, 4, and 8 wks. In this dissertation, I focused of 4 and 8 wks to simplify the study. Co: chow diet, LDC: Lieber-DeCarli, and L-HFr: LDC+ 70% kcal fructose.

Fatty liver models that were developed in Sprague-Dawley Rats			
Diet	Feeding status before sacrifice	Experimental time (wks)	Use
Chow pellets (Co)	Fasted	1,2,4, 8	Thesis
Lieber-DeCarli diet (LDC)			
LDC + high (70% kcal) fructose (L-HFr)			
Chow pellets (Co)	Unfasted	4	Preliminary work
Lieber-DeCarli diet (LDC)			
LDC + 30% kcal ethanol (L-Et)			
LDC + 30% kcal fructose (L-Fr)			
LDC + high (70% kcal) fructose (L-HFr)	Unfasted Fasted	4 1,2,4, 8	Preliminary work
LDC + 30% kcal ethanol + 30% kcal fructose (L-EF)			

Appendix Figure 2 Illustration of rat fatty liver models induced by various diets.

Appendix Table 1 Summary of LCN2 studies in recent literature

	Author	Model/design	Tissue	Treatment	Title/Conclusion
1	Semba 2013	Fatty liver Shionogi vs. dd Shionogi Mice	Liver	Chow pellets	The FLS mouse reveals local expressions of LCN2 and CXCL9 in the liver with NASH, suggesting significant roles of these proteins in the pathogenesis of NASH
2	Borkham- Kamphors t 2013	<i>Lcn2</i> ^{-/-} Mice	Liver Serum	Acutely with CCl ₄ , LPS and or subjected to bile duct ligation	Protective effects of LCN2 in acute liver injury suggest a novel function in liver homeostasis.
3	Jun 2011	<i>Lcn2</i> ^{-/-} vs. WT Mice	Liver, Serum Adipose	Chow vs. high-fat diet (HFD) (60% kcal fat)	A minor role for LCN2 in HFD induced glucose intolerance.
4	Liu 2011	18-yr-old men	Serum	cross-section study	LCN2 is not an independent predictor of metabolic risk factors.
5	Borkham- Kamphors t 2011	Primary liver cell isolation Sprague–Dawley rats	Liver	<i>i.p.</i> CCL ₄ in mineral oil	Induction of LCN2 expression in acute and chronic exp. liver injury moderated by pro-inflammatory IL-1 β through NF-kB activation.
6	Liu 2011	<i>Lcn2</i> -KO Mice	Serum Carotid artery	HFD, 45% kcal Inject with Recomb. LCN2	LCN2 deficiency prevents endothelial dysfunction associated with obesity.
7	Guo 2010	<i>Lcn2</i> ^{-/-} vs. WT Mice	Liver Adipose	Chow vs. HFD adaptive thermogenes is	LCN2 deficiency impairs thermogenesis and potentiates diet-induced IR in mice.
8	Law 2010	C57BL/6J vs. C57BL/6J db/db diabetic Mice. <i>Lcn2</i> ^{-/-} Mice	Serum Muscle Fat and liver	Chow and HFD Anti-TNF α treatment	LCN2 deficiency protects mice from developing aging- and obesity-induced IR.
9	Wang 2007	People C57BL/KsJ <i>db/db</i> Mice	Serum Muscle Fat and liver	Cross- sectional, Rosiglitazone administratio n	LCN2 Is an Inflammatory marker closely associated with obesity, IR, and hyperglycemia in Humans.

HFD: high fat diet.

Acknowledgments

Before all else, I am greatly indebted for my research and success to Merciful and Almighty “ALLAH” Who blessed me with the ability to achieve this milestone in my life, and all respects are for the Holy Prophet, Hazrat Muhammad (Peace Be Upon Him).

There are so many nice people who supported me with this thesis. First, I would like to thank Prof. Dr. S. Barghouti, Dean of Research & Cooperation, and Dr. Rania Abu Seir, Al-Quds University, Palestine. She recommended me and supported me to obtain the scholarship to the Georg-August-University of Göttingen. In addition, many thanks for Prof. Ramadori who offers me the opportunity to pursue my post-graduate studies in Germany.

Endless thanks to Dr. med. FC Schultze who has been my academic advisor for this project for the last two years: your enthusiasm for my project and science in general is truly inspirational.

I would also like to thank the professors that guided my graduate career, specifically my committee. Great appreciation, gratitude and deepest thanks are directed to my thesis' committee (Prof. Dr. Groß and Prof. Dr. Hoppert). I am grateful for them for serving on the committee, and for their constructive criticism and endless help throughout this study. Special thanks go to Prof. Dr. med. Sauerbruch, Prof. S. Mihm and Dr. med. S. Cameron, Gastroenterology and Endocrinology Dept., to Prof. Witling, Anatomy and Cell Biology Dept, and to Dr. med. Schaefer, Institute of Pathology.

Next, I owe to my colleagues in the Gastroenterology & Endocrinology Dept. Mentioning some people by name is not as important as it is to admire and admit their valuable role in keeping me mobile and energetic: Dr. Min Xu, Dr. Sadaf Sultan, Dr. Sajjad Khan, Dr. Naila Naz, and Dr. Ihtzaz Malik.

I would like to thank my friends for all of their support, especially Ali Abu Quttam, Eng. Alaa Qatrawi, Dr. Ahmad Ghazi, Ahmad and Yasser Jaffal, and Dr. Wafi Dhman: thank you for the endless hours of entertainment and encouragement. Eng. Wajdi Alwahsh and Dr. Hesham Hameeda: thank you for everything. Last but not least, I would like to acknowledge all the support and encouragement provided by my family: Mom, Dad, and my brothers and sisters, and for my Uncle Salama, and especial thanks to my wife Lubaba Shtaya and her nice family.

SALAMAH M. ALWAHSH

Publications and Conferences

Publications

- Ahmad S, Sultan S, Naz N, Ahmad G, **Alwahsh SM**, *et al.* (2013). Regulation of iron uptake in primary culture rat hepatocytes: The role of acute phase cytokines. SHOCK (Accepted)
- **Alwahsh SM**, Xu M, Seyhan HA, Schaefer IM, Ahmad S, *et al.* (2013). *Diet high in fructose leads to an overexpression of lipocalin-2 in rat fatty liver.* WJG (In press)
- Schultze FC, Andag R, **Alwahsh SM**, Toncheva D, Maslyankov S, *et al.* (2013). FoxP3 demethylation is increased in colorectal cancer and intrahepatic cholangiocarcinoma tissues. Clin Biochem

Conferences

Alwahsh SM, Xu M, Mihm S, Ramadori G, and Schultze FC (2013)

Fructose-enriched diet induced an overexpression of lipocalin-2 in rat fatty liver
Journal of Clinical & Experimental Hepatology [JCEH]; Volume 3, Issue 1, Supplement,
Pages S31-S32

Alwahsh SM, Xu M, Ramadori G, Schultze FC (2013)

Lipocalin-2 is a biomarker in rat fatty liver induced by fructose-enriched diet
Z Gastroenterol;51-P_3_01

D. Petrova, K. Luchs, F. Schultze, **S. Alwahsh**, *et al.* (2012)

Kidney function and histopathological differences induced by mycophenolate mofetil in a mouse model for progressive renal disease
Clin Chem Lab Med;50: A227

Resume

PERSONAL DATA

NAME **Salamah Mohammad Alwahsh**
 DATE & PLACE OF BIRTH November 11th, 1985, Bethlehem, PALESTINE

EDUCATION

POST-GRAUDATE

2010-2013 Doctorate (Dr.rar.nat.) in Biology
 Internal Medicine, Gastroenteriology & Endocrinology Dept.
 University Medical Center Goettingen (UMG), Germany

2010-2011 "Diploma" equivalent
Thesis: "Study the effect of glucose versus fructose on the gene expression, growth, and metabolism in HepG2 cells"
 Anatomy & Cell Biology Institute, UMG, Germany

GRADUATE

2005-2009 Bachelor's Degree (B.Sc.) in Medical Laboratory Sciences
 Health Professions Faculty
 Al-Quds University, West-bank, Palestine
(In addition to the scientific part; this field as a profession concerns in executing a clinical lab diagnosis for the patients including Hematology, Coagulation & Blood banking, Clinical chemistry, Serology, Body fluids, Medical Microbiology & Parasitology, Histology, and Endocrinology tests).

SCHOOL

2003-2004 Baccalaureate degree (Certificate of General Secondary School Examination (Tawjihi)), the prerequisite for University studies
Scientific Stream, evaluation **95.1%**, ranking: EXCELLENT
 Muhamad Salem Althweb Secondary School, Bethlehem, Palestine

1992-2003 Primary School (1st- 7th grade) and Middle school (8th- 11th grade)

DISTINCTIONS & AWARDS

2010-2013 Scholarship for post-graduate studies in Gastroenterology Dept., UMG, Goettingen, Germany

2009 First position holder in Health Professions Faculty as well as in the Dept. of Medical Lab Sciences, Al-Quds University, Palestine.
EXCELLENT with **HONOR** degree in **B.Sc.**, Cum. average **91.1%**.

SKILLS/EXPERIENCE

2011-2013 Exemplary *ad hoc* reviewer for *Lab Invest.*, and PloS one Journals
 Primary hepatocytes and neutrophils isolation and manipulation
 Handling of Lab Animals (rats & mice) and establishing of models

2010-2011 Experience in 2-DE proteomics and other scientific lab techniques

2009-2011 Member of "Medical Technology Association", PALESTINE

RESEARCH OF INTEREST

Fatty liver, Hepatic ischemia-reperfusion injury, NASH, Metabolic syndrome, Lipocalin-2

"And with Him are the keys of the unseen; none knows them except Him. And He knows what is on the land and in the sea. Not a leaf falls but that He knows it. And no grain is there within the darkneses of the earth and no moist or dry [thing] but that it is [written] in a clear record", Chapter 7:59 "The Cattle" (Al-A'n'ām), **QURAN**.